Resuspension, Flocculation, and Transport of Drilling Muds and Fine-grained Sediments

Final Technical Summary

Final Study Report

MMS

**U.S. Department of the Interior
Minerals Management Service
Pacific OCS Region**

Resuspension, Flocculation, and Transport of Drilling Muds and Fine-grained Sediments

Final Technical Summary

Final Study Report

Authors

Wilbert J. Lick
Principal Investigator
and
Hening Huang

U.S. Department of the Interior
Minerals Management Service
Pacific OCS Region

Camarillo
March 2003

Disclaimer

This report has been reviewed by the Pacific Outer Continental Shelf Region, Minerals Management Service, U.S. Department of the Interior and approved for publication. The opinions, findings, conclusions, or recommendations in this report are those of the author, and do not necessarily reflect the views and policies of the Minerals Management Service. Mention of trade names or commercial products does not constitute an endorsement or recommendation for use. This report has not been edited for conformity with Minerals Management Service editorial standards.

Availability of Report

Suggested Citation

Table of Contents

FINAL TECHNICAL SUMMARY

STUDY TITLE: Resuspension, Flocculation, and Transport of Drilling Muds and Fine-grained Sediments

REPORT TITLE: Resuspension, Flocculation, and Transport of Drilling Muds and Fine-grained Sediments

CONTRACT NUMBER: 14-35-0001-30471

SPONSORING OCS REGION: Pacific

APPLICABLE PLANNING AREA(S): Southern California

FISCAL YEAR(S) OF PROJECT FUNDING: FY 89, FY 90, FY 91

COMPLETION DATE OF REPORT: March 1993

COST(S): FY 89: $70,000; FY 90: $76,532; FY 91: $76,532

CUMULATIVE PROJECT COST: $223,064

PROJECT MANAGER: Wilbert J. Lick

AFFILIATION: University of California, Santa Barbara

ADDRESS: Department of Mechanical and Environmental Engineering, University of California, Santa Barbara, CA 93106

KEY WORDS: drilling muds; sediments; offshore oil; pollution; transport; resuspension; flocculation.

BACKGROUND: The disposal of drilling muds from offshore oil platforms is of concern because of potential effects of pollution from these muds. A related problem is the concentration of pollutants from produced waters and other sources in bottom (especially fine-grained) sediments. Fine-grained sediments (silts and clays) are especially important because of their great capacity for adsorbing contaminants which are then transported with the sediments. Both drilling muds and fine-grained bottom sediments are similar in their general physical and chemical characteristics and can be studied by similar methods.

In an accurate description of the transport of fine-grained sediments, it is essential to realize that (1) in a real mud sample, the particle sizes vary by more than three orders of magnitude, from less than one micrometer to several hundred micrometers, and (2) the effective particle size is a dynamic quantity which changes with time depending on the rates of aggregation and disaggregation (flocculation). Neither the parameters that govern these factors nor their influence on transport are well understood, but they were investigated as part of this project.

1

OBJECTIVES: The purpose of this project was to quantitatively understand and be able to predict the transport of drilling muds and bottom sediments. This included a quantitative study of their resuspension, deposition, and flocculation. This project was similar to previous work that we have done on fine-grained sediments in both lake and oceanic waters. It emphasized laboratory experiments but also incorporated the experimental results into mathematical models of resuspension, deposition, and flocculation of drilling muds and sediments.

DESCRIPTION: Specific studies are (a) laboratory experiments on flocculation, particle sizes, and settling speeds of the flocculated particles; (b) resuspension experiments using our annular flumes in the laboratory and using the shaker to study resuspension of undisturbed sediments in the field; (c) numerical modeling of the resuspension, flocculation, and hence transport of muds and other finegrained sediments.

STUDY RESULTS:

Laboratory experiments on flocculation, particle sizes, and settling speeds: It should be emphasized that the formation of flocs is a dynamic process with the state of aggregation at any particular location and time depending on the rates of aggregation and disaggregation. The fact that flocculation is a dynamic process also indicates that aggregate properties, such as the settling speed, also change in a dynamic manner. For example, as a particle settles in the water column, it may increase or decrease in size depending on the rates of aggregation and disaggregation. Corresponding to this increase or decrease in size, the settling speeds will also increase or decrease.

Figure 1 shows the result of some of our work (Xu 1989) on the flocculation of bentonite, a major component of most drilling muds. In these experiments, bentonite was first disaggregated in a blender and then placed in a Couette flocculator. Initially, the median particle size was about 4 microns but then increased with time and eventually reached steady state. This steady-state particle size depends on the shear stress and also on the particle concentration.

Figure 1. Time variations of median floc diameters for bentonite at a shear stress of 2 dynes/cm^2.
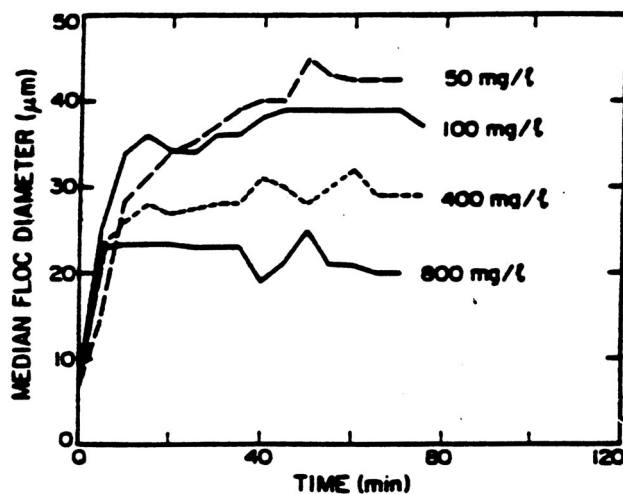
A numerical model which describes these flocculation processes has been developed and shows good agreement with the experiments. In the original model, thousands of states were used in the description of the flocs, i.e., each state corresponded to a different number of particles making up the floc. Although this model was quite accurate, it also required a great deal of computer time. In order for this model to be included in transport calculations, the model must be made more efficient. This has now been done, and the computation times have been reduced by several orders of magnitude.

The above experiments and analyses investigated the effects of an applied fluid shear on flocculation. As the applied fluid shear decreases, the flocs increase in size, and the settling speeds of these flocs also increase. As this happens, the induced fluid shear due to flow around the flocs as they settle through the water becomes more significant than the applied shear. To investigate this situation, flocculation experiments were done in a unique rotating fluid disk device, essentially an infinitely long settling tube. Flocculation at concentrations from 100 mg/l to 1 mg/l was investigated.

Of course, in predicting transport, the most important particle property is its settling speed. This is dependent upon the size, or diameter, of the particle but not simply through Stokes' law, for example. Results of direct measurements of settling speeds of flocculated bentonite are shown in Figure 2. These flocs were produced in the flocculator at a sediment concentration of 100 mg/l and a fluid shears of 100, 200, and 400 s^{-1}. It can be seen that all of the settling speeds are considerably less than those predicted by Stokes' law for a solid particle, some by almost a factor of 1000.

Figure 2. Settling speeds of bentonite flocs formed at a concentration of 100 mg/l and fluid shears of 1, 2, and 4 dynes/cm^2.
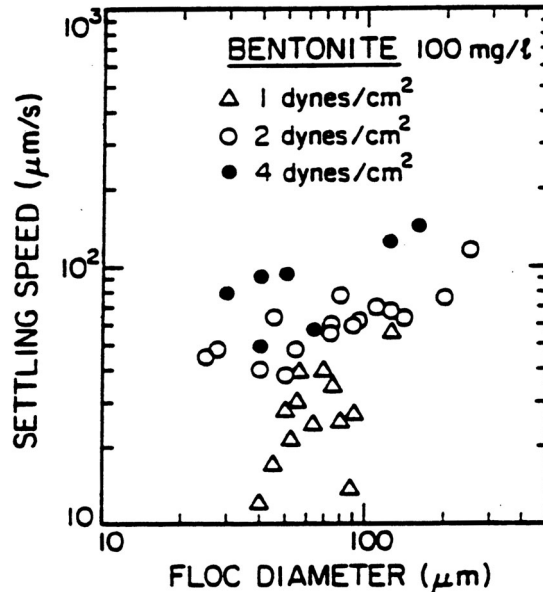
Similar experiments to those described above have been done for barite, another major component of most drilling muds, and also for used drilling muds.

<u>Laboratory resuspension experiments</u>: Drilling muds and effluents are generally disposed of from platforms by either discharging at or near the surface (for maximum dispersion) or by shunting to depths (to minimize dispersion). In either case, drilling muds are eventually transported to the bottom by a combination of density-driven flows, currents, turbulent diffusion, and settling of the particles relative to the surrounding waters.

Here they may be buried and compacted by sediments and other particles being deposited over them, and they may also be processed and transformed by chemical reactions and benthic organisms. At some later time, depending on environmental conditions, they may be resuspended and again transported and dispersed by currents and wave action. This series of events will continue until the particles are buried deep enough so that they become a permanent part of the bottom sediments or until they are transported out of the region of interest.

Considerable work has been done in general on the resuspension properties of fine-grained sediments, but nothing specifically on drilling muds previous to the present work. What is known in general about the resuspension of fine-grained sediments is as follows (Lick 1991). A sediment bed composed mostly of cohesive, fine-grained materials will be compacted with the compaction generally increasing with depth and time. Because of this, the sediments near the surface are relatively easy to resuspend while deeper sediments are more difficult to resuspend. Particle size variations also affect the resuspension since, at any particular shear stress, only the finer particles on the surface of the sediment bed can be resuspended while the larger particles are left behind and armor the bed. For both of these reasons, at any particular stress, only a finite and relatively small amount of sediment can be resuspended. This is in contrast to uniform-size, non-cohesive sediments where the resuspension rate is approximately constant with time.

<u>Numerical modeling of the transport of drilling muds</u>: As part of our previous modeling efforts, both two-dimensional vertically integrated time-dependent and three-dimensional, time--dependent hydrodynamic and transport models have been developed (Lick 1976; Sheng *et al* 1978; Lick and Ziegler 1988). These models have been coupled with a three-dimensional, time-dependent model of the sediment bed and its properties. The sediment bed model is layered in the vertical direction with an arbitrary number of layers and arbitrary initial thickness. The properties of each layer depend on time after deposition and composition (relative fraction of medium and coarse sediments). Settling speeds and sediment resuspension parameters needed in the model have been determined by laboratory and field tests.

SIGNIFICANT CONCLUSIONS:

<u>Laboratory experiments on flocculation, particle sizes, and settling speeds</u>: From this and related experiments, it can be shown that the median particle size decreases as the shear stress increases and decreases as the particle concentration increases. The rates of aggregation and disaggregation can also be deduced from these experiments.

It is also clear that the settling speed of a floc depends on the conditions under which it was produced, i.e., flocs produced at low shears have lower settling speeds than do flocs produced at higher shears. It can also be shown that flocs produced at lower concentrations have lower settling speeds that do flocs produced at higher concentration (Burban *et al* 1990).

<u>Laboratory resuspension experiments</u>: The experimental work on resuspension of bentonite, barite, and used drilling muds has determined the dependence of the resuspension rate and the total amount of sediment that can be resuspended at a particular stress as a function of (a) the turbulent stress at the sediment-water interface, and (b) the water content of the deposited sediments (or the time after deposition).

STUDY PRODUCT:

Huang, Hening. 1992. Transport Properties of Drilling Muds and Detroit River Sediments. Ph.D. Dissertation, University of California, Santa Barbara. 191 pp.

FINAL STUDY REPORT

UNIVERSITY OF CALIFORNIA
Santa Barbara

Transport Properties of Drilling Muds and
Detroit River Sediments

Thesis submitted in partial satisfaction of the requirements for the degree
of

Doctor of Philosophy
in
Environmental Sciences / Civil Engineering

by
Hening Huang

Advisor:
Wilbert J. Lick

May 1992

.

ABSTRACT

Transport Properties of Drilling Muds and Detroit River Sediments

by
Hening Huang

The purpose of this study was to improve our understanding of the transport properties of drilling muds and Detroit River sediments. These properties include those of resuspension, flocculation, and settling speeds.

From experiments in an annular flume, the resuspension properties of a drilling mud were obtained as a function of fluid shear stress and bed consolidation period; empirical expressions for these properties were also obtained. The drilling mud was found to be much easier to resuspend than lake sediments but more difficult than bentonite.

From flocculation tests for the drilling mud in a Couette flocculator, the median diameter and standard deviation of the floc size distribution were obtained as a function of fluid shear and solid concentration; self-similar size distributions and three flocculation stages were observed. It is demonstrated by dimensional analysis that the effects of fluid shear and solid concentration can be accounted for in terms of a dimensionless parameter F_l, which is defined as the flocculation number. The data were found to be well correlated with the flocculation number, and semi-empirical equations for these relations were obtained.

The validity of using disc flocculators to investigate flocculation due to differential settling was examined both theoretically and experimentally. The criteria for dynamic and collision similarity are presented. Compared with tests in the Couette flocculator, particles flocculated much slower in the disc flocculators, and floc sizes in the steady state were much larger.

A preliminary investigation of the effects of organic coatings on flocculation was made by using sediments with the organic matter removed. For Detroit River sediments in seawater, treated samples flocculated faster than did untreated samples; in fresh water, treated samples flocculated faster at high concentrations but slower at low concentrations. Treated drilling muds flocculated much slower than did untreated samples.

Settling speeds of flocs were measured in a settling tube by a double-exposure photographic method. The results show that the settling speed of a floc is a function of its size and the conditions at which the floc is formed. Empirical expressions for the settling speed-size relationships were obtained. Using the settling speed data and a floc settling speed model, effective densities of flocs were obtained.

1. INTRODUCTION

The general purpose of this study is to improve our understanding of the transport properties of fine-grained sediments, with specific applications to drilling muds and Detroit River sediments. The transport properties include those of resuspension, flocculation, and settling speeds and effective densities of flocs. These properties are essential in the quantitative prediction of the transport and fate of fine-grained sediments in natural water bodies.
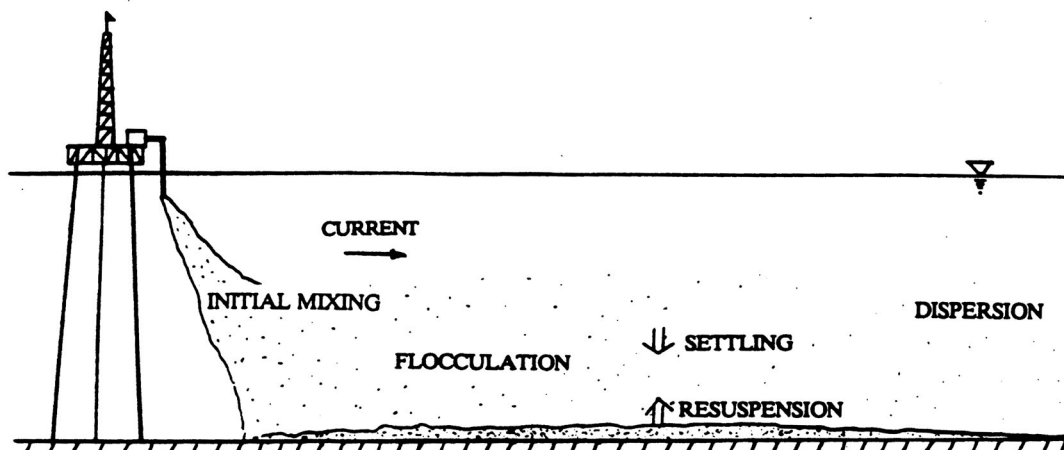
Drilling Muds

The exploration for and development of offshore oil and gas resources have prompted concerns about the environmental impact of used drilling muds discharged into the ocean. Drilling muds are water-based or oil-based suspensions of clays. Only a water-based drilling mud will be considered here. The major components of drilling muds are barite (barium sulfate) and bentonite, whose functions are to increase density and viscosity respectively. To meet a variety of requirements for drilling operations, many kinds of chemicals are added, such as lignosulfonates to control filtration and flow properties, caustic soda and lime to control the pH, hydrated lime and amine salts to control corrosion, and bactericides to control bacteria. Various types of contaminants are adsorbed on or are part of drilling mud particles, including hydrocarbons and metals such as chromium, mercury, copper, zinc, lead, and cadmium, many of which are toxic to marine species.

The main functions of drilling muds are (a) to remove and transport cuttings from the drill-hole, (b) to cool and lubricate the bit and drill string, (c) to insure controlled and efficient drilling through maintenance of well pressures and well properties of the borehole, and (d) to support the drill pipe and casing weight.

During the drilling operation of a well, the drilling mud is pumped down the center of a rotating string of drill pipe where it exits through nozzles at the drill bit, picks up drill cuttings (rock fragments), and returns to the surface through the annulus between the drill string and the walls of the borehole and/or casing. Back at the surface, the drilling mud is passed through various mechanical devices (solid control equipment) that selectively separate cuttings from the drilling mud. Separated cuttings are then discharged into the ocean. This type of discharge is continuous in the sense that it occurs while drilling is on location. The separated mud goes back to the mud pits for recirculation. As time goes on, the concentration of fine particles in the mud continues to increase and eventually reaches a point where the mud becomes too viscous. At this time a portion of the mud is discharged and the remainder is diluted with water and appropriate quantities of mud additives to bring the concentration of fine solids back to an acceptable level. Bulk mud discharges may occur if a completely different type of mud is needed or if the mud becomes seriously contaminated. In addition, discharge of the entire mud occurs at the completion of each exploratory well. Typically, over the life of a well, some 3000 to 30000 barrels of spent drilling muds are disposed of into the ocean (Ayers, 1983).

Drilling muds are generally disposed of from platforms by either discharging through a pipe at or near the water surface or by shunting to depth. The discharged drilling muds encounter both short-term and long-term transport processes in the ocean. The short-term transport (also known

as near-field transport) includes the initial mixing and passive diffusion of drilling mud plumes (jets) and the initial sedimentation of mud solids. The long-term transport (also known as far-field transport) includes the resuspension, dispersion, and deposition of drilling mud particles over longer periods of time. Flocculation will affect both the short-term and long-term transport processes (Fig.1-1).

Fig.1-1 Transport processes of ocean disposed drilling muds

In order to assess the effects of drilling mud discharges on the marine environment, it is important to understand and predict the transport and fate of disposed muds. At the present time, the hydrodynamics of initial mixing and passive diffusion in the short-term is reasonably well understood (Lick, 1989), and some numerical models (e.g. the OOC model, Brandsma and Sauer, 1983) describing the motion of drilling mud plumes (jets) and initial sedimentation of drilling mud solids are available. However, an accurate prediction of the transport can not be made if the flocculation of drilling muds, the settling speeds, and the effective densities (known as the physical properties) of the resulting flocs are not well understood and not incorporated into the hydrodynamic model. This is because the solid particles in drilling muds are very fine, usually in the silt or clay range (a few microns in diameter); after being discharged into the ocean, these fine particles generally do not exist as individual particles, but rather as flocs. The sizes of flocs may be several hundred microns, and the settling speeds and effective densities of these flocs are quite different from the fine solid particles from which these flocs are made. Field tests of drilling mud discharges performed by Ayers *et al* (1982) indicated rapid flocculation and aggregate settling. It is obvious that both the short-term and the long-term transport of discharged drilling muds are greatly influenced by the flocculation process as well as by the settling speeds of the flocs formed in this process.

Following the initial mixing and passive diffusion, though some particles will remain and be dispersed in the water column, significant amounts of drilling muds will generally deposit on the sea bed. This is called the initial sedimentation and results in a layer of drilling mud over the natural sediments. The thickness and covered area of this drilling mud bed depend on the local environmental conditions such as water depth, currents, waves, density stratification, discharge

conditions such as rate and total amount of discharges, and the dynamics of initial mixing, passive diffusion, flocculation, and settling. The drilling mud bed may later be resuspended due to the turbulent shear stress on its surface due to currents and waves. The resuspended particles will be transported away from the discharge site by ocean currents and will then generally deposit again depending on the local environmental conditions. Therefore, the resuspension properties of drilling mud beds are very important parameters in the prediction of the long-term transport.

Although, as mentioned above, the transport properties of drilling muds are very important in the accurate prediction of both the short-term and the long-term transport of ocean disposed drilling muds, to our knowledge, no laboratory studies on this subject using real drilling muds have been reported. Only Xu (1988) has done some experiments using pure barite and bentonite, the major components of drilling muds.

This study focuses on the transport properties of ocean disposed drilling muds. The material used in the study was a used drilling mud from a platform in the Santa Barbara Channel. Table 1-1 shows the components of this drilling mud (Johnson, 1992). Excluding water, approximately 65% of the mud is barite and 30% is bentonite, while the rest consists of small amounts of additives. The properties of resuspension, flocculation, settling speeds, and effective densities for this drilling mud were determined from extensive experiments using an annular flume, a Couette flocculator, disc flocculators, and a settling tube.

Table 1-1 Components of the drilling mud used in this study

Components	Weight (lb/bbl)	Generic description
Water	335.4	
Barite	46.9	
Therma-Thin	1.15	
Drispac (starch)	1.8	Polyanionic cellulose
Caustic	0.25	
Barabrine (60 % alcohol)	0.4	Alcohol based defoamer
Aquagel	21.50*	Bentonite

* This measured value includes some formation clays that enter the mud system
   during drilling operations.

The significance of the present work is an improvement of our understanding of the transport properties of drilling muds; one of the applications of the results is to provide some important parameters (such as the net resuspension, floc size distribution, and settling speeds) for the numerical modeling of the transport of drilling muds discharged from oil platforms in the Santa Barbara Channel and in the Gulf of Mexico as well as elsewhere.

Detroit River Sediments

The transport properties of Detroit River sediments have been extensively studied by Lick and Lick (1988), Tsai *et al* (1987), and Burban *et al* (1989, 1990). However, they did not examine flocculation due to differential settling and the effects of natural organic coatings on flocculation. To extend their experiments, we performed experiments using disc flocculators in which flocculation was dominated by differential settling. In addition, some samples were treated using sodium hypochlorite to remove the organic coating. Both the treated and untreated samples were tested, so that the effects of the natural organic coating on flocculation and settling speeds, as well as on effective densities were examined.

Outline

In the following section, previous work is reviewed. Although, as mentioned above, no laboratory work on the transport properties of real drilling muds has been done before, many studies on the resuspension, flocculation of fine-grained sediments, and the settling speeds and effective densities of flocs have been made in many different fields such as natural sediment transport, water purification, and waste water treatment. Achievements from these studies provide useful information related to the present study.

The description and findings of the present study are presented in Section 3 through Section 6. Section 3 describes the resuspension experiments performed in an annular flume. Section 4 describes the flocculation experiments using Couette and disc flocculators. The effects of organic coatings on the flocculation properties of sediments are also discussed in Section 4. Section 5 describes the experiments to determine settling speeds. Section 6 discusses the effective densities of flocs. Finally, Section 7 discusses and summarizes the main findings from the present study.

2. PREVIOUS WORK

Resuspension

Resuspension properties of fine-grained sediments are important in predicting the transport of these sediments. Fine-grained sediments are characterized by their cohesive nature which is strongly dependent on the attractive electro-chemical surface forces between particles; these forces are different from one sediment to another. Because of this, the transport properties of a sediment can not be predicted from physical properties such as particle size distribution and density of the sediment, and must be determined experimentally.

In experimental studies of the resuspension properties of cohesive sediments in flumes or other devices, a sediment bed must be prepared in some manner. Two different kinds of sediment beds can be distinguished. One is called the placed bed and is produced by placing the sediment in the apparatus manually or by pouring a pre-prepared slurry. The shear strength of the placed bed remains relatively invariant over depth.

The other kind of bed is called the deposited bed and can be produced by allowing a fully mixed sediment suspension to settle and consolidate. The shear strength of the deposited bed varies more with depth, because the sediments near the surface are fine and less compacted, while the sediments further down are coarser and more compacted. For a constant applied shear stress, the rate of resuspension of such a bed decreases with time, and only a finite and relatively small amount of sediment can be resuspended (Massion, 1982; Tsai and Lick, 1987). Generally speaking, the upper portion of a sediment bed in natural water bodies can be represented by the deposited bed.

For cohesive sediments from lakes or oceans, experimental work (Krone, 1962; Partheniades, 1972; Mehta, 1973; Lee *et al*, 1981; Kusuda *et al*, 1984; Lick and Kang, 1987; Tsai and Lick, 1987; MacIntyre *et al*, 1990; Xu, 1991) has revealed that the resuspension rate and the total amount of sediment that can be resuspended at a particular stress are a function of the turbulent stress at the sediment-water interface and the consolidation period (or the water content) of the sediments. In addition, other parameters such as temperature, salinity, cation exchange capacity (CEC), the sodium adsorption ratio $SAR = Na^+ / [0.5(Ca^{++} + Mg^{++})]^{1/2}$, and organisms also affect the resuspension properties (McCave, 1984), though their effects may be less important than those of stress and consolidation period.

An empirical formula for resuspension as a function of fluid shear stress and bed consolidation period for a deposited bed was proposed by Lick (1989) as:

$$\epsilon = \frac{a_o}{t_d^n}(\tau - \tau_c)^m \qquad\qquad \tau > \tau_c \qquad\qquad\qquad (2\text{-}1)$$

$$\epsilon = 0 \qquad\qquad\qquad\qquad \tau \leq \tau_c$$

where ϵ is the resuspension in mg/cm^2, τ and τ_c are the shear stresses of the flow at the water-sediment interface and the effective critical stress respectively, both in $dynes/cm^2$, t_d is the consolidation period in *days*, and a_0, *m,* and *n* are coefficients to be determined by experiments. The determination of these coefficients was discussed by Xu (1991).

Although, as mentioned in Section 1, resuspension properties are very important for the prediction of the transport of drilling muds in the ocean, no experimental studies on these properties have been reported. Xu (1991) did resuspension tests in an annular flume using pure bentonite, one of the major components of drilling muds. However, usually only about 10 percent of a drilling mud is bentonite. Therefore, the resuspension properties of drilling muds may not be dominated by bentonite.

Flocculation

General
The study of the flocculation of fine particles is of significance in many fields, such as waste water treatment, water purification, ocean disposal of particulate wastes, and sediment transport.

Generally speaking, flocculation results when two or more particles collide and adhere. This means that flocculation involves: (a) fluid mechanic aspects, i.e. the transport mechanisms to bring particles into close proximity, leading to collisions between particles; and (b) coalescence mechanisms of physics, chemistry, and biology.

The transport mechanisms involved in flocculation are: (1) Brownian motion, (2) fluid shear due to laminar or turbulent flow, and (3) differential settling of particles. Among these three mechanisms, Brownian motion is important only for particles less than about 1 μ*m*, which is generally not the situation for typical fine-grained sediments (in the clay and silt size ranges). The importance of differential settling depends on the differences of settling speeds of particles. Fluid shear is often the dominant mechanism for typical fine-grained sediments.

The coalescence mechanisms include short-range interfacial forces (such as hydrodynamic forces, electrostatic forces, and van der Waals' force), steric interaction, and polymer bridging.

At a fundamental level, flocculation can be analyzed by the collision rate theories originally developed by Smoluchowski (1917). Smoluchowski's rate theory assumes binary collisions between particles and no break-up of flocs into discrete particles. The main parameters (rate coefficients or collision-frequency functions) in the floc growth expressions are well understood for each of the transport mechanisms (i.e. Smoluchowski, 1916, for Brownian motion; Smoluchowski, 1917, for laminar shear; Camp and Stein, 1943, for turbulence in the viscous subrange; Saffman and Turner, 1956, and Amirtharajah and Trusler, 1986, for turbulence in the inertial subrange; Findheisen, 1939, for differential settling). Because of the no breakage assumption, however, the rate theory is only valid for the early stage of flocculation, when the rate of floc break-up is very small in comparison with the rate of floc growth.

In fact, flocculation is a dynamic process in which the growth of flocs as well as the breakage of these flocs continuously take place, particularly for the flocculation due to fluid shear. Argaman and Kaufman (1970) developed a floc break-up rate theory to model the flocculation and de-flocculation process in a turbulent flow. This theory gives a floc break-up rate expression similar to the floc growth rate expression. More general dynamic equations incorporating floc growth and break-up have been given by several investigators, such as Jeffrey (1982), Tsai *et al* (1987), and Lick and Lick (1988) for flocculation due to fluid shear. However, the breakup rate coefficients in the break-up rate expressions are difficult to determine from experiments (Hunt, 1986).

Although the rate theory as well as its extensions provides a fundamental description of flocculation, the flocculation properties of a sediment are not predicted by the rate theory. This is because the coalescence mechanisms are strongly dependent on the type of the sediment and on the ambient water; these can not be determined without experiments. Therefore, experimental studies of flocculation are essential for understanding the flocculation properties of sediments.

Experimental work on flocculation in the areas of sediment transport and sedimentation for natural sediments or sewage sludge has been conducted by many investigators such as Krank (1975), Edzwald *et al* (1974), McCave (1975), Krone (1978, 1986), Hunt (1980,1982), Hunt and Pandya (1984), Eisma (1986), Fancy and Morel (1986), Morgan and Lovorn (1986), Gibbs *et al*

(1986, 1989), Tsai *et al* (1987), Lick and Lick (1988), and Burban *et al* (1989). However, studies of the flocculation of drilling muds are almost nonexistent. Only Xu (1987) conducted some flocculation tests using a Couette flocculator for barite and bentonite, the main components of drilling muds.

Flocculation due to Fluid Shear
Fluid shear is often large near the sediment/water interface, in shallow, near-shore areas, and in drilling mud plumes (jets) during the initial mixing process. In these situations, among the three collision mechanisms (Brownian motion, fluid shear, and differential settling) involved in flocculation, fluid shear dominates the flocculation for medium size particles such as fine-grained natural sediments as well as drilling muds.

To study flocculation due to fluid shear, two kinds of flocculators are usually used. One is the Couette type flocculator. The other one is the blade type flocculator. The advantage of the former is that the fluid shear generated by this device is well defined and fairly uniform. The laminar flow in a Couette flocculator is usually maintained during a flocculation test, while most flows in the near shore regions of oceans or lakes are turbulent. However, as long as the floc size is less than the size of the smallest eddies, the flocculation properties in a laminar flow can be related to those in a turbulent flow by relating laminar shear to the effective turbulent shear G_e as follows (Camp and Stein, 1943):

$$G_e = \left(\frac{\epsilon}{\nu}\right)^{1/2} \qquad\qquad d_p \leq \eta \qquad\qquad\qquad (2\text{-}2)$$

where ϵ is the turbulent energy dissipation rate, ν is the kinematic viscosity of the fluid, d_p is the particle diameter, and η is the Kolmogorov microscale length defined by:

$$\eta = \left(\frac{\nu^3}{\epsilon}\right)^{\frac{1}{4}} \qquad\qquad\qquad\qquad (2\text{-}3)$$

For estuaries and coastal seas, the estimated smallest eddies are on the order of a few millimeters (Eisma, 1986). Since the sizes of flocs produced in the Couette flocculator in the present study are less than 500 μm, the above relation is generally valid and the results obtained from the Couette flocculator can be related to turbulent flows.

On the other hand, the flow in a blade type flocculator is turbulent but far from isotropic with very high shears near the edges of blades which may dominate the flocculation and de-flocculation processes. An average shear can be estimated using a similar relation to Eq.(2-2).

Flocculation due to Differential Settling
When fluid shear or turbulence is very low, for example in the open lake or ocean away from shore, differential settling may become the governing mechanism for flocculation. Although the flocculation due to differential settling can be significant, no experimental studies on it have been reported. This may be due to the difficulty in the design of an appropriate device to mimic and measure the flocculation purely due to differential settling. In other words, it seems that an infinitely long settling tube is needed, which makes it impossible in practice.

This difficulty has been recently solved by the design and use of disc flocculators, which will be described in detail later. Three disc flocculators with different sizes have been used in the present study. The fluid in a disc flocculator rotates as a rigid body. The particles in the disc flocculator keep settling due to gravity and at the same time are kept from settling out by the rotating fluid. To a good approximation, the particles are then settling in an infinitely long settling tube; the flocculation in a disc flocculator is governed by the differential settling of particles, and no applied fluid shear is involved.

Effects of Organic Coatings on Flocculation
Natural sediments are usually coated by some organic matter. Gibbs (1977) reported the existence of organic coatings on all the clay size fractions in rivers and estuaries. It is widely accepted that the surface electrical properties of aquatic particles are strongly affected by adsorbed organic compounds, particularly humic substances (Beckett and Ngoc, 1990). Subsequently, the electrical double-layer property of a particle undergoes changes. The van der Waals' force between particles is also modified by the organic coating (Gregory, 1983). Both of these result in the change of the flocculation properties of sediments.

The change of surface electrical properties of particles due to the natural organic coating has been studied by many investigators such as Neihof and Loeb (1972, 1974), Hunter (1980), Hunter and Liss (1982), and Beckett and Ngoc (1990). The electrophoretic mobility (or zeta potential) of particles is found to be low when the surfaces of these particles are coated with natural organic matter (Hunter and Lisa, 1982; Gregory, 1989; Beckett and Ngoc, 1990).

Gibbs (1983) measured the effects of natural organic coatings on flocculation from tests in Couette and blade-type flocculators using Amazon River material with and without organic coatings. Jekel (1986) examined flocculation in the presence of humic acids from tests in a stirred cell using silica and kaolinite particles. These studies indicated that the coated material flocculated significantly slower than the uncoated samples. However, the effects of organic coatings on flocculation are not well understood at the present time and much work is needed to improve our knowledge in this area.

Settling Speeds of Flocs

As mentioned in Section 1, the settling speeds of flocs are important in modeling the transport of fine-grained sediments. For solid spherical particles and low Reynolds numbers (Re < 1), the settling speed can be obtained from Stokes' law. However, the settling speeds of flocs generally can not be predicted by Stokes' law because the factors affecting settling speed, such as the floc density, surface roughness, and shape irregularity, are not included in Stokes' law, are generally unknown, and are strongly dependent on the floc size as well as the conditions under which the flocs are formed. Therefore, the settling speeds of flocs must be determined experimentally.

The settling speeds of flocs made from a variety of materials have been studied by many investigators, such as Gibbs (1985a) for flocs of illite, kaolinite, and montmorillonite; Matsumoto and Mori (1975) for bentonite and alum flocs; Li and Ganczarczyk (1987) for activated sludge flocs; Kajihara (1971), Kawana and Tanimoto (1976, 1979), Chase (1979), Hawley (1982), and Alldredge and Gotschalk (1988) for marine aggregates; Gibbs (1985b) for

estuarine flocs; Tambo and Watanabe (1979) for alum flocs; and Burban *et al* (1990) for river and lake sediment flocs. However, the study of the settling speeds of drilling mud flocs has not been reported.

Usually, the data on floc settling speeds as a function of floc size are approximated by a power expression:

$$w_s = A d_f^m \qquad\qquad\qquad\qquad (2\text{-}4)$$

where d_f is the floc size (diameter), and A and m are empirical constants which depend on the type of the materials from which the flocs are made and the conditions under which the flocs are formed (Burban *et al*, 1990).

All studies mentioned above, except Burban *et al* (1990), do not consider the effects of floc formation conditions, such as fluid shear and sediment concentration, on the floc settling speeds. Burban *et al* (1990) have found that the settling speed of a floc is a function of fluid shear and sediment concentration as well as the size of the floc; for the same size, flocs formed at lower fluid shears and sediment concentrations have lower settling speeds than do the flocs formed at higher fluid shears and sediment concentrations.

Effective Densities of Flocs

Flocs typically have a tenuous and loose porous structure. Because of the highly porous structure, the average density of a floc is often much less than that of the solid particles from which the floc is made and often close to that of the ambient water. Moreover, the density of a floc is strongly dependent on the floc size. This makes the major contribution to the deviation of the settling speed-size relationship from Stokes' law.

In order to get some insight into floc structure, a determination of the average density of a floc is useful. However, to discuss the nature of floc density, the average relative density $\Delta\rho_f$ is more often adopted than the average density. The average relative density of a floc is defined as the excess value of the average density of the floc over that of the ambient water. That is:

$$\Delta\rho_f = \rho_f - \rho_w \qquad\qquad\qquad\qquad (2\text{-}5)$$

where ρ_f is the average density of a floc and ρ_w is the density of the water.

Experimental studies on the floc density-size relationship have been performed by many investigators for flocs formed from a variety of materials, such as Lagvankar and Gemmell (1968) for $Fe_2(SO_4)_3$ flocs; Matsumoto and Mori (1975) for bentonite and alum flocs; Magara *et al* (1976) and Li and Ganczarczyk (1987) for activated sludge flocs; Glasgow and Hsu (1984) for kaolin-polymer flocs; Gibbs (1985a) for clay flocs; Tambo and Watanabe (1979) for alum flocs; Weitz and Oliveria (1984) for gold colloid flocs; Klimpel and Hogg (1986) for pure quartz flocs; Gibbs (1985b) for estuarine flocs; and Kajihara (1971), McCave (1975) Hawley (1982), and Alldredge and Gotschalk (1988) for marine aggregates. These studies have shown that a power

17

law for the floc relative density-size relationship is approximately valid, but only over a limited range of floc sizes.

In the experimental studies mentioned above, three methods were used in the determination of the floc density. One of these three methods is the equivalent density method (Lagvankar and Gemmell, 1968; Gibbs, 1985a, b). This method is based on the principle that if the density of a floc is equal to the density of the solution in which it is suspended, it will not sink or rise. However, this is not generally a usable method because the measurements must be made in a matter of seconds; the pore water of a floc is quickly replaced by the standard density solutions, thereby changing the floc density (Gibbs, 1985a, b).

Matsumoto and Mori (1975) measured floc densities by using the Oden balance method and photo-extinction method simultaneously; this assumes that the relationship between the size and settling speed of flocs is known. However, this method has not been used by others.

The most frequently used method for floc density measurements is an indirect method. The floc size and settling speed are first measured in a settling tube. Assuming that the settling of each individual floc satisfies Stokes' law, an effective relative density $\Delta\rho_f$ of a floc is defined by and determined from:

$$\Delta\rho_f = \frac{18\mu}{g}\frac{w_s}{d_f^2} \tag{2-6}$$

where w_s is the floc settling speed, μ is the dynamic viscosity of water, and g is the gravitional acceleration (McCave, 1975; Magara *et al*, 1976; Tambo and Watanabe, 1979; Glasgow and Hsu, 1984; Gibbs, 1985a, b; Klimpel and Hogg, 1986; Li and Ganczarczyk, 1987).

The density obtained in this way is an effective relative density (in short, called effective density hereafter). This effective density is only an approximation to the true relative density of a floc because Stokes' law is only valid for solid (impermeable) spheres, while flocs are porous (permeable) particles. Since a floc is a highly porous structure, the ambient fluid will penetrate the floc; the settling speed of the floc is therefore higher than that of a solid particle with the same size and the same average density as the floc (Ooms *et al*, 1970; Neale *et al*, 1973; Matsumoto and Suganuma, 1977; Masliyah and Polikar, 1980).

3. RESUSPENSION

The resuspension properties of a used drilling mud from a platform in the Santa Barbara Channel were determined from experiments in an annular flume. Although, as mentioned in Section 2, several parameters, such as temperature, salinity, CEC, SAR, organisms, as well as fluid shear stress and bed consolidation period, affect the resuspension properties, the latter two parameters are most important. Therefore, the emphasis here is placed on the effects of shear stress and con-solidation period.

In this section, we first describe the experimental methods and apparatus. Then we present the data, the empirical equation obtained by fitting the data, and the comparison of the resuspension properties of the drilling mud with those of Green Bay and Fox River sediments and bentonite.

Experimental Methods

Annular Flume

The annular flume used in the resuspension experiments is 2 m in diameter; the annular channel is 0.15 m in cross-section and 0.21 m high (Fig.3-1). A rigid lid fits inside the channel and just touches the top of the water in the channel. The distance between the lid and the surface of the sediment bed on the bottom of the channel is adjusted to 7.62 cm. This lid is driven by an adjustable speed motor; a Couette-type turbulent flow is produced in the channel through the friction exerted on the surface between the rotating lid and the water.
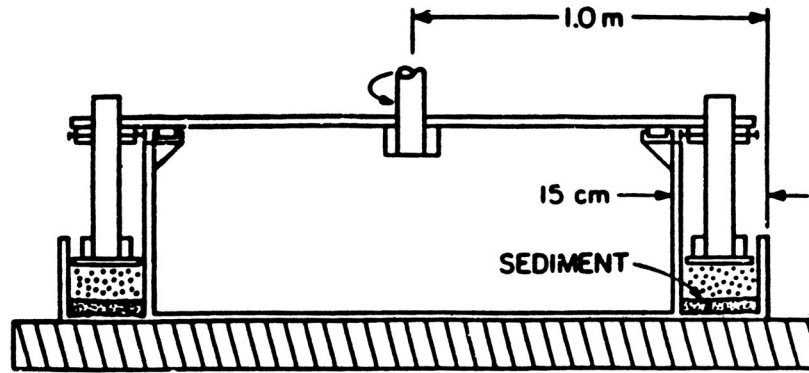
Fig.3-1 A schematic of the annular flume

The fluid shear stress on the surface of the sediment bed can be determined from the velocity profile with the assumption that the flow is a fully developed turbulent flow with the average velocity varying only in the vertical direction; in this case, the logarithmic profile of velocity is valid and is given by:

$$u_z = \frac{u_*}{k}\ln(\frac{zu_*}{v})+5.56 \qquad (3\text{-}1)$$

where u_z is the horizontal velocity at a height z, v is the kinematic viscosity of the fluid, k is von Karman's constant, and u_* is the friction velocity. The shear stress on the surface of a sediment bed is related to u_* by:

$$\tau = \rho u_*^2 \qquad (3\text{-}2)$$

where ρ is the density of the fluid.

This flume has been calibrated by MacIntyre *et al* (1990). They used a one-dimensional laser-Doppler velocimeter (LDV) in backseatter mode to measure the velocity profiles and obtained a relationship between the shear stress and the rotation rate of the lid.

It should be noted that, in the channel, the shear stress varies in the radial direction by as much as a factor of two at the higher rotation rates. The average value of the shear stress is used in the stress-rotation rate relationship (MacIntyre *et al*, 1990). In addition, a secondary flow is present in the channel. The circulation induced by the secondary flow is inward near the bottom, upward near the inner wall of the flume, outward near the lid, and downward near the outer wall. Dye and hot-wire experiments by Fukuda (1978) showed that the secondary flow is small compared to the primary azimuthal flow. Deardorff and Yoon (1984) performed extensive radial and azimuthal velocity measurements in an annular flume comparable in dimensions and operating principle to the flume used here. Their results support Fukuda's contention that the contribution of the radial velocity to the bottom shear stress is minor.

Procedure

The first step in an experiment was to prepare the drilling mud bed. An appropriate amount of drilling mud was put in the channel and mixed with natural sea water (from the Santa Barbara Channel); the solids were fully resuspended and uniformly dispersed using a stirring disc. Then the suspension was allowed to settle and consolidate for a desired period (e.g., 1, 2, 3, 7, or 30 days) to form a drilling mud bed. The height of this bed varied from 5 cm to 7 cm depending on the consolidation period. If a bed was higher than 7 cm, some drilling mud was taken out of the channel; if lower than 5 cm, some drilling mud was added. After this, the drilling mud was resuspended and allowed to settle again. The bed formed in this way is known as a deposited bed.

To start an experiment, the lid was slowly accelerated to the rate of rotation corresponding to the desired shear stress on the bed and kept at this rate for a period of time (usually about 2 hours). During this period, several samples at different times were withdrawn from a port on the outer wall of the channel. These samples were filtered, dried, and weighed to determine the solid concentrations in the overlying water. At the beginning of the experiment, the solid concentration increased rapidly. However, as time went on, the rate of change of concentration decreased and the concentration eventually approached a constant value. Then the lid was accelerated to a higher rate and the same procedure was repeated. This kind of test is known as a multi-shear stress test; that is, a test at a higher stress is performed using the bed which has been already run at a lower stress. Tsai and Lick (1987) have demonstrated that the results of the net resuspension obtained from a multi-stress test are the same as those from a single-stress test for the same shear stress.

In addition, all experiments were carried out at room temperature ranging from 23 to 26 C and with the salinity of the sea water at 33.4.

Results and Discussion

Resuspension and Effective Critical Stress

Fig.3-2 shows a typical plot of the time variation of solid concentration from the multi-stress test. Usually the solid concentration reached a steady state within 1 hour. To ensure that the steady state had been reached, we ran experiments for 1.5 to 2 hours at each shear stress.
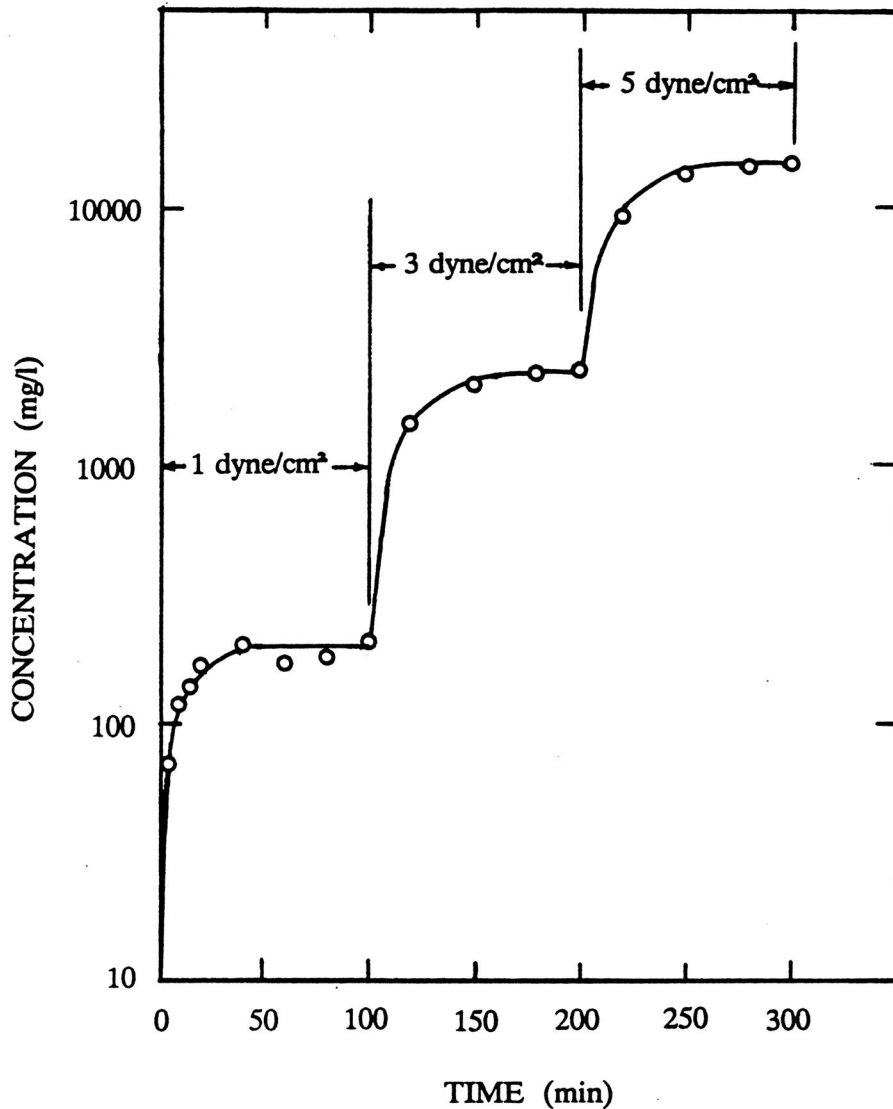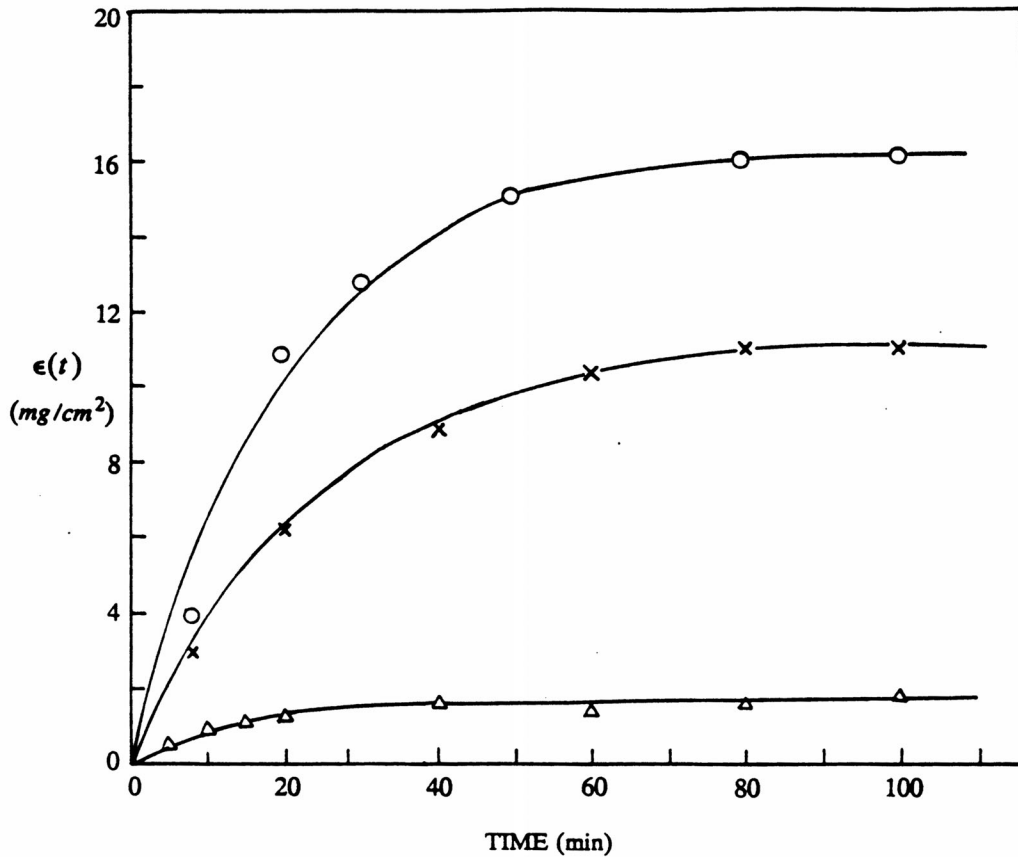

Fig.3-2 A typical plot of the time variation of solid concentrations from the muti-stress test for the drilling mud. Consolidation period $t_d = 2$ *days*

Fig.3-3 shows the typical plots of the time variation of resuspension ϵ (t), where ϵ (t) is the amount of material in resuspension at time t per unit area. ϵ is obtained from the following expression:

$$\epsilon(t)=C_m(t)h(t) \tag{3-3}$$

where C_m is the solid concentration in the overlying water in the channel and h is the water depth. h is initially adjusted to 7.62 cm and changes little at low shear stresses. However, at high stresses, large amounts of sediment are resuspended and the bed height is reduced significantly. In this case, the change of h must be taken into account.

Fig.3-3 Typical plots of the time variation of the drilling mud resuspension. $\triangle-t_d=1$ *days* **and** $\tau=1$ *dyne/cm*^{2} ; $\circ-t_d=7$ *days* **and** $\tau=3$ *dyne/cm*^{2} ; $\times-t_d=21$ *days* **and** $\tau=3$ *dyne/cm*^{2} .

We can see from Fig.3-3 that at the beginning, the rate of resuspension is very high. However, as time goes on, the rate of resuspension decreases, and eventually approaches zero as the steady state is reached.

Fig.3-4 and Table 3-1 show the data for the steady state resuspension ϵ_s (i.e., the total amount of sediment resuspended per unit area). To a reasonable approximation, ϵ_s represents the total amount of sediment which can be resuspended at a given stress (Tsai and Lick, 1987; MacIntyre *et al*, 1990).
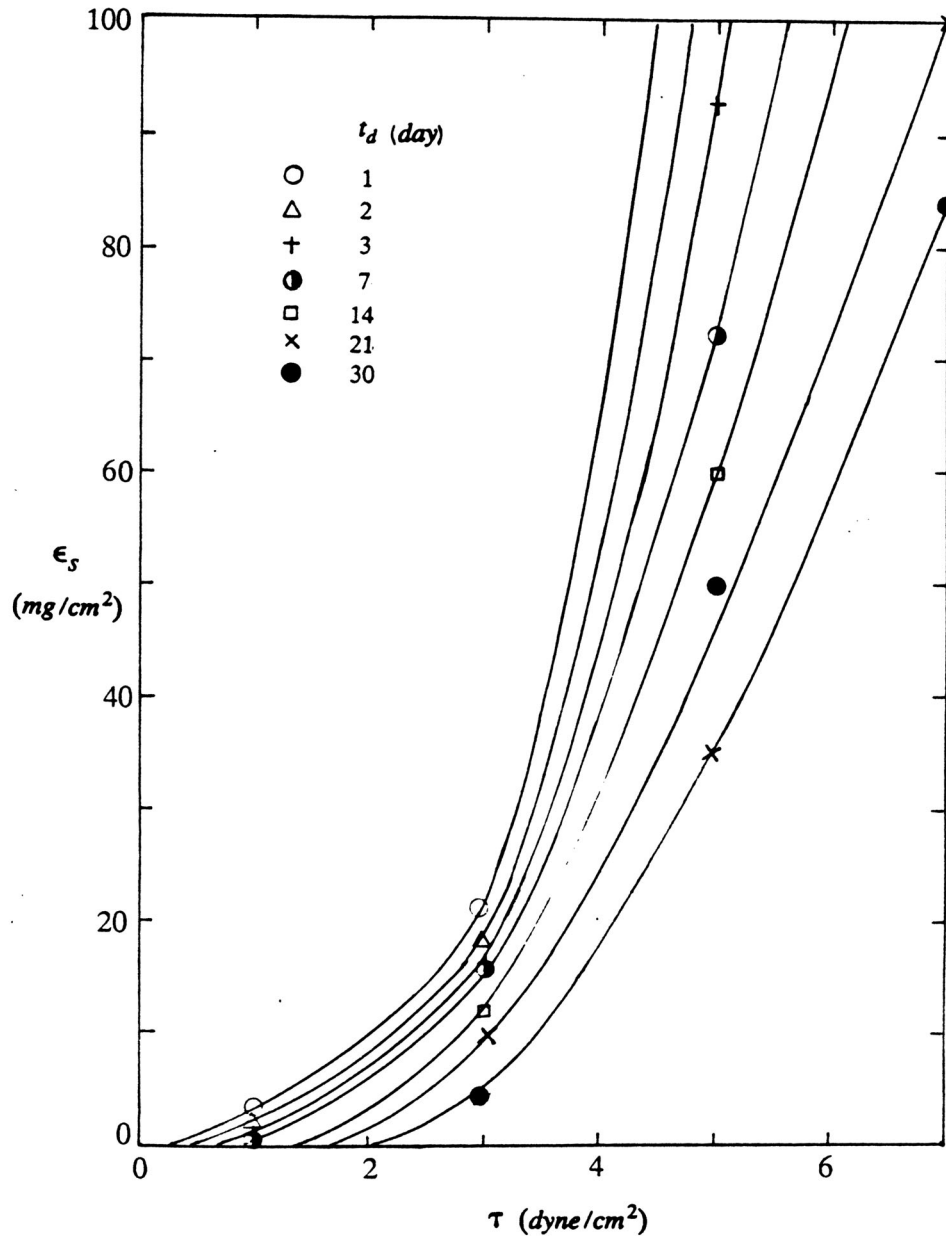
Fig.3-4 Resuspension of the drilling mud: experimental data and the best fitted lines for determining critical stresses

Table 3-1 Resuspension of the drilling mud (mg/cm^2)

Consolidation (days)	Shear stress ($dyne/cm^2$)			
	1	3	5	7
1	3.1	21.9	–	–
2	1.5	18.7	126.4	–
3	0.45	15.2	93.1	–
7	0.14	16.2	73.0	146.3
14	0.0	12.9	60.4	140.3
21	–	10.7	36.2	104.2
30	–	5.0	50.9	84.5

From Fig.3-4 and Table 3-1, we can see that ϵ_s is a strong function of shear stress and consolidation period. Generally speaking, the higher the shear stress and the shorter the consolidation period, the higher the resuspension. It is also noticed that no data were obtained for the 1 day consolidation beyond a stress of 3 $dyne/cm^2$, for the 2 and 3 day consolidation beyond 5 $dyne/cm^2$, and for the 7, 14, 21, 30 day consolidation beyond 7 $dyne/cm^2$. This is because in all these cases the drilling mud beds were either almost totally eroded or became very non-uniform. On the other hand, for the cases of 14, 21, and 30 day consolidation and a stress of 1 $dyne/cm^2$, the solid concentrations in the overlying water were too small to distinguish them from the background concentration, though some particles on the bed were seen to have been moved by the flow.

From Fig.3-4 we can estimate an effective critical stress by extrapolating a best fit line through the data points to the resuspension $\epsilon_s = 0$ axis; the corresponding value of the resuspension at $\epsilon_s = 0$ is considered to be the effective critical stress τ_c (Fig.3-5). If this extrapolation is valid, the physical meaning of τ_c is that, in a flume experiment, the solid concentration in the overlying water is just distinguishable from the background concentration at this stress. Some particles may have been resuspended even at a stress below τ_c, but this entrainment is too small to be considered of significance.

The extrapolation for τ_c (Fig.3-5) can be fitted by a power law as follows:

$$\tau_c = 0.28 \, t_d^{0.60} \tag{3-4}$$

where t_d is the consolidation period in *days,* and τ_c is in *dyne/cm²*. With Eq.(3-4), we replot the data such that the resuspension at steady state is a function of the excess shear stress $\tau - \tau_c$
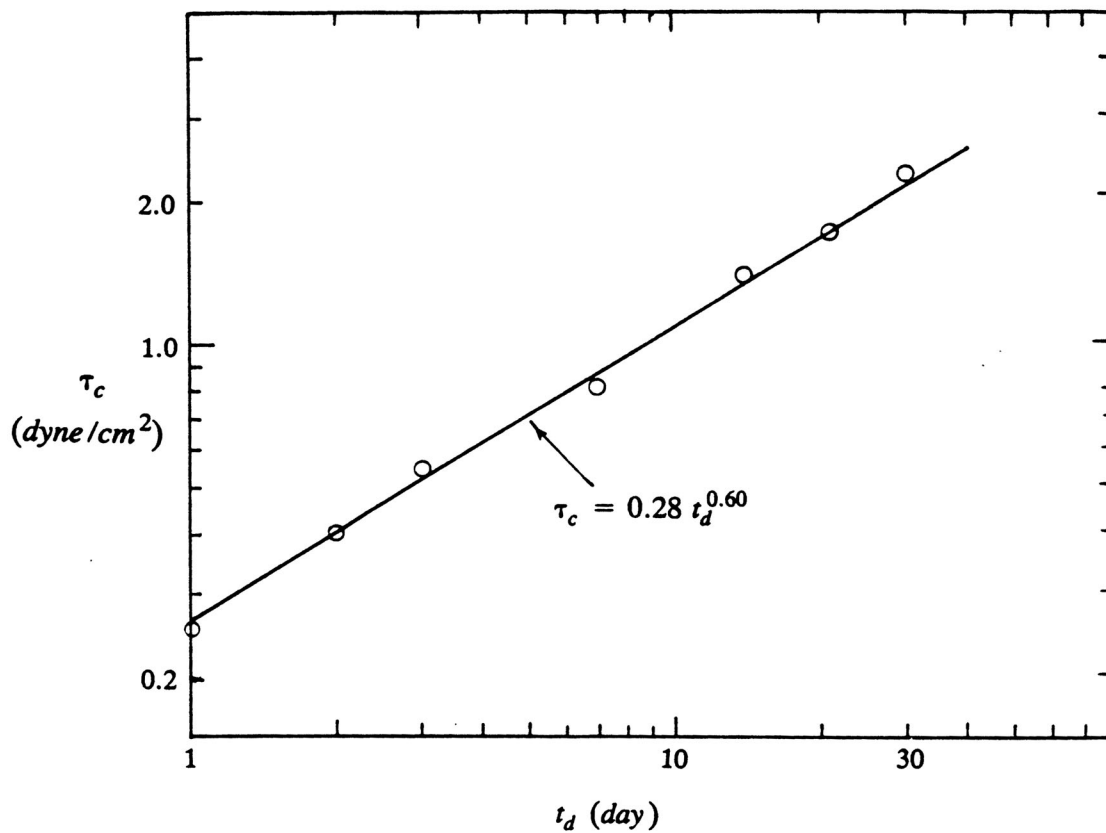
(Fig.3-6). The power law is also employed to regress the data and the expression can be written as:

$$\epsilon_s = 3.9169(\tau-\tau_c)^{1.984} \qquad \tau > \tau_c \qquad \text{(3-5)}$$
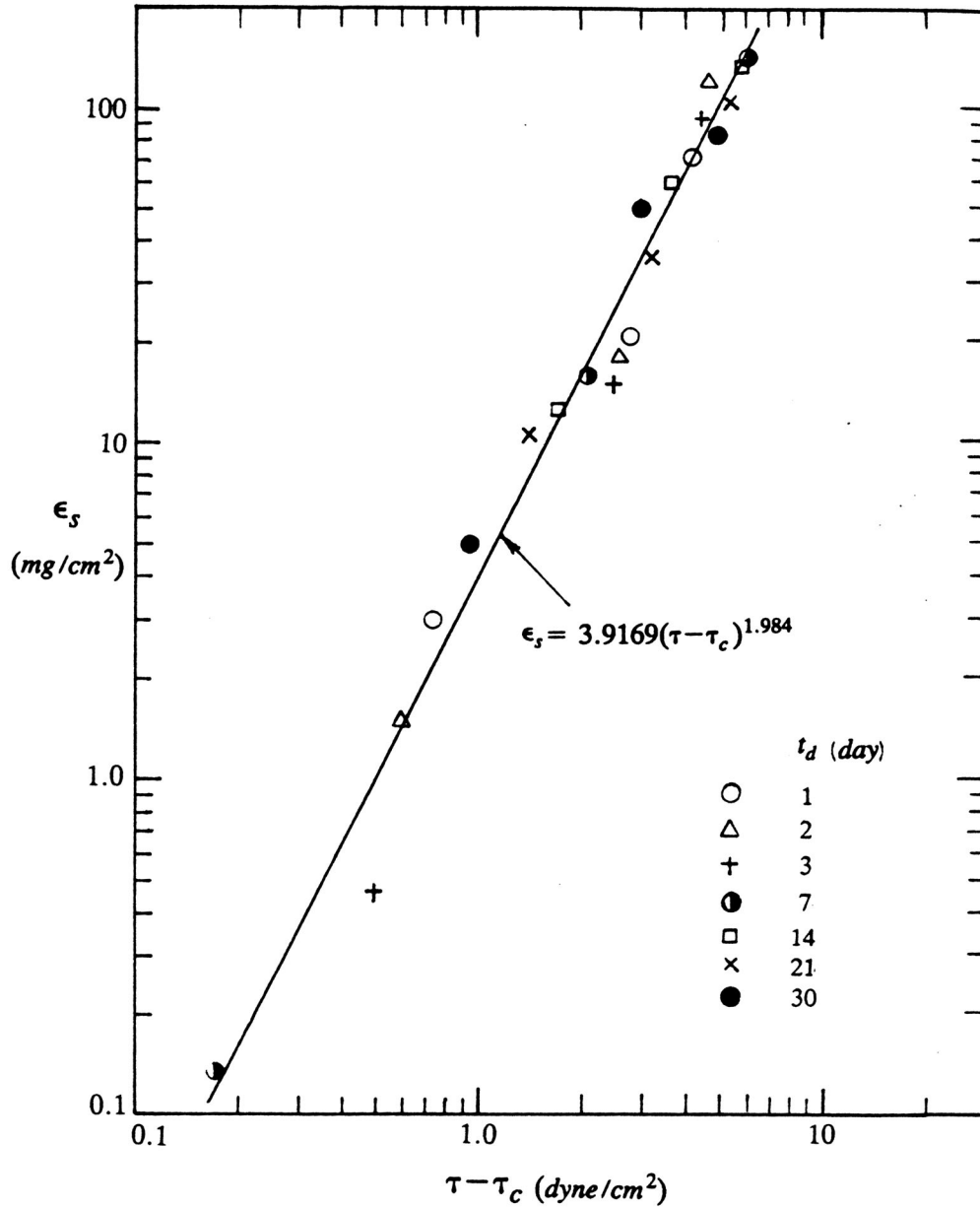
$$\epsilon_s = 0 \qquad \tau \leq \tau_c$$

where ϵ_s is in mg/cm^2 and stresses are in $dyne/cm^2$. The correlation coefficient is 0.9860.

It should be noted that Eq.(3-5) pertains to the drilling mud used in this study.

$$\tau_c = 0.28\, t_d^{0.60}$$

Fig.3-5 Critical stress-consolidation period relationship for the drilling mud

$$\epsilon_s = 3.9169(\tau - \tau_c)^{1.984}$$

	t_d (day)
○	1
△	2
+	3
◐	7
□	14
×	21
●	30

Fig.3-6 Resuspension-excess stress relationship for the drilling mud

Comparison

To compare the resuspension of the drilling mud with that of other sediments, we plot the best fit lines for the data of resuspension of the drilling mud and for Xu's (1991) data for Fox River sediments, Green Bay sediments, and bentonite (Figs.3-7 and 3-8). It can be seen from these figures that the resuspension of the drilling mud is less than that of bentonite by a factor of 2 to 2.5 and larger than those of Fox River and Green Bay sediments by a factor of 5 to 10. In

addition, we have found (data on the other sediments are not shown) that, at the same consolidation period, the effective critical stress of the drilling mud is larger than that of bentonite but smaller than those of Fox River and Green Bay sediments. This suggests that the drilling mud is much easier to resuspend than the natural sediments but more difficult than bentonite.
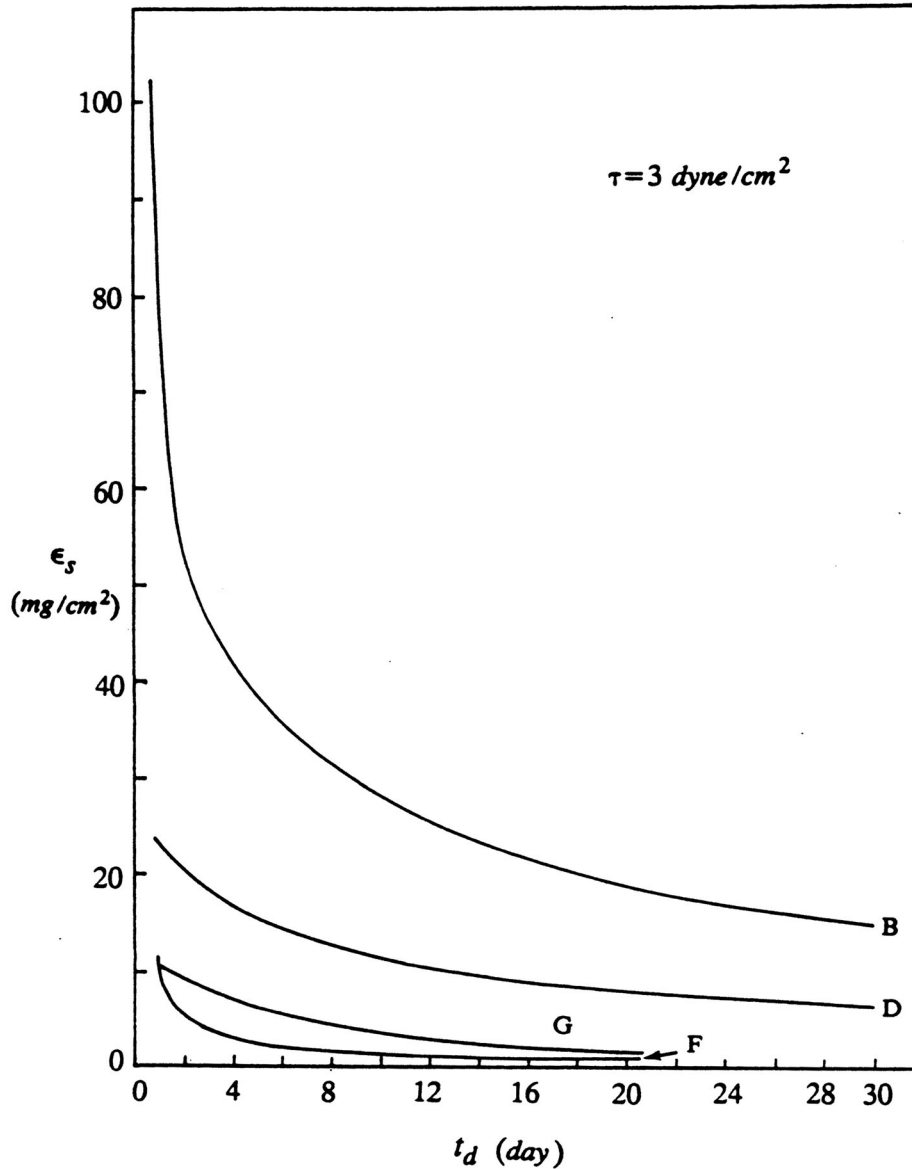
Fig.3-7 Comparison of the resuspension between different sediments. B-bentonite, D-drilling mud, G-Green Bay sediment, F-Fox River sediment. Stress $\tau = 3$ *dyne/cm²*
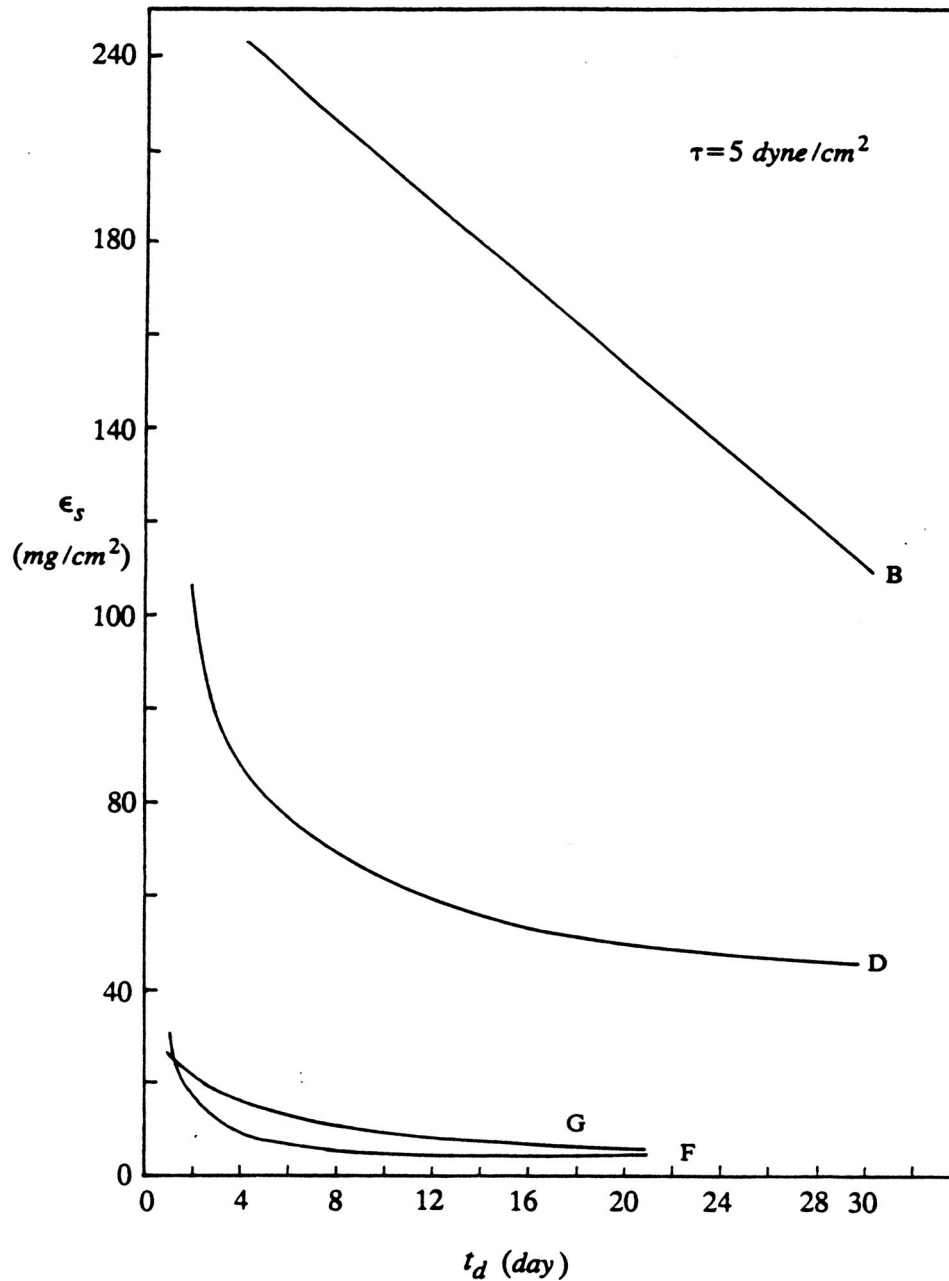
Fig.3-8 Comparison of the resuspension between different sediments. B-bentonite, D-drilling mud, G-Green Bay sediment, F-Fox River sediment. Stress $\tau = 5\ dyne/cm^2$

We may not be surprised by such differences in the resuspension properties of these sediments, because, as mentioned in Section 2, the resuspension properties are strongly dependent on the type of sediments. Differences in the particle surface electro-chemical properties, which were neither determined in this study nor in Xu's study, may make the major contribution to the differences in the resuspension properties of these sediments. Other factors, such as organic

matter, particle size and density, may also contribute to the differences (Table 3-2). We can see from Table 3-2 that, among these sediments, bentonite contains no organic matter and has the finest size and smallest density. This may account for the fact that bentonite is easiest to resuspend. Young and Southard (1978) have also found that in their experiments using natural marine muds, the effective critical stress increased with organic carbon content.

Table 3-2 Some properties of the sediments

Sediment	Organic matter* (% by weight)	Median size (μm)	Density (g/cm^3)
Drilling mud	1.77	9.0	2.65
Bentonite	0.0	7.0	2.20
Green Bay sediment	3.2	19.0"	2.65
Fox River sediment	–	22.0"	2.65

* The sum of organic carbon, hydrogen, and nitrogen.
" From Xu (1991).

For the drilling mud used in this study, we have presented the empirical formula for the resuspension (Eq.3-5) and for the effective critical stress (Eq.3-4). These formula are now written in a general form as follows:

$$\epsilon_s = A\,(\tau - \tau_c)^B \qquad \tau > \tau_c \qquad\qquad (3\text{-}6)$$

$$\tau_c = C t_d^D \qquad\qquad (3\text{-}7)$$

where *A, B, C,* and *D* are experimentally determined constants mainly depending on the type of sediments.

To examine the validity of these equations for other sediments, we plot Xu's data for Green Bay sediments and bentonite (Figs.3-9 and 3-10) in the form of ϵ_s versus $\tau - \tau_c$. The effective critical stresses are determined as follows:
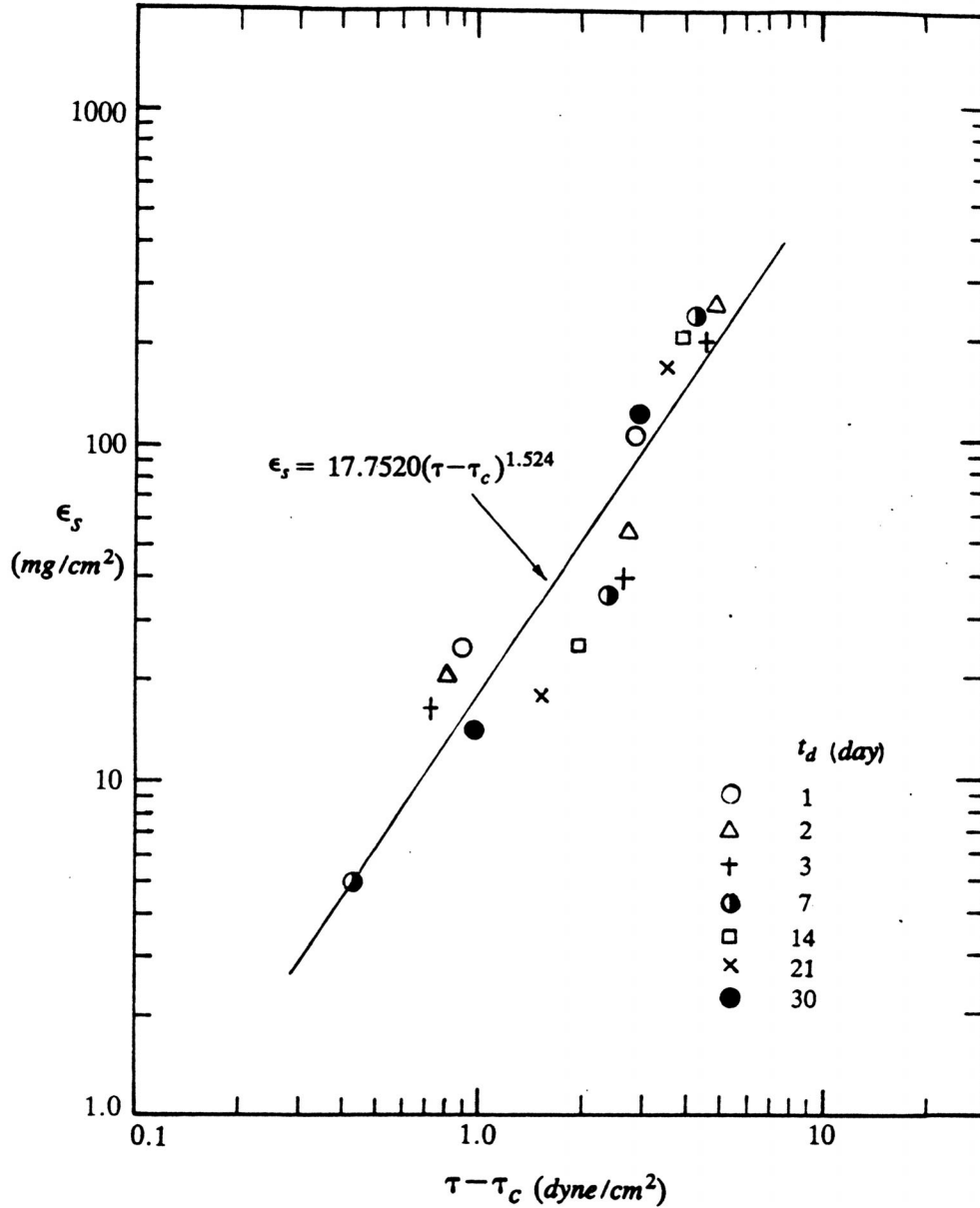
$$\tau_c = 0.6 t_d^{0.48} \qquad \text{for } Green\ Bay\ sediment \qquad\qquad (3\text{-}8)$$

$$\tau_c = 0.1 t_d^{0.884} \qquad \text{for } bentonite \qquad\qquad (3\text{-}9)$$

The best fit lines and the regression equations are also shown in Fig.3-9 and Fig.3-10. The correlation coefficients of the regression are 0.9807 for Green Bay sediment and 0.9265 for bentonite.
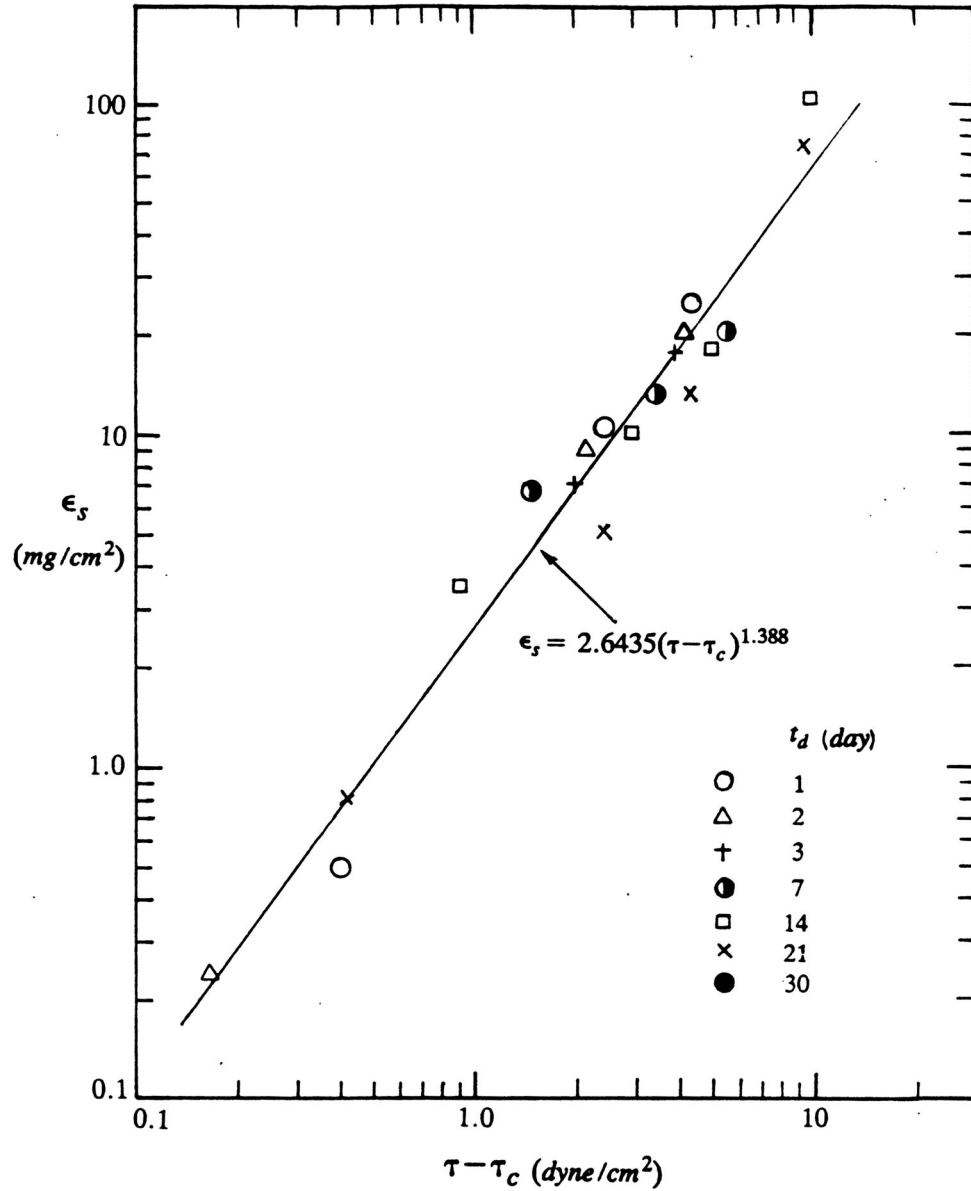
Fig.3-9   Resuspension-excess stress relationship for Green Bay sediment (data from Xu, 1990)

Fig.3-10 Resuspension-excess stress relationship for bentonite (data from Xu, 1990)

It should be mentioned that Eq.(3-6) is another version of Eq.(2-1) used previously. To use Eq.(2-1) to regress the data, τ_c is usually taken as a constant. In Figs.3-11 to 3-13, we plot the data shown above in the form of $\epsilon_s t_d^n \sim (\tau - 1.0)$ (i.e., $\tau_c = 1.0$ *dyne/cm^2*). From these plots, we have determined the coefficients in Eq.(2-1); they are $a_0 = 3.75,\ 1.461,\ 15.604$; $n = 0.35,\ 0.50,\ 0.57$; and $m = 2.5,\ 2.25,\ 2.68$ for the drilling mud, Green Bay sediment, and bentonite respectively.
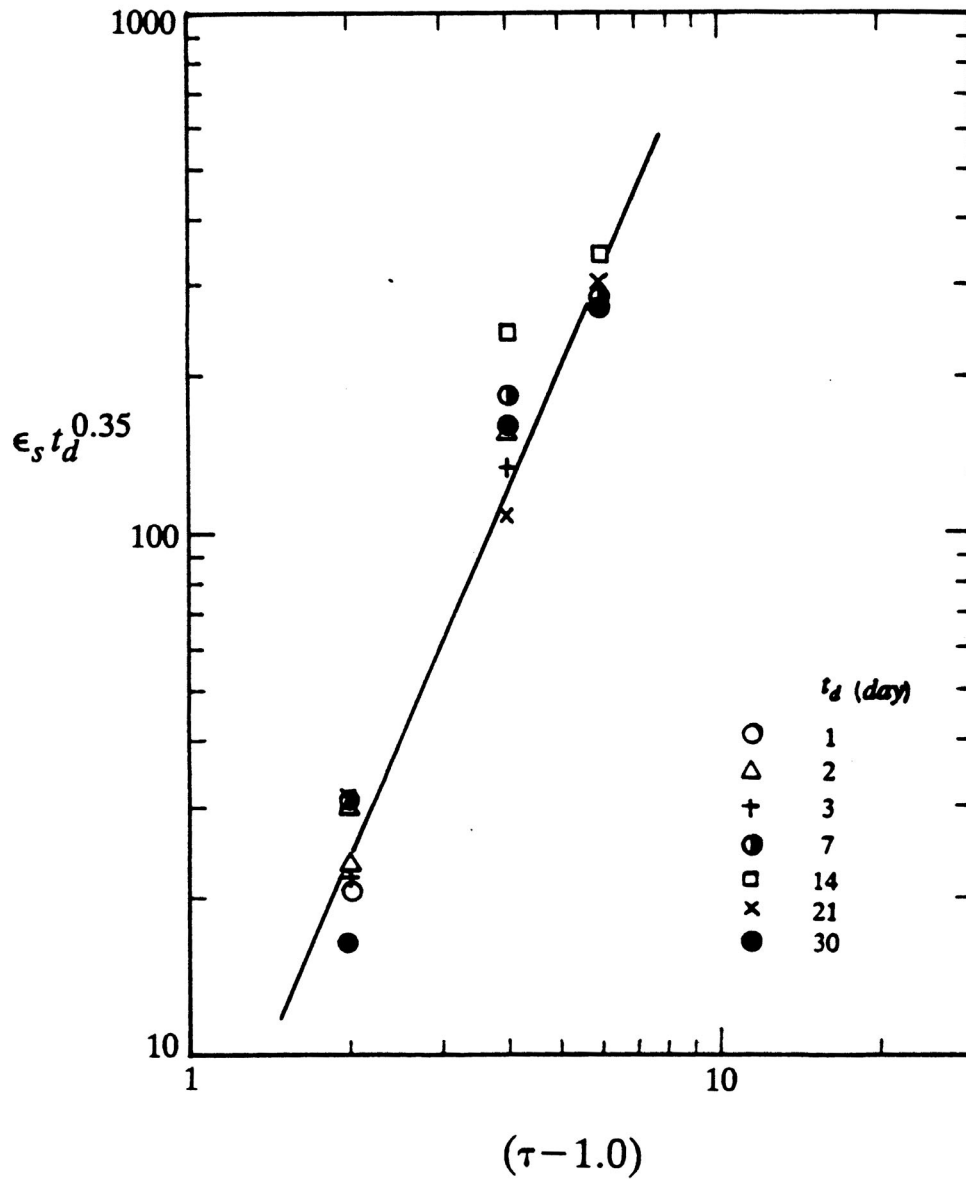
Fig.3-11 $\epsilon_s \sim (\tau - 1.0)$ **relationship for the drilling mud**
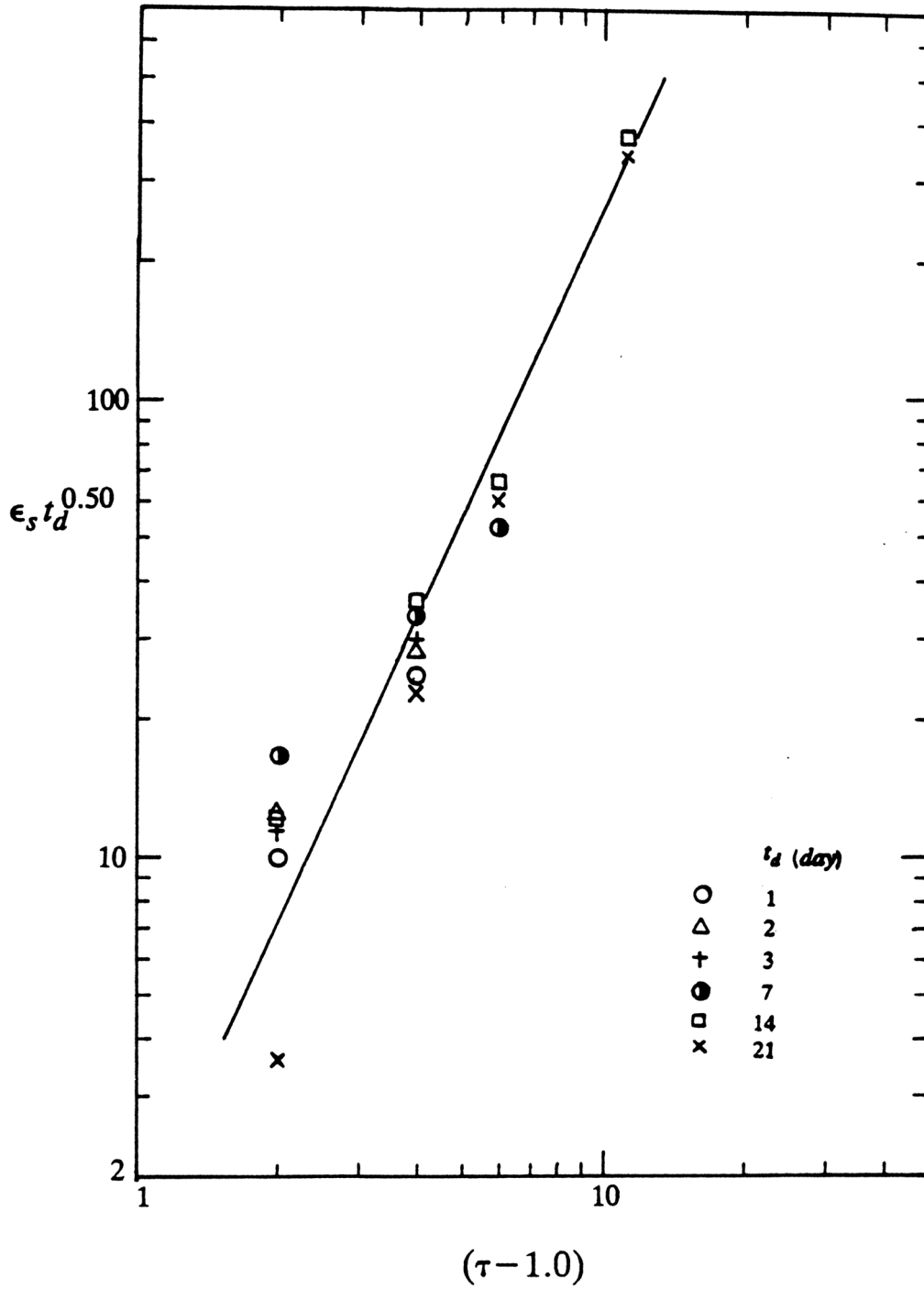
Fig.3-12 $\epsilon_s \sim (\tau - 1.0)$ **relationship for Green Bay sediment (data from Xu, 1991)**
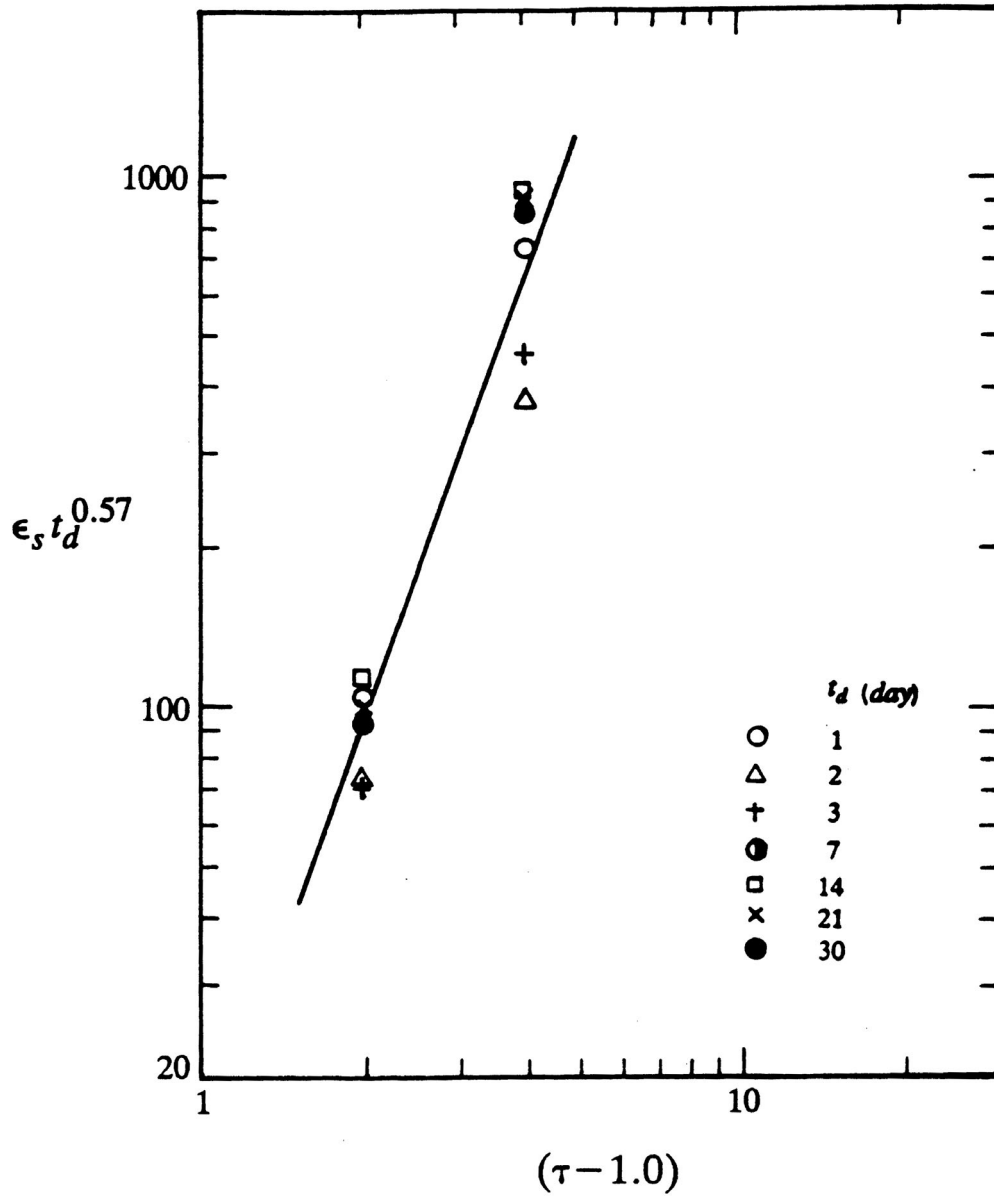
Fig.3-13 $\epsilon_s \sim (\tau - 1.0)$ **relationship for bentotine (data from Xu, 1991)**

4. FLOCCULATION

This section contains three parts. The first part is concerned with tests in a Couette flocculator which were made in order to examine the flocculation properties of the drilling mud due predominately to fluid shear. The second part is concerned with tests in disc flocculators which were made in order to examine the effects of differential settling of particles on flocculation. Both the drilling mud and Detroit River sediment were used in the disc flocculator tests. The third part is on the effects of organic coatings on flocculation. Both the drilling mud and Detroit River sediment samples were treated to remove organic matter and then used in the disc flocculator tests.

4.1 FLOCCULATION DUE TO FLUID SHEAR

In this subsection, we first describe the experimental methods. Results of the tests are then presented and discussed. Finally, a dimensional analysis is performed for the fluid shear dominated flocculation at steady state; the relationship between the flocculation characteristics and a nondimensional number is demonstrated.

Experimental Methods

Couette Flocculator

Fig.4.1-1 shows a schematic of the Couette flocculator used in this study. This flocculator consists of two concentric cylinders. The gap between the two cylinders is 2 mm. The diameter and length of the inner cylinder are 50 mm and 254 mm respectively, with a length to gap ratio of 125.
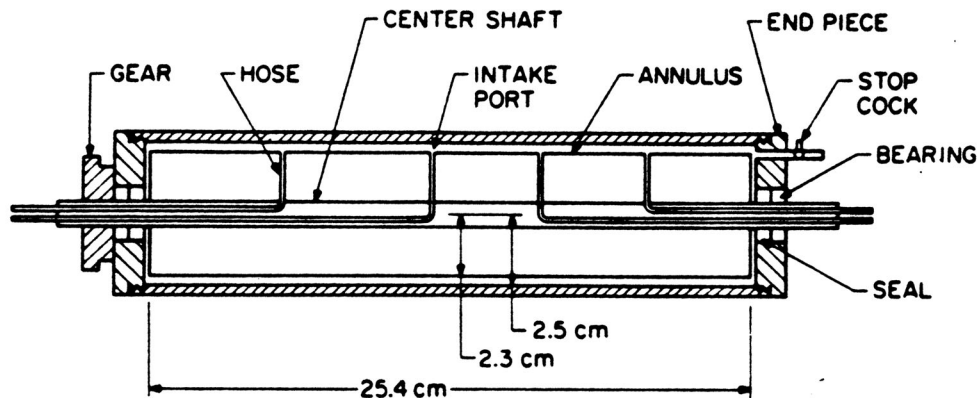
Fig.4.1-1 A schematic of the Couette type flocculator

The detailed analysis for the flow field in this type of device (also known as a Couette viscometer) can be found in the references by Taylor (1923, 1936), Van Duuren (1968), and Iacobellis (1984). The outer cylinder rotates at a constant angular speed ω, while the inner cylinder is stationary. By solving the Navier-Stokes equations, the velocity gradient G' across the annular gap can be obtained as:

$$G' = \frac{2\omega R_1^2 R_2^2}{(R_2^2 - R_1^2)r^2} \qquad (4.1\text{-}1)$$

where R_1 and R_2 are the radii of the inner and outer cylinders respectively, and r is the radial coordinate.

Intergrating across the gap, the mean velocity gradient G can be obtained:

$$G = \frac{2\omega R_1 R_2}{R_2^2 - R_1^2} \qquad (4.1\text{-}2)$$

The limit for the flow field in a flocculator to remain laminar was found (Van Duuren, 1968) to be:

$$\omega_{limit} = 3.16 \times 10^5 \frac{\nu (R_2 - R_1)^{0.7}}{R_2^{2.7}} \qquad (4.1\text{-}3)$$

For the flocculator used in this study, according to Eq.(4.1-3), $\omega_{limit} = 87$ *rad/s,* which corresponds to a maximum average fluid shear of 1050 s^{-1}. Moreover, the red dye tests by Iacobellis (1984) showed that the transition to turbulence occurred when the fluid shear increased above 900 s^{-1}

Procedure

The procedure for the flocculation experiments was similar to that by Tsai et al (1987), Burban *et al* (1989) and Xu (1991). Therefore, only a brief description is given here.

The first step was to prepare the test sample suspension. To do this, 100 ml of the drilling mud slurry stored in an air-supplied container at a concentration of about 200 *g/l* was taken out and put into a 1-liter cylinder, and mixed with 900 ml of sea water (which was from the Santa Barbara Channel with a salinity of 33.4). The diluted slurry in the cylinder was then stirred and allowed to settle for 5 to 10 minutes. After this, 100 ml of the top portion of the mixture was removed and placed into a beaker with 350 ml of sea water. The concentration of the suspension in the beaker was then measured, and the suspension was diluted to a desired concentration. It is noted that due to the sedimentation method used in the test sample preparation, the sizes of the particles in test samples (6 μ*m* in median diameter) were smaller than those of the original drilling mud solids (9 μ*m* in median diameter).

In doing the experiments, the sample suspension at a known concentration was first disaggregated in a blender and was then put into the flocculator. The flocculator was run at a constant rotational speed to produce a uniform fluid shear in the flocculator. At certain time intervals (5, 10, or 20 minutes, depending on flocculation conditions), the flocculator was stopped, and samples were withdrawn from the flocculator for particle size analysis using a Malvern Particle Sizer 3600E. Then the flocculator was filled and run again. This procedure was continued until successive samples showed that the average median diameter over time approached a constant. It was then assumed that a steady state of flocculation had been reached.

In order to examine the effects of flocculation conditions, we conducted the experiments at a variety of combinations of fluid shear and solid concentration. The fluid shears used in the tests were 25, 50, 100, and 200 s^{-1}, and the solid concentrations were 5, 10, 25, 50, 100, 200, and 400 *mg/l*. Tests on a total of 20 combinations were performed.

Results and Discussion

Variation of Size Distributions

Before it is put into the flocculator, the particle suspension has been disaggregated at an extremely high fluid shear in a blender. Therefore, at the beginning of a flocculation test, it is assumed that all particles in suspension are the individual solid particles of test samples. A typical solid particle size distribution is shown in Figs.4.1-2 and 4.1-3 (t=0 curve). This distribution can be fitted with a log-normal distribution with a median diameter of 6 μ*m* and a standard geometric deviation (σ_g defined by Eq.(4.2-17)) of 2.4. During a flocculation test, flocs are formed from the solid particles, and the floc size distribution changes with time. Figs.4.1-2 and 4.1-3 show two examples of such size distribution variations during the flocculation tests.
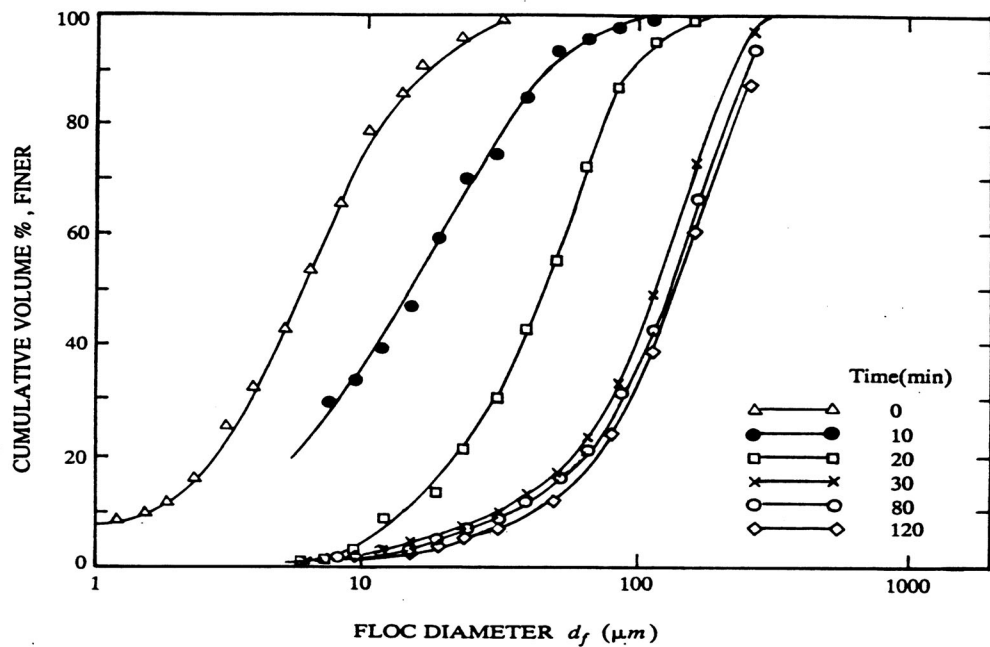
Fig.4.1-2 Size distributions at various times at fluid shear of 50 s^{-1} and at solid concentration of 10 mg/l
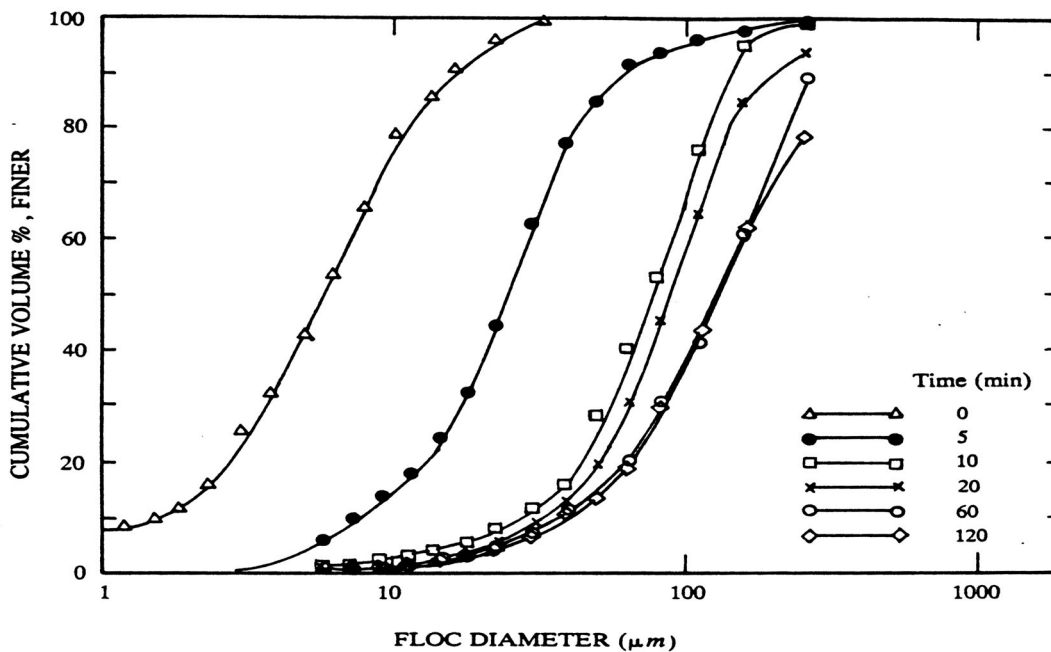

Fig.4.1-3 Size distributions at various times at fluid shear of 50 s^{-1} and at solid concentration of 25 mg/l

To characterize a size distribution, some statistical quantities such as median diameter and standard deviation are necessary. Figs.4.1-4a to 4.1-4d show the floc median size (diameter) as a function of time for all combinations of fluid shear and solid concentration. From these figures we can see that the median size changes significantly during the flocculation processes, from the order of a few microns at the beginning of the tests to the order of hundreds of microns at the steady state.
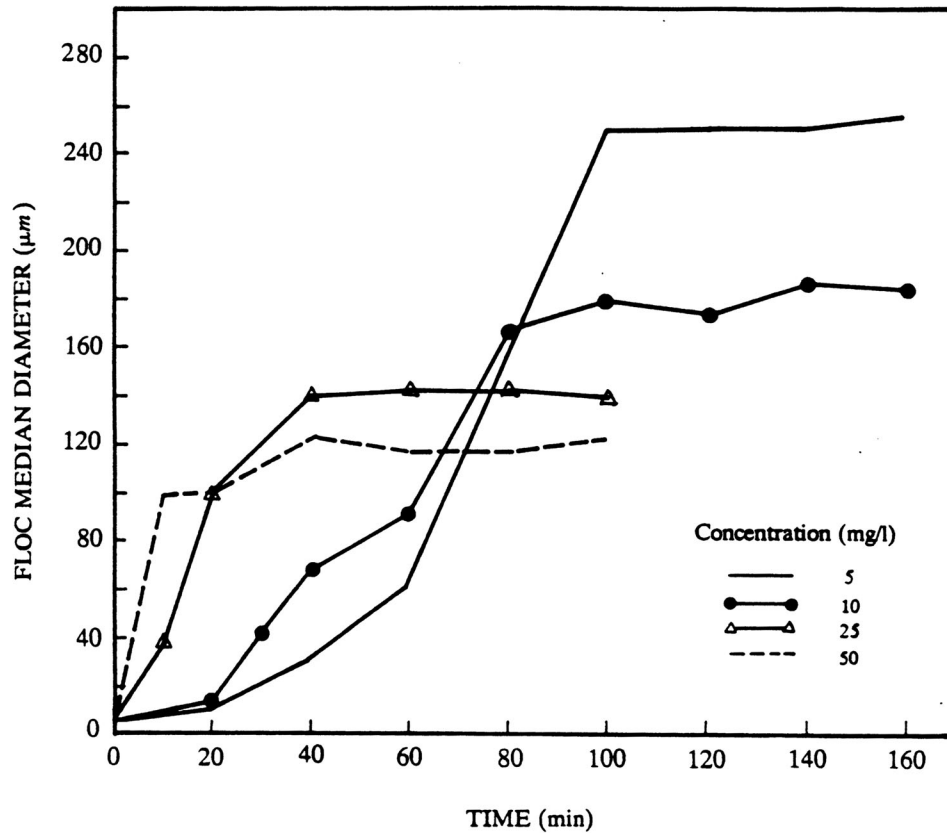
Fig.4.1-4 Time variation of the floc median diameter for drilling mud at fluid shears: (a) 25 s^{-1} ; (b) 50 s^{-1}; (c) 100 s^{-1} ; (d) 200 s^{-1} .
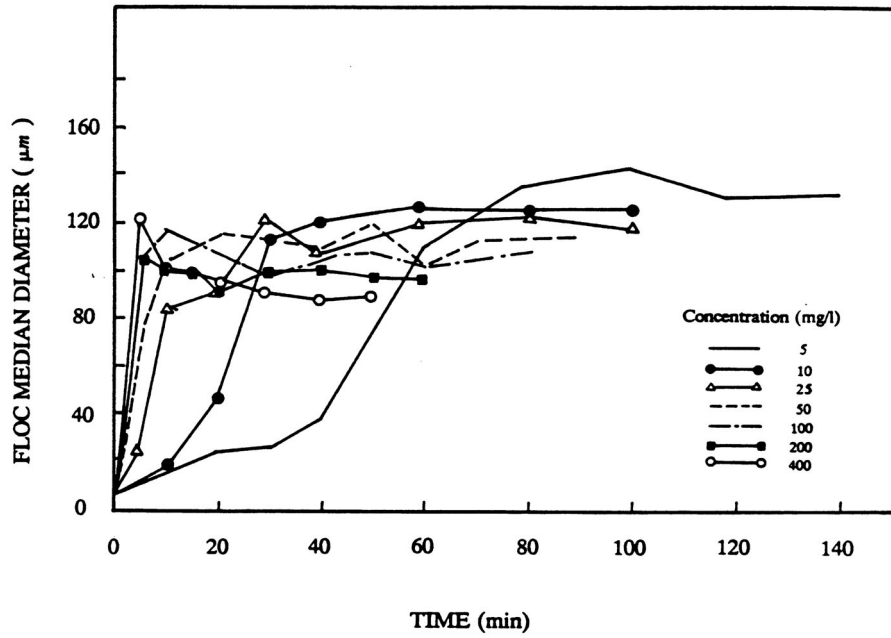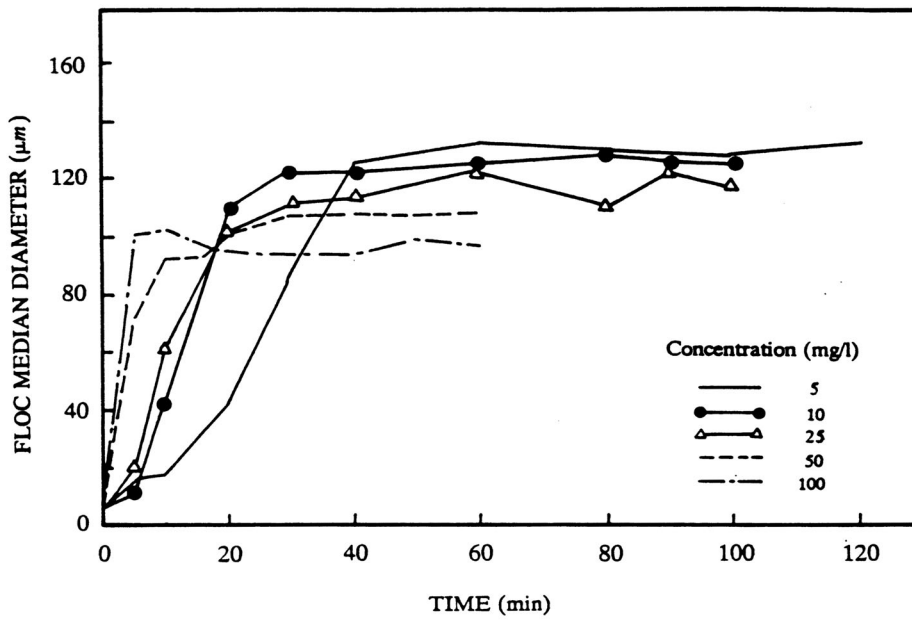
Fig.4.1-4a

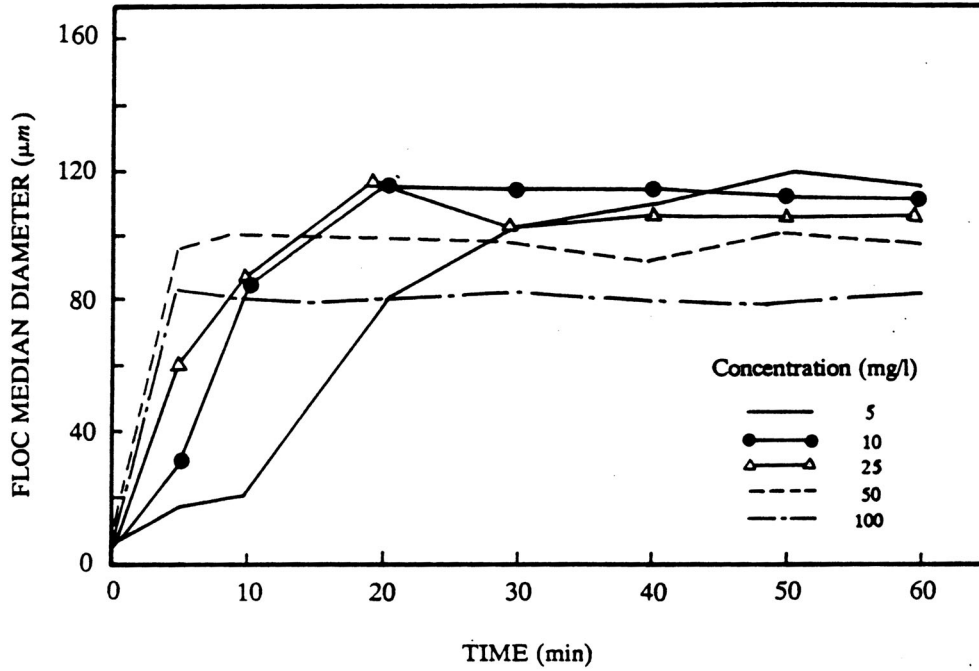**Fig.4.1-4b**

Fig.4.1-4c

Fig.4.1-4d

Like the median size, the standard deviation of the floc size distribution also changes with time. The standard deviation $\sigma(t)$ at time t is defined as:

$$\sigma(t) = [\sum_{k=1}^{\infty} (d_k - d_m(t))^2 P_k(t)]^{1/2} \qquad (4.1\text{-}4)$$

where d_k and $P_k(t)$ are the diameter and volume percent of floc k respectively, and $d_m(t)$ is the median diameter of flocs at time t.

Now we define the normalized standard deviation σ_n as follows:

$$\sigma_n = \frac{\sigma(t)}{d_m(t)} = [\sum_{k=1}^{\infty} (\frac{d_k}{d_m(t)} - 1)^2 P_k(t)]^{1/2} \qquad (4.1\text{-}5)$$

We can plot the floc size distribution as the floc cumulative volume percent versus normalized size $d_f/d_m(t)$. Two examples of such normalized floc size distributions are shown in Figs.4.1-5 and 4.1-6, which correspond to the distributions shown in Figs.4.1-2 and 4.1-3 respectively. We can see from these figures that beyond a short period of early flocculation, the data of normalized

floc size distributions at different times fall into a single curve. This feature suggests that a self-similar size distribution exists, and consequently, the normalized standard deviation is independent of time.
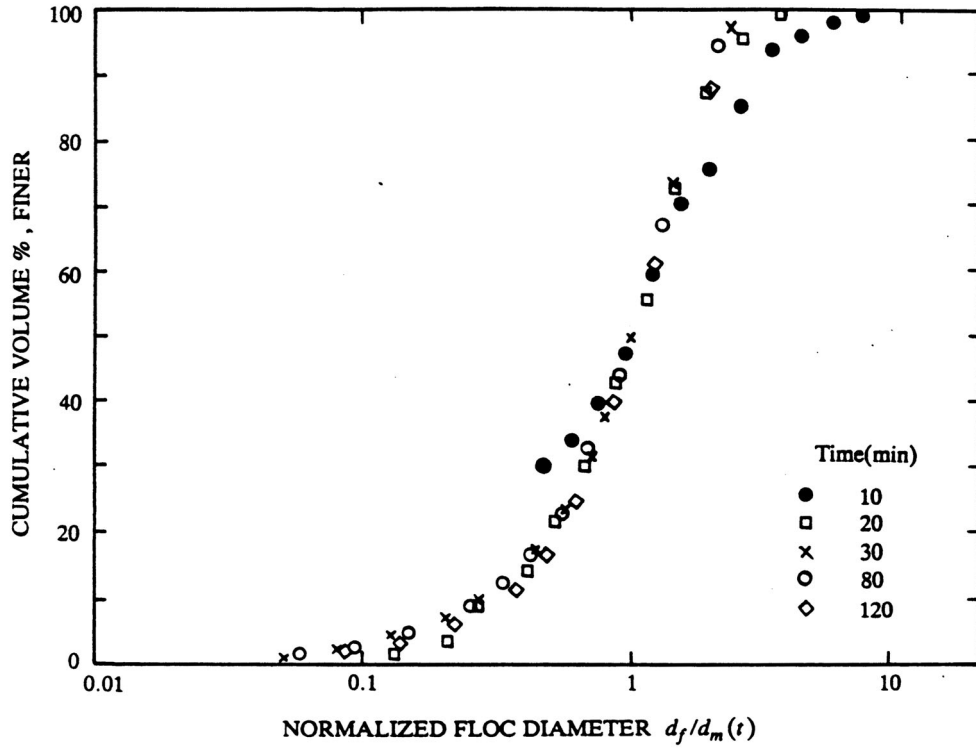
Fig.4.1-5 Self-similar size distribution of drilling mud flocs in the Couette flocculator test at fluid shear of 50 s^{-1} and solid concentration of 10 mg/l
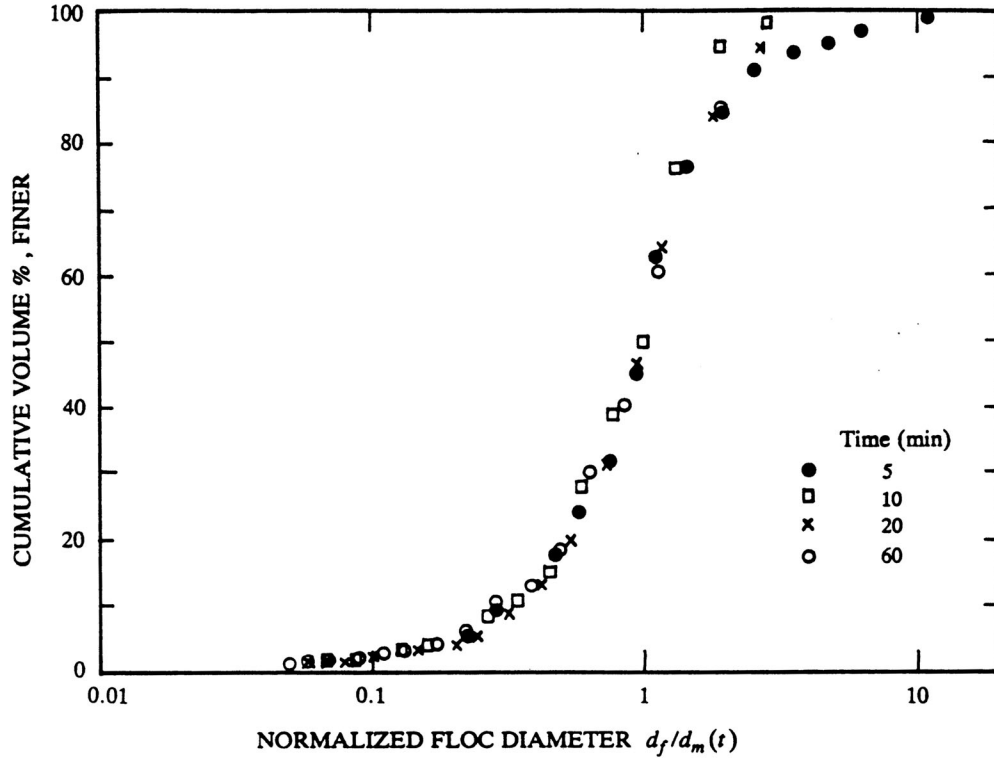
**Fig.4.1-6 Self-similar size distribution of drilling mud flocs
in the Couette flocculator test at fluid shear of 50 s^{-1}
and solid concentration of 25 mg/l**

Since Malvern outputs the volume percent corresponding to floc groups within different size ranges, Eq.(4.1-5) can not be used to calculate σ_n. Instead, we calculate σ_n from the normalized floc size distribution, that is:

$$\sigma_n^2 = \int_0^\infty (x-1)^2 \frac{dF(x)}{dx} dx \tag{4.1-6}$$

where x = $d_f/d_m(t)$, and $F(x)$ is the normalized size distribution function (i.e., the best fit curve in Fig. 4.1-5 or 4.1-6).

To obtain σ_n from Eq.(4.1-6), the Simpson integrating scheme for the integral and the Lagrangian interpolating scheme for the estimation of $dF(x)/dx$ were employed. A computer program named SIGMA2.FOR (Appendix 1) was written to perform the calculation.

Fig.4.1-7 shows σ_n for all combinations of fluid shear and solid concentration. We can see from this figure that σ_n is a very weak function of fluid shear and solid concentration. As a first

approximation, σ_n may be considered to be a constant as:

$$\sigma_n = 0.6742 \qquad\qquad (4.1\text{-}7)$$

for all combinations of fluid shear and solid concentration.
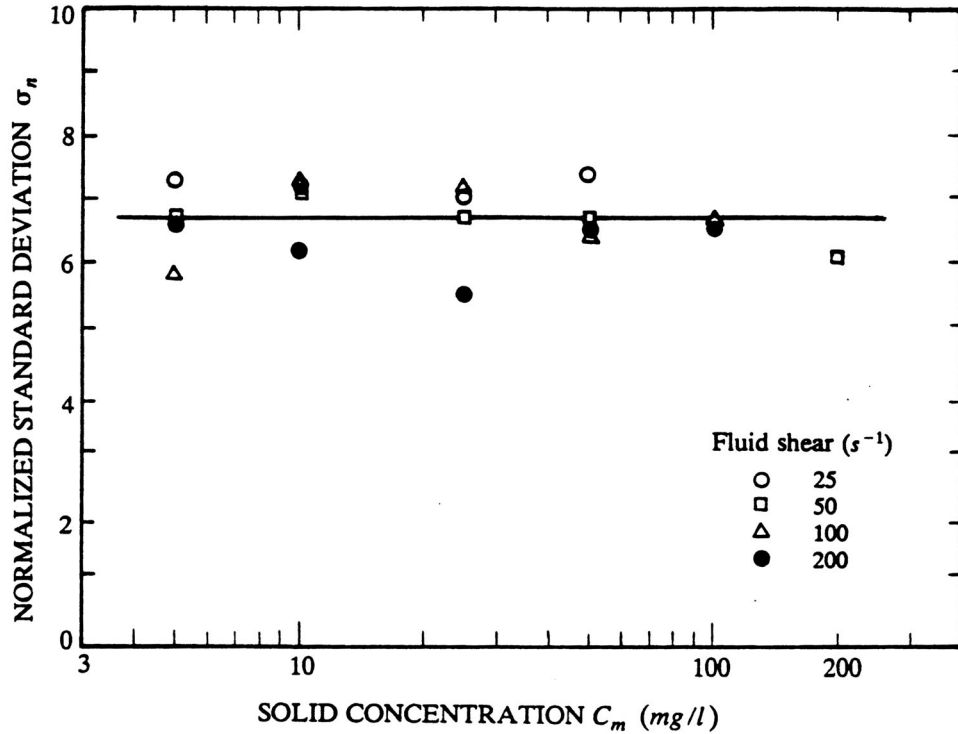
Fig.4.1-7 Normalized standard deviation of the drilling mud floc size distributions in the Couette flocculator tests

Then the standard deviation of the floc size distribution for the drilling mud is related to the median diameter as:

$$\sigma(t) = \sigma_n d_m(t) = 0.6742 d_m(t) \qquad\qquad (4.1\text{-}8)$$

This equation is valid beyond the initial stage of flocculation (which will be defined later).

Tables 4.1-1 and 4.1-2 show the steady state floc median diameter and the time to reach the steady state respectively. We can see from these tables as well as from Fig.4.1-4 that the flocculation process depends on the combination of fluid shear and solid concentration. For a fixed fluid shear, the higher the solid concentration, the faster the flocculation process, the shorter the time to reach steady state, and the smaller the floc median size at steady state. The

same can be seen for a fixed solid concentration at the higher fluid shear. This suggests that both fluid shear and solid concentration have the same effects on the flocculation time scale as well as the floc size distribution, and they can offset each other (Fair and Gemmell, 1964; Tambo and Watanabe, 1979).

Table 4.1-1 Steady state floc median diameter (μm) for the drilling mud in the Couette flocculator tests

Concentration (mg/l)	Fluid shear (s^{-1})			
	25	50	100	200
5	251.6	134.2	127.0	115.2
10	183.8	126.7	124.7	112.0
25	140.8	121.5	116.0	105.5
50	119.7	113.7	107.1	97.3
100	–	108.3	98.0	82.6
200	–	97.9	89.0	69.5
400	–	94.3	81.3	65.7

Table 4.1-2 Time (min) to reach steady state of flocculation for the drilling mud in the Couette flocculator tests

Concentration (mg/l)	Fluid shear (s^{-1})			
	25	50	100	200
5	100	80	50	40
10	90	50	35	20
25	50	35	25	15
50	35	25	20	10
100	–	15	10	5

Flocculation Stages

From the experimental results, we can distinguish three stages of flocculation process. Let us take the test for a fluid shear of 50 s^{-1} and a solid concentration of 10 *mg/l* as an example to illustrate these stages.

Stage I: This is the initial stage of flocculation. At this stage the floc growth rate is much higher than the floc break-up rate, but the floc size has not increased much. Large amounts of both flocs and solid particles exist in suspension (Fig.4.1-2, t = 10 mm curve). The size distribution is not self-similar as in stage II. We may distinguish the initial stage from stage II by $d_m(t) < 4d_{m0}$, where d_{m0} is the median diameter of primary solid particles.

Stage II: This is the transition stage. At this stage, the floc size increases rapidly. On the other hand, the floc break-up rate increases and becomes comparable with the floc growth rate. Most of the particles in suspension are flocs and only a few solid particles exist (Fig.4.1-2, t = 10, 20, 30 mm curves). The most important feature of this stage is that the floc size distributions are self-similar. This means that the normalized floc size distributions at different times fall on a single curve (Fig.4.1-5), and the normalized standard deviation is independent of time.

Stage III: This is the steady state. At this stage, the floc growth rate is equal to the floc break-up rate, i.e. a dynamic equilibrium is reached. The floc size distributions do not change with time, though they may have some small fluctuations (Fig.4.1-2, t = 80, 120 mm curves).

We have noticed that for the combinations of low fluid shear and low solid concentration, these three stages are clearly distinguished. However, for the combinations of high fluid shear and high solid concentration, the flocculation takes place rapidly and the time to reach the steady state is too short to determine the initial stage from the size measurements.

The three stages of flocculation have also been noticed by Koh *et al* (1986) in their study of the flocculation of scheelite in a stirring tank. Self-similar floc size distributions have been found experimentally or theoretically by Friedlander (1960a, b), Swift and Friedlander (1964), Kawashima and Capes (1974), Tambo and Watanabe (1979), Tsurui and Takamori (1981), Hunt (1982), and Koh *et al* (1986). Moreover, the steady state of flocculation in a laminar flow or in a turbulent flow has been demonstrated by Fair and Gemmell (1964), Argaman and Kaufman (1970), Boadway (1978), Hunter and Frayne (1980), Hsu and Glasgow (1983), Tsai *et al* (1987), Xu (1988, 1991), and Burban *et al* (1989). However, they do not give the details on the shifts of the size distributions at different flocculation stages.

<div align="center">**Dimensional Analysis**</div>

In the following, we use the dimensional analysis method to correlate the characteristics of flocculation, such as the median size of flocs in the steady state, with the flocculation parameters (i.e. fluid shear and solid concentration) for the fluid shear dominated flocculation process at the steady state.

Considering the steady state of flocculation due to fluid shear, the floc median size d_{ms} at the steady state has the functional form:

$$d_{ms} = f(G, C_m, d_{m0}, \mu) \tag{4.1-9}$$

where d_{m0} and C_m are the diameter and concentration of primary solid particles respectively, G is the fluid shear in the flocculator, and μ is the dynamic viscosity of the fluid.

It is readily shown that Eq.(4.1-9) can be written in the following non-dimensional form:

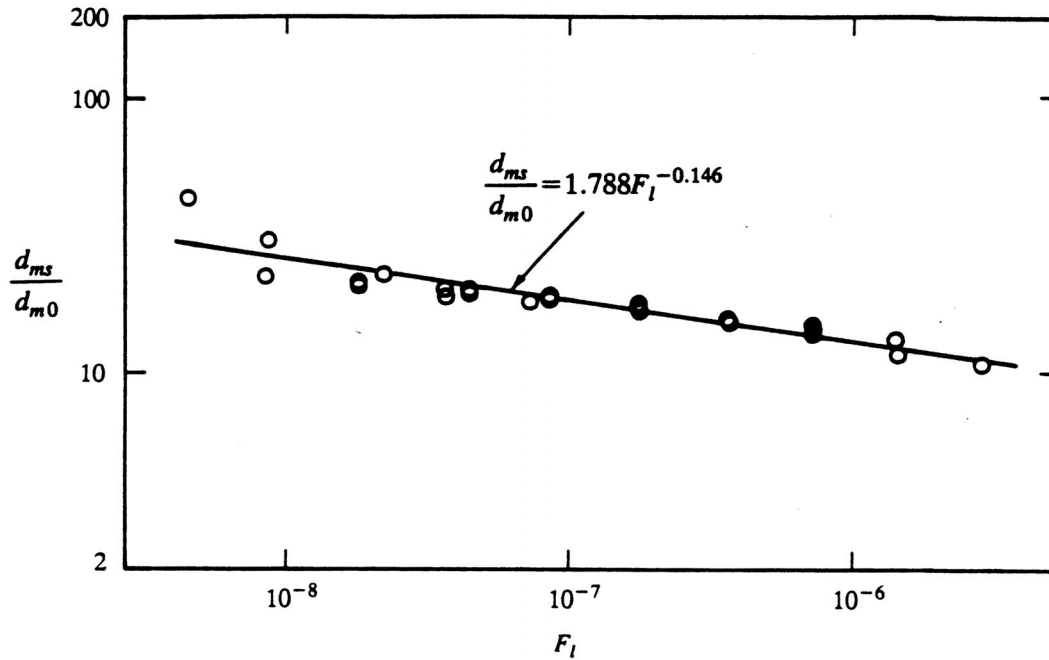$$\frac{d_{ms}}{d_{m0}} = f\left(\frac{GC_m d_{m0}^2}{\mu}\right) \tag{4.1-10}$$

Eq.(4.1-10) indicates that the floc median size at the steady state is correlated to a non-dimensional number, which is defined as the flocculation number F_l:

$$F_l = \frac{GC_m d_{m0}^2}{\mu} \tag{4.1-11}$$

The experimental data for the steady state floc sizes are shown in Table 4.1-1. These values are plotted in Fig.4.1-8 in the form of Eq.(4.1-10). It is seen that a power law can be used to regress the data. Using the least-square method, we obtain a semi-empirical expression for the steady state median sizes of the drilling mud flocs as a function of the flocculation number as:

$$\frac{d_{ms}}{d_{m0}} = 1.788 \, F_l^{-0.146} \tag{4.1-12}$$

The correlation coefficient is 0.9251.

The plotted equation reads:

$$\frac{d_{ms}}{d_{m0}} = 1.788 F_l^{-0.146}$$

with axes labeled $\frac{d_{ms}}{d_{m0}}$ (vertical) and F_l (horizontal).

Fig.4.1-8 Relationship of the steady state floc median diameter with the flocculation number for drilling mud

To verify further the validity of the correlation between the steady state floc diameter and the flocculation number for other types of sediments, we plot the data from the studies by Tsai et al. (1987), Burban et at. (1989), Xu (1988), and Hunter and Frayne (1980) (Figs.4.1-9 to 4.1-13).

Figs.4.1-9 and 4.1-10 show the $d_{ms}/d_{m0} \sim F_l$ relationship for the Detroit River sediments in sea water and in fresh water respectively. The median sizes of the solid particles vary from 3.5 to 5.4 µm. The experiments were conducted using a Couette flocculator similar to that used in this study. The applied fluid shears ranged from 100 to 600 s^{-1}, while the solid concentrations ranged from 10 to 800 *mg/l* (Tsai *et al*, 1987; Burban *et al*, 1989).
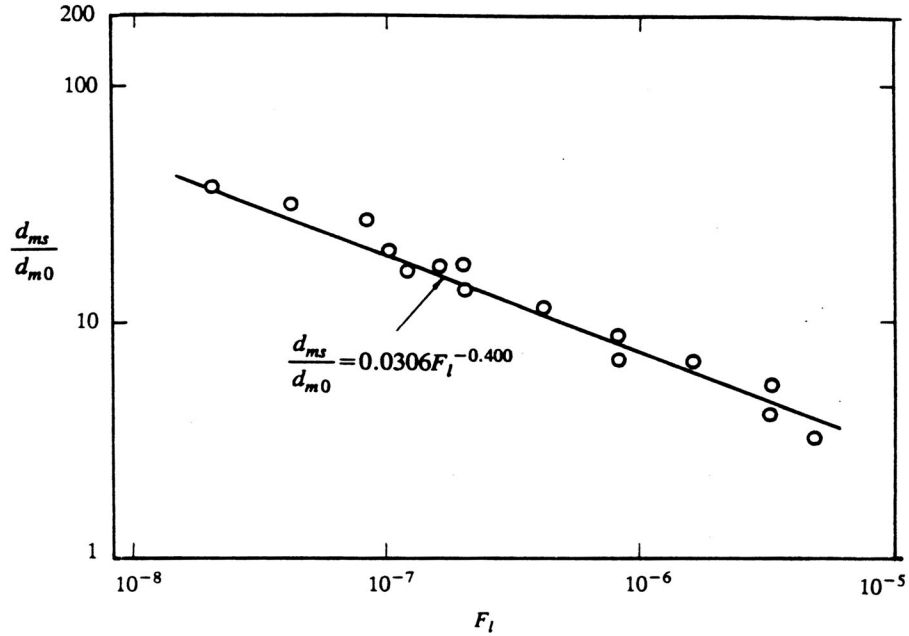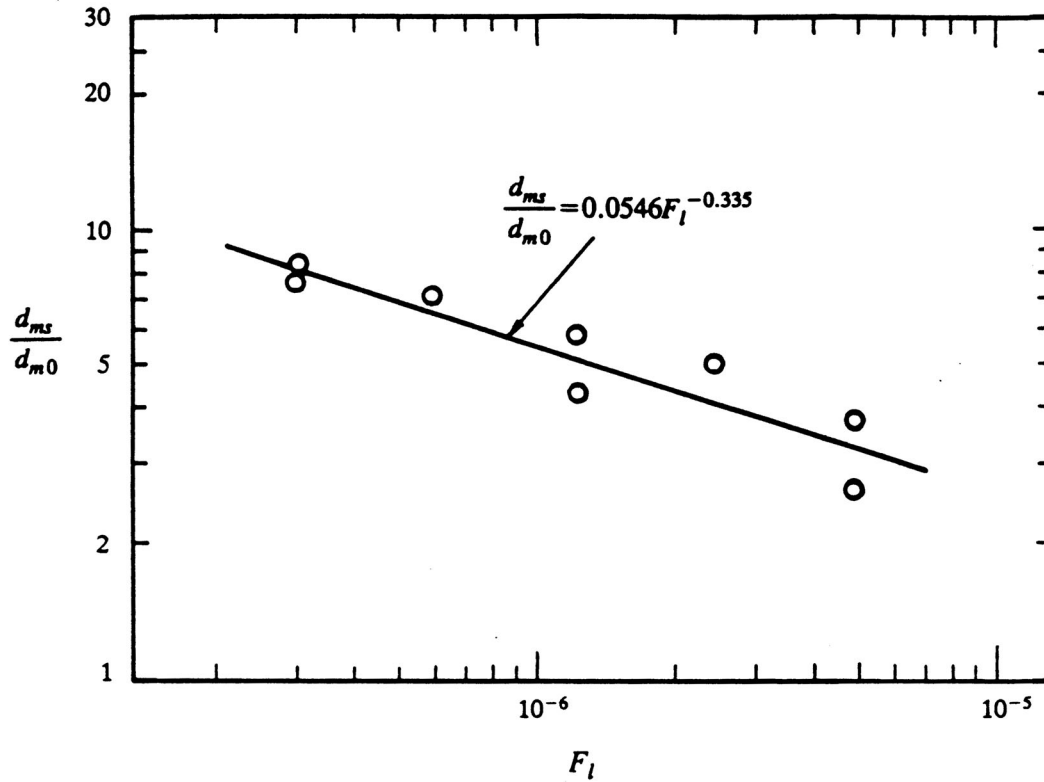
Fig.4.1-9 **Relationship of the steady state floc median diameter with the flocculation number for Detroit River sediment in seawater (modified from Burban et al., 1989).**
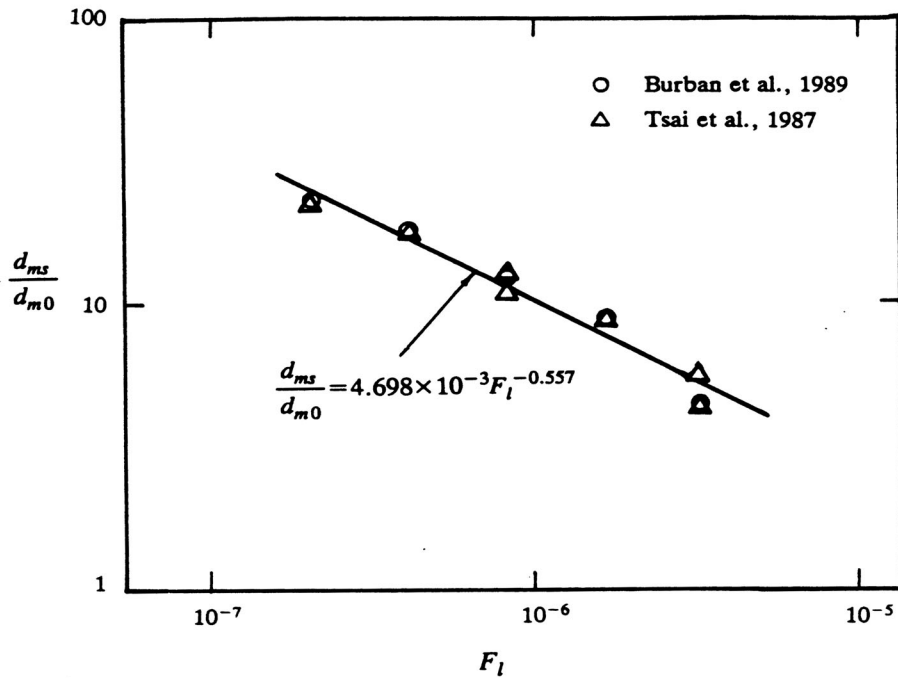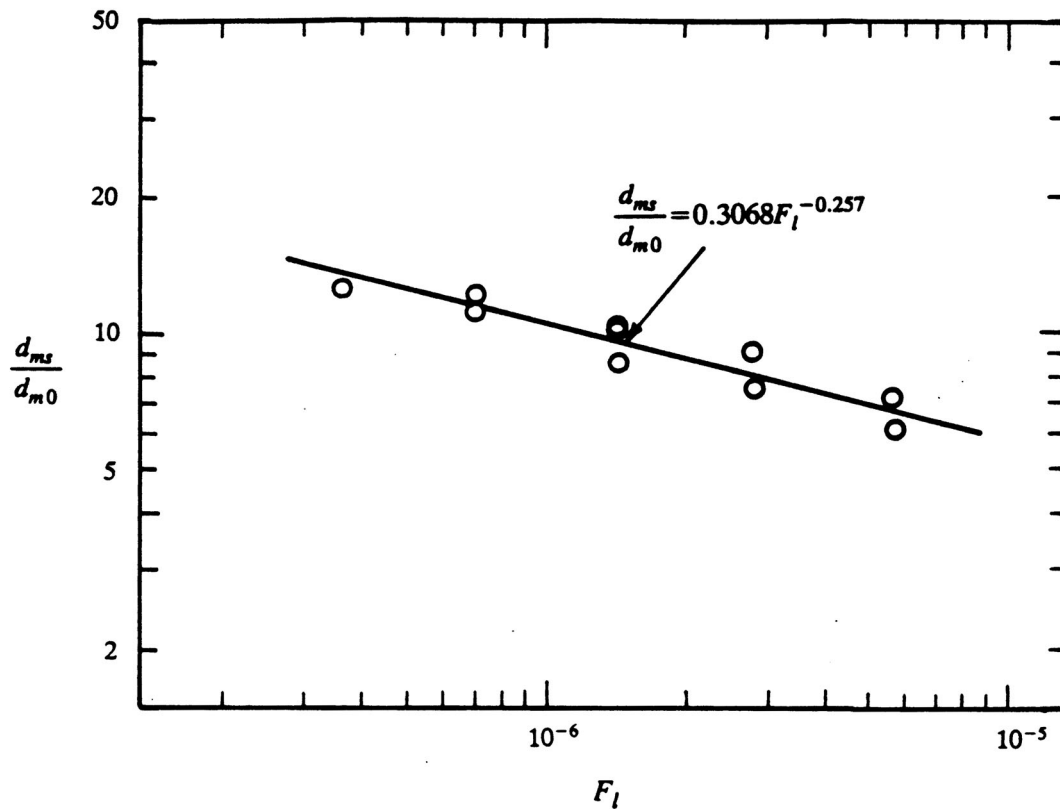

Fig.4.1-10 **Relationship of the steady state floc median diameter with the flocculation number for Detroit river sediment in fresh water (modified from Burban et al., 1989; and Tsai et al., 1987).**

Figs.4.1-11 and 4.1-12 show the $d_{ms}/d_{m0} \sim F_l$ relationship for bentonite and barite in sea water respectively. The median size of the solid particles is about 6 μm. The experiments were conducted using a Couette flocculator similar to that used in this study. The applied fluid shears ranged from 100 to 400 s^{-1}, while the solid concentrations ranged from 50 to 800 mg/l (Xu, 1988).

Fig.4.1-11 Relationship of the steady state floc median diameter with the flocculation number for bentonite (modified from Xu, 1988).

$$\frac{d_{ms}}{d_{m0}} = 0.3068 F_l^{-0.257}$$
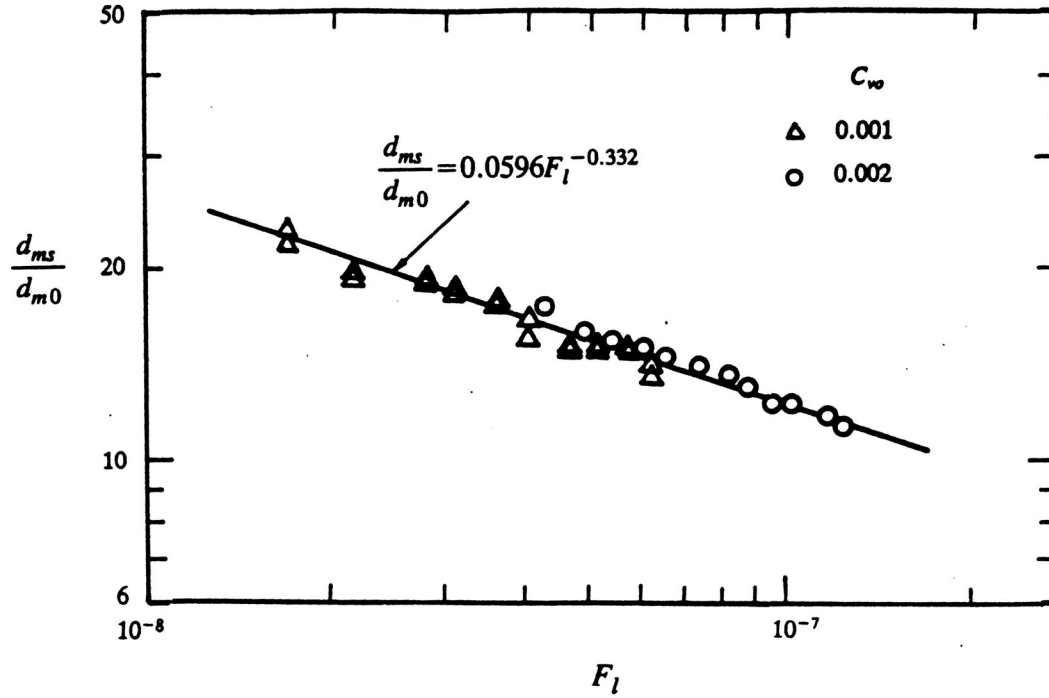
**Fig.4.1-12 Relationship of the steady state floc median
diameter with the flocculation number for barite
(modified from Xu, 1988).**

Fig.4.1-13 shows the $d_{ms}/d_{m0} \sim F_l$ relationship for poly (methylmethacrylate) (PMMA) lattices of a uniform size (238 nm in diameter) (here d_{ms} represents the steady state average diameter). The experiments were conducted in a variable-speed stirrer (IKARW18) at the equivalent fluid shears of 450 to 1800 s^{-1} and particle volume concentrations (C_{vo}) of 0.001 and 0.002 (Hunter and Frayne, 1980).

Fig.4.1-13 Relationship of the steady state floc average diameter with the flocculation number for poly lattice (modified from Hunter and Frayne, 1980).

The data shown in Figs.4.1-9 to 4.1-13 can also be fitted by a power law:

$$\frac{d_{ms}}{d_{m0}} = aF_l^b \tag{4.1-13}$$

where a and b are constants which depend on the type of the sediment and the properties of the fluid in which the sediment is suspended. Using the least-square method, we have obtained a and b for the above data (see Table 4.1-3). We can see that the plots in Figs.4.1-9 to 4.1-13 also show a strong correlation between the steady state floc median size and the flocculation number.

Table 4.1-3 Summary of experimental constants in the relationship
$(d_{ms}/d_{m0}=aF_l^b)$ **of the steady state floc median diameter and**
flocculation number

Sediment	a	b	r
Drilling mud	1.788	-0.146	0.9251
DR-S	0.0306	-0.400	0.9737
DR-F	0.0047	-0.557	0.9802
Bentonite*	0.0546	-0.335	0.9236
Barite*	0.3068	-0.257	0.9254
Poly lattice"	0.0596	-0.332	0.9794

Note: DR-S --Detroit River sediment in seawater, primary data from Burban
et al. (1989).
DR-F --Detroit River sediment in fresh water, primary data from Burban
et al.(1989) and Tsai et al. (1987).
* --primary data from Xu (1988).
" --primary data from Hunter and Frayne (1980).
r --correlation coefficient.

It should be mentioned that, for the Detroit River sediment in fresh water, based on the experimental data of Tsai *et al* (1987), Lick and Lick (1988) presented an empirical equation for the steady state floc size as a function of fluid shear and solid concentration:

$$C_m d_{ms}^2 G_s = \alpha_o \qquad (4.1\text{-}14)$$

where G_s is the fluid shear stress in *dynes/cm²* , d_{ms} is in *cm* , C_m is the solid mass concentration in *g/cm³*, and $\alpha_0 = 10^{-8} g dynes/cm^3$.

This equation can be rearranged as follows:

$$\frac{d_{ms}}{d_{m0}} = 10^{-2} F_l^{-0.5} \qquad (4.1\text{-}15)$$

On the other hand, the semi-empirical equation obtained from the present study, using the same data and some additional data from Burban *et al* (1989), is:

$$\frac{d_{ms}}{d_{m0}} = 4.698 \times 10^{-3} F_l^{-0.557} \tag{4.1-16}$$

It is seen that Eqs.(4.1-15) and (4.1-16) are consistent.

In addition, for the drilling mud used in this study, we have obtained the time to reach the steady state of flocculation as a function of fluid shear and solid concentration (see Table 4.1-2). Although the correlation between the time (T_s) to reach the steady state and the flocculation number can not be deduced from a dimensional analysis, we find that an empirical relationship of T_s with F_l exists. This relationship is shown in Fig.4.1-14. The empirical expression for this relationship is obtained by power regression as follows:

$$T_s = 1.340 \times 10^{-3} F_l^{-0.564} \tag{4.1-17}$$

where T_s is in min. The correlation coefficient is 0.9849.
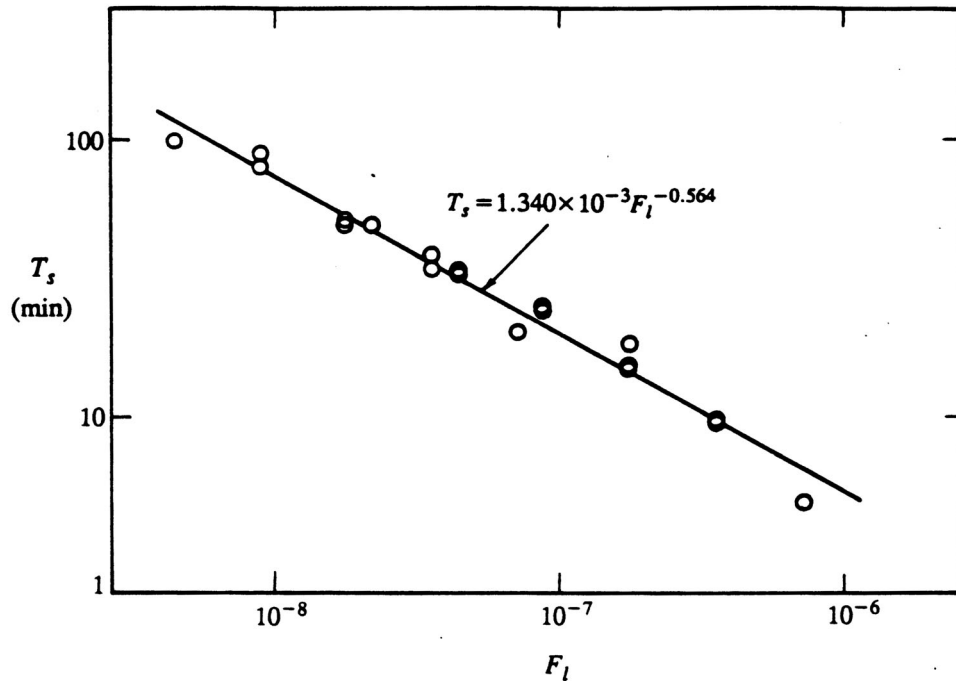
Fig.4.1-14 Relationship of the time to reach steady state of flocculation with the flocculation number for drilling mud

4.2 FLOCCULATION DUE TO DIFFERENTIAL SETTLING

In this subsection, we describe the experiments performed in disc flocculators. The validity of using disc flocculators to investigate flocculation due to differential settling is first examined and is followed by a description of the experimental procedures. Finally, the results of the experiments are presented and discussed.

Experimental Methods

Disc Flocculators

Fig.4.2-1 shows a schematic of the three disc flocculators with different sizes used in the experiments. The big disc has a diameter of 1 m, the medium one 0.3 m, and the small one 0.2 m. The thickness of the big disc is 35 mm, while the thicknesses of the medium and small discs are 26 mm. The volumes of these discs are 31, 2.1, and 0.84 liters respectively. The small and medium discs are driven by rollers which are connected to motors. The big disc is driven by gears connecting the axis of the disc to a motor.
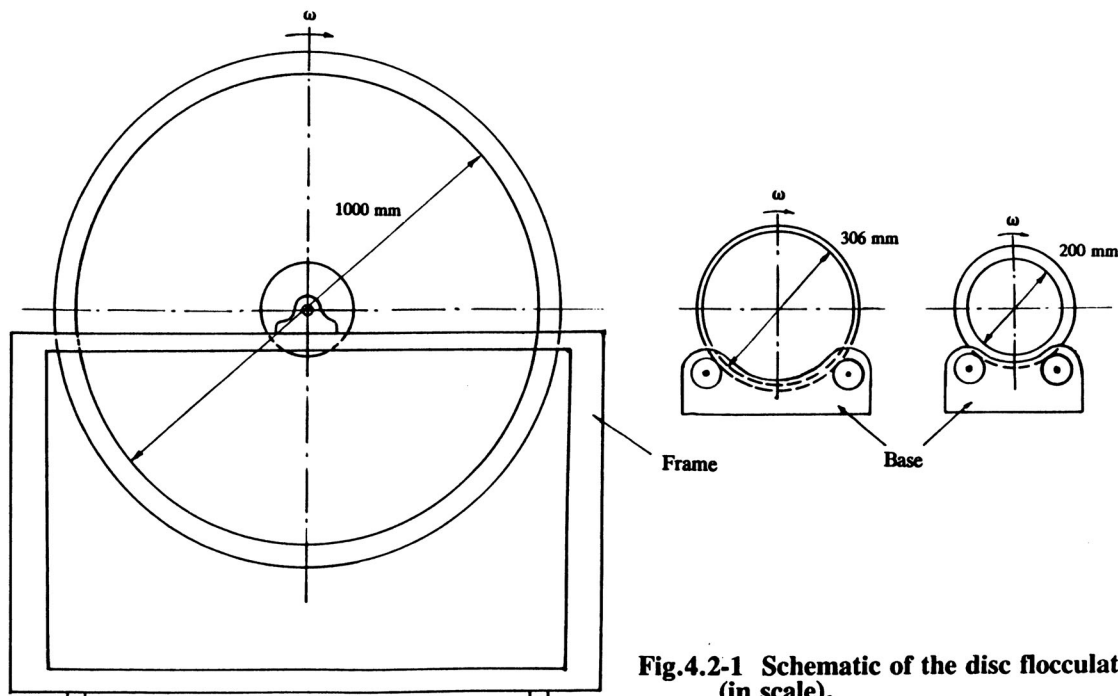
Fig.4.2-1 Schematic of the disc flocculators (in scale).

When a disc flocculator is rotated at a constant rate, after an initial transient of about two minutes, the fluid in the disc thereafter rotates as a rigid body. The particles in the disc flocculator keep settling due to gravity and at the same time are kept from settling out by the rotating fluid. We may use the disc flocculators to investigate the flocculation process purely due to differential settling. However, before the disc flocculators can be used for this purpose, we must answer three questions: (a) does dynamic similarity exist for the settling of a particle in a disc flocculator and in a settling tube? (b) is the collision coefficient for flocculation in the disc

flocculators the same as that in a settling tube? and (c) does the scale of the discs affect flocculation? We answer these questions in the following.

Dynamical Similarity
The first question means that dynamical similarity must exist for the settling of a particle in a disc floceulator and in a settling tube, as far as the forces acting on a particle are concerned. Fig.4.2-2 shows the free body diagram of the forces acting on a particle in a rotating fluid. These forces are F_G, the gravity buoyancy force, $F_G = V(\rho_p - \rho_w)g$; F_D , the drag force,

$F_D = \boxed{F_D = C_D \dfrac{u \, |u|}{8} \rho_w \pi d^2}$; F_C, the centrifugal-buoyancy force, $Fc = \omega^2 r(\rho_p - \rho_w)V$; F_L, the lift force; and F_P, the perturbing force (where ω is the rotation rate of the disc; ρ_p and ρ_w are the densities of the particle and the water respectively; d is the diameter of the particle; u is the velocity of the particle; V is the volume of the particle; and C_D is the drag coefficient). For the settling of a small particle in a viscous fluid, the Reynolds number is very low, i.e., the viscous force is much larger than the inertial force. On the other hand, if the disc is rotated slowly, which will create only a very small pressure gradient, the lift and centrifugal-buoyancy forces may be much smaller than the first-order drag and gravity-buoyancy forces (Tooby *et al*, 1977). We may use the ratio of centrifugal-buoyancy and gravity-buoyancy forces as a criterion for dynamical similarity, i.e.:

$$\frac{F_C}{F_G} = \frac{\omega^2 r}{g} \ll 1 \tag{4.2-1}$$

where r is the radius of the orbit of a particle which is assumed to have the maximum value of the radius of a disc. For the rotation periods of 30 s for the big disc and 25 s for the small and median discs, this ratio is 0.002 and 0.001 respectively. It is seen that the centrifugal-buoyancy force is very small and can be neglected.
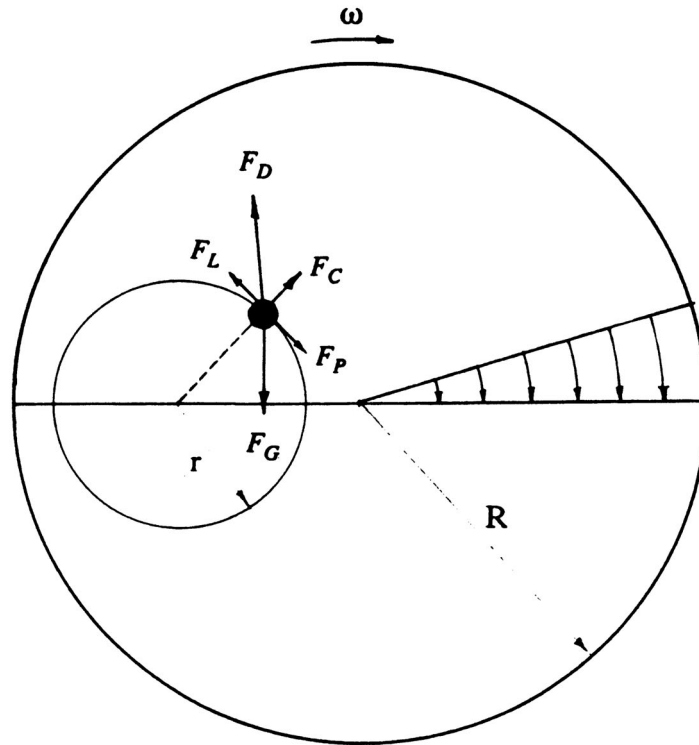
Fig.4.2-2 Forces on a particle in a rotating fluid field. For a small sphere, a nearly circular orbit is observed.

Additionally, the perturbing force is even smaller than the lift and centrifugal-buoyancy forces. Therefore, the drag and the gravity-buoyancy forces are the dominant forces acting on a particle in a rotating fluid. This is the same situation for a particle settling in a settling tube or in a real water body. So that, dynamic similarity exists in these situations.

Collision Similarity
Although dynamical similarity exists, the motion of a particle in a disc is somewhat different from that in a settling tube. However, from the point of view of flocculation, the collisions (or relative motions) of particles need to be considered instead of the motions of individual particles. Therefore, for the flocculation process to be the same in two systems, the collision coefficients for flocculation in these two systems must be the same. We define this as collision similarity.

To examine the collision similarity, we first write the collision coefficient for flocculation due to differential settling in a settling tube (Findheisen, 1939):

$$\beta_{ij} = \frac{\pi g}{72\mu}(\rho_p - \rho_w)(d_i + d_j)^3 \, | \, d_i - d_j \, | \tag{4.2-2}$$

$$= \frac{\pi}{4}(d_i + d_j)^2 \Delta w_{sij}$$

where d_i and d_j are the diameters of particles i and j respectively, and Δw_{sij} is the settling speed difference, or the relative velocity of the two particles:

$$\Delta w_{sij} = \frac{g}{9\mu}(\rho_p - \rho_w)\frac{(d_i + d_j)}{2} \, | \, d_i - d_j \, | \tag{4.2-3}$$

In Eq.(4.2-2) or (4.2-3), Stokes' law for the settling speeds of solid spheres is assumed.

On the other hand, the collision coefficient for flocculation in a disc flocculator may be written as:

$$\beta_{ij} = \frac{\pi}{4}(d_i + d_j)^2 \Delta u_{rij} \tag{4.2-4}$$

where Δu_{rij} is the relative velocity of particles i and j in the disc and is discussed in the following.

Considering the two dominant forces, the drag and gravity-buoyancy forces acting on a small particle, the governing equation for the motion of the particle in a rotating fluid is written as:

$$-C_d\left(\frac{dx}{dt} + \omega y\right) = 0 \tag{4.2-5a}$$

$$-C_d\left(\frac{dy}{dt} - \omega x\right) - F_G = 0 \tag{4.2-5b}$$

where $C_d = 3\pi\mu d$ is the Stokes expression for drag in a low Reynolds number flow.

For a particle started at the point $(x_0, 0)$ on the horizontal plane through the disc axis, the solutions are (Tooby *et al*, 1977):

$$x(t) = (x_0 - r_0)\cos\omega t + r_0 \tag{4.2-6a}$$

$$y(t) = (x_0 - r_0)\sin\omega t \tag{4.2-6b}$$

These solutions indicate that the motion of a particle in a rotating fluid follows a circular orbit in the vertical plane perpendicular to the disc axis with the center r_0 at:

$$r_0 = \frac{w_s}{\omega} \tag{4.2-7}$$

For a given settling speed of the particle and the rotation rate of the disc, there is a family of circular solutions about the same orbit center, with the particular orbit radius determined by the initial conditions. These solutions correspond closely to observations (Tooby *et al*, 1977).

From Eq.(4.2-6), the velocity of a particle is written as:

$$\frac{dx}{dt} = -\omega(x_0 - r_0)\sin\omega t \tag{4.2-8a}$$

$$\frac{dy}{dt} = \omega(x_0 - r_0)\cos\omega t \tag{4.2-8b}$$

Then, it is readily shown that the relative velocity between particles i and j is:

$$\Delta u_{rij} = |\Delta x_{0ij}\omega - \Delta r_{0ij}\omega| \tag{4.2-9}$$

Making use of Eq.(4.2-7) and considering the fact that when the two particles collide, the distance between them must be about the average of their size, Eq.(4.2-9) is rewritten as:

$$\Delta u_{rij} = |\frac{1}{2}(d_i + d_j)\omega - \Delta w_{sij}| \tag{4.2-10}$$

This equation indicates that collision similarity between a disc flocculator and a settling tube may exist, as long as the first term of the right side of the equation is much smaller than the second term.

Since we are dealing with fine-grained sediments which generally have a wide size distribution, and consequently a wide settling speed distribution, to evaluate collision similarity from Eq.(4.2-10), we must consider the relative velocities between all particles. This is too complex, if not impossible. Instead, we can consider the average relative velocity $\overline{\Delta u_r}$ between particles. With the assumption of Stokes' law for the settling speed of solid particles, we then have:

$$\overline{\Delta u_r} = d_m |\omega - \frac{g}{9\mu}(\rho_p - \rho_w)\overline{\Delta d}| \qquad \text{for } \textit{solid particles} \tag{4.2-11}$$

where $|\overline{\Delta d}|$ is the average difference of particle diameters and d_m is the median diameter of the particles.

Now we have a criterion for collision similarity as follows:

$$\frac{\omega}{\omega_e} \ll 1 \qquad \qquad (4.2\text{-}12)$$

where

$$\omega_e = \frac{g}{9\mu}(\rho_p - \rho_w)\,|\overline{\Delta d}| \qquad \text{for } \textit{solid particles} \qquad (4.2\text{-}13)$$

The statistical meaning of $|\overline{\Delta d}|$ is similar to that of the standard deviation of a size distribution. However, the difference is that the standard deviation is measured relative to the median size, while $|\overline{\Delta d}|$ is measured relative to all sizes. Therefore, we may construct an expression to estimate $|\overline{\Delta d}|$ as follows:

$$(\overline{\Delta d})^2 = \sum_{i=1}^{\infty}\sum_{j=1}^{\infty}(d_i - d_j)^2 P_i P_j \qquad (4.2\text{-}14)$$

where P_i and P_j are the percentages of particles i and j respectively.

Moreover, if a particle size distribution density exists, Eq.(4.2-14) can be replaced by the following:

$$(\overline{\Delta d})^2 = \int_{-\infty}^{\infty}\int_{-\infty}^{\infty}(x-y)^2 p(x)p(y)\,dxdy \qquad (4.2\text{-}15)$$

where x or y represents the particle diameter and $p(x)$ or $p(y)$ is the size distribution density.

Most fine-grained sediments follow a log-normal distribution law:

$$p(x) = \frac{1}{\sqrt{2\pi}\ln\sigma_g x}\exp\left[-\frac{(\ln x - \ln d_m)^2}{2\ln^2\sigma_g}\right] \qquad x > 0 \qquad (4.2\text{-}16)$$

$$p(x) = 0 \qquad \qquad x \leq 0$$

where σ_g is the standard geometric deviation defined by:

$$\ln^2\sigma_g = \int_{-\infty}^{\infty}(\ln x - \ln d_m)^2 p(x)\,dx \qquad (4.2\text{-}17)$$

With the log-normal size distribution, it is not difficult to show that:

$$|\overline{\Delta d}| = \sqrt{2}d_m[\exp(\ln\sigma_g)^2(\exp(\ln\sigma_g)^2-1)]^{1/2} \qquad (4.2\text{-}18)$$

To give quantitative results, we calculate ω/ω_e assuming a log-normal size distribution with different d_m and σ_g. In the calculation, we assume $\rho_p = 2.65 \ g/cm^3$, $\rho_w = 1.02466 \ g/cm^3$ and $\omega = 2\pi/T$ with $T=25 \ s$. Results are shown in Fig.4.2-3. We can see from this figure that ω/ω_e decreases as σ_g and d_m increase. For the test samples of the drilling mud, $d_m =6 \ \mu m$, and $\sigma_g = 2.4$, resulting in $\omega/\omega_e =0.011$. For the test samples of the Detroit River sediment, $d_m =4.8 \ \mu m$, and $\sigma_g=2.3$, resulting in $\omega/\omega_e =0.015$.
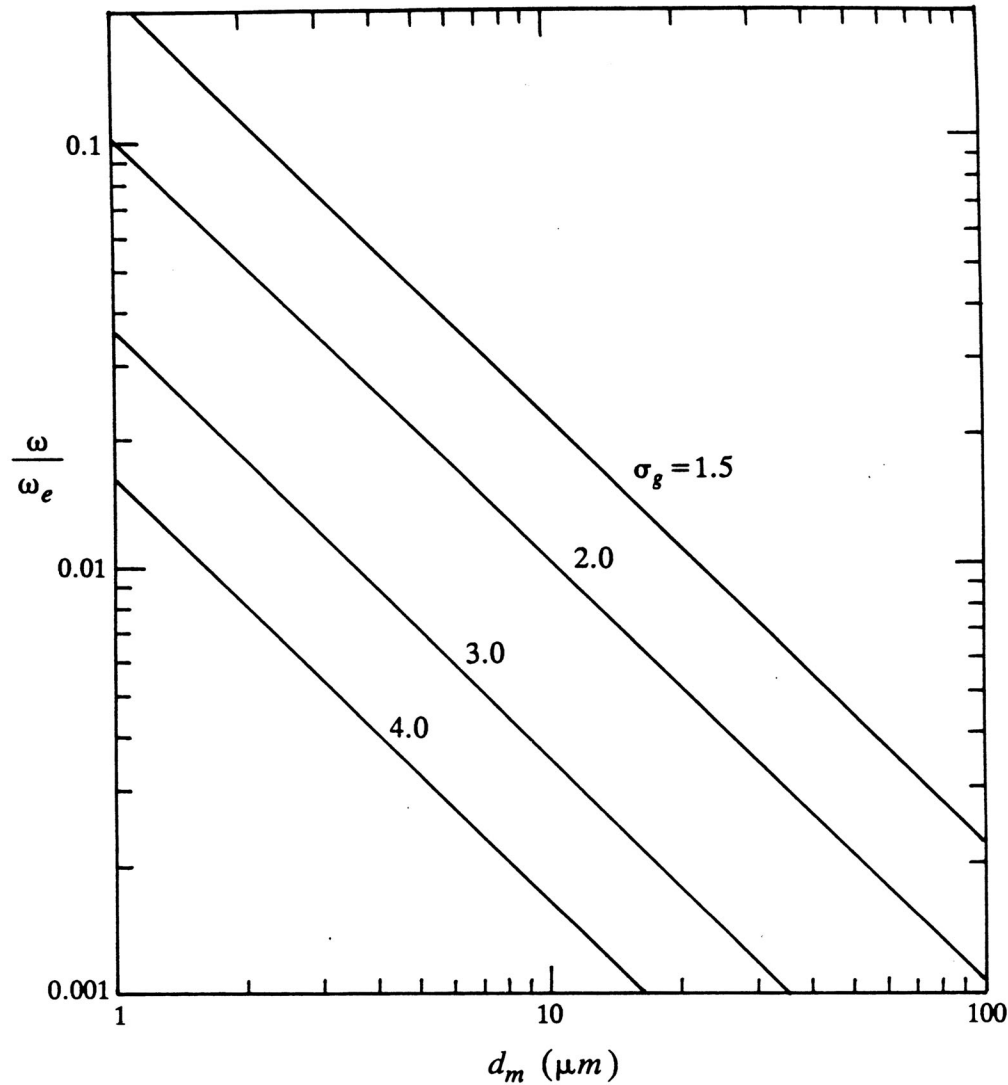

Fig.4.2-3 Collision similarity examination for solid particles

The results shown in Fig.4.2-3 are meaningful for the initial stage of flocculation, when large amounts of solid particles are present in suspension. As the flocculation process goes on, more and more flocs are formed. Therefore, we also need to examine the collision similarity for the stages in which large amounts of flocs are present in suspension. We note that, in this case, Eq.(4.2-11) is no longer valid because it is based on Stokes' law for the settling of solid particles. However, we can make use of the empirical expression for floc settling speeds which has a general form (see Section 5):

$$w_s = A d_f^m \qquad\qquad (4.2\text{-}19)$$

where d_f is the floc diameter, and A and m are experimental constants.

Then the average relative velocity between flocs in a disc is written as:

$$\overline{\Delta u_r} = d_m \mid \omega - m A d_m^{m-2} \overline{\Delta d} \mid \qquad \text{for } flocs \qquad (4.2\text{-}20)$$

So that,

$$\omega_e = m A d_m^{m-2} \mid \overline{\Delta d} \mid \qquad \text{for } flocs \qquad (4.2\text{-}21)$$

To give quantitative results for ω/ω_e, we use the empirical expression (Eq.(5-4)) for the settling speeds of drilling mud flocs from the disc flocculator tests, resulting in $\omega_e = 0.24\, d_m^{-0.562} \mid\overline{\Delta d}\mid$, and assume that the floc size distribution also follows the log-normal distribution law. The results for ω/ω_e as a function of d_m and σ_g are shown in Fig.4.2-4. For $\sigma_g = 4.0$, estimated from the experimental data, ω/ω_e ranges from 0.026 to 0.004 for the floc median diameter ranging from 30 to 2000 μm.
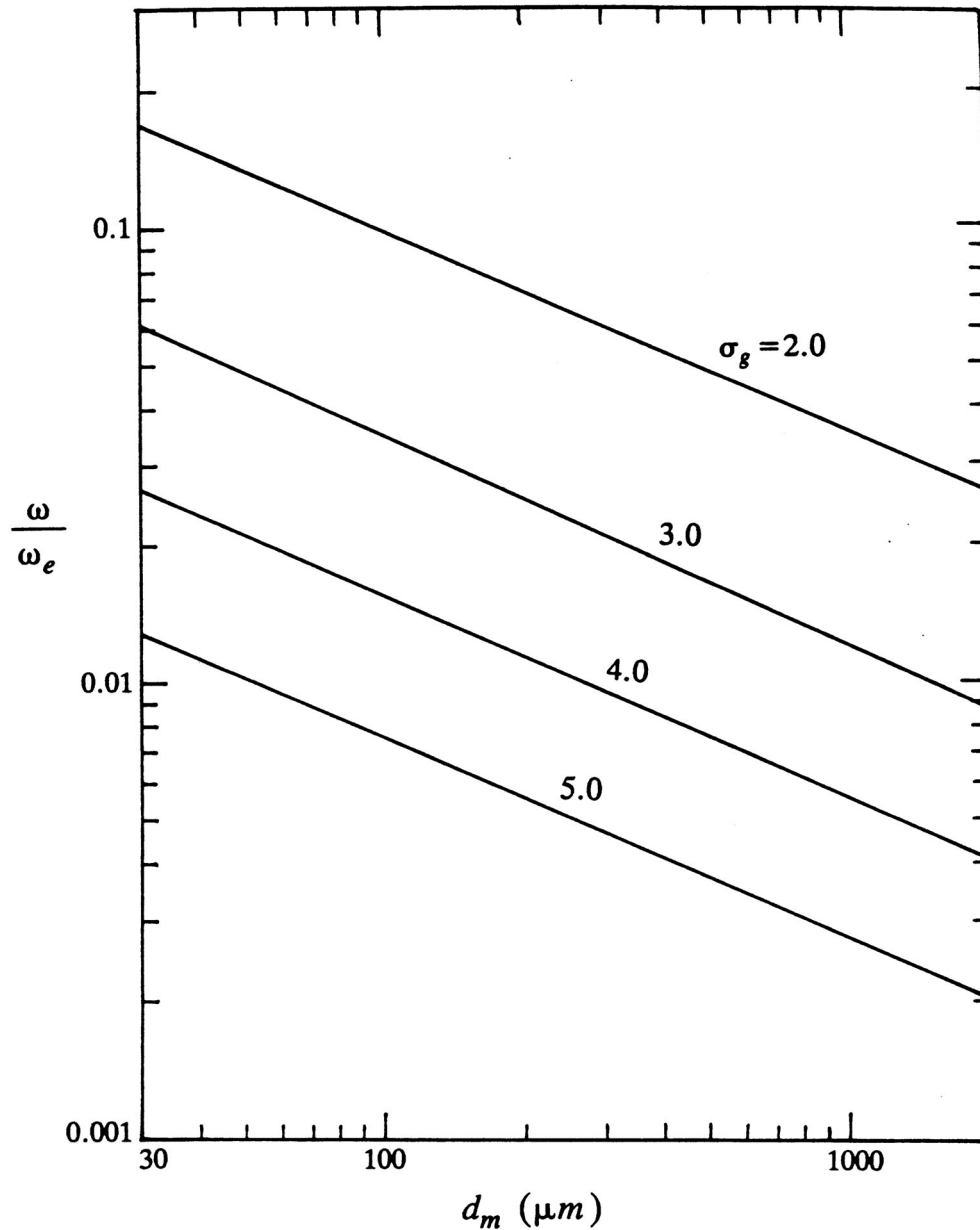
Fig.4.2-4 Collision similarity examination for flocs

From the above analysis, we may conclude that for the low rotation rate (e.g., $T = 25\ s$) of the discs, collision similarity approximately exists for the whole flocculation process.

In addition, collision similarity requires that the flocculation in a disc must be independent of the rotation rate of the disc. The above analysis has indicated that this will be true when the rotation rate is low. To examine this further, we did experiments in the small disc flocculator, using the

drilling mud at a concentration of 100 *mg/l* and at rotation periods of 25, 50, 100, and 160 *s*. The results are shown in Fig.4.2-5. We can see from this figure that the rotation rate does not have an effect on flocculation. This is consistent with the theoretical analysis.
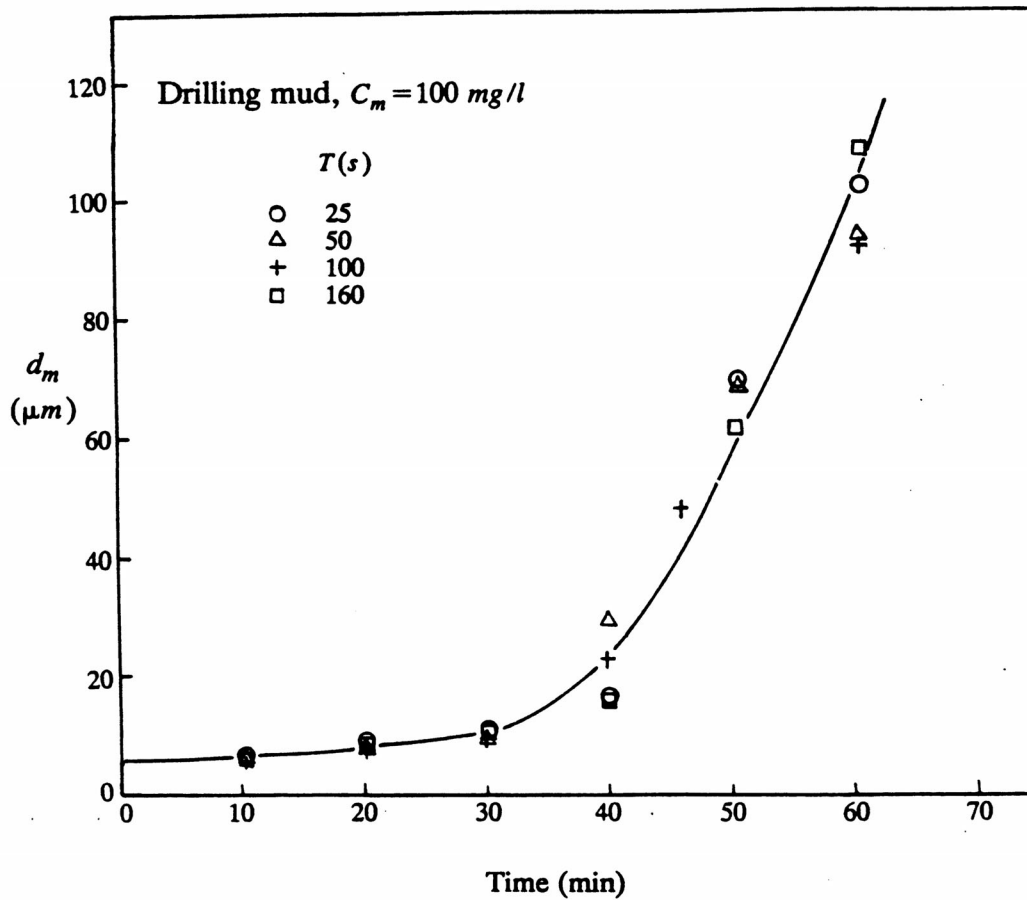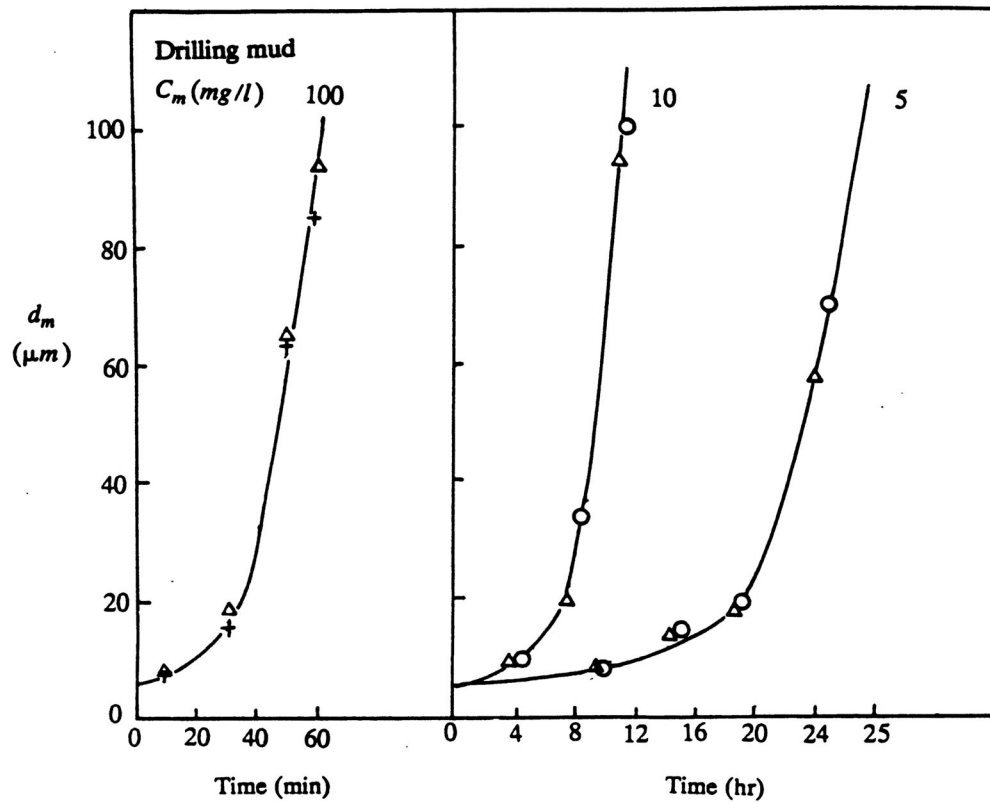

Fig.4.2-5 Examination of the effect of the rotating speed of the disc on flocculation. (*T* is the rotation period)

However, we noticed in the tests that, when flocs became bigger, they might settle down on the bottom of the disc if the rotation rate was too low. The criteria for choosing the rotation rate may therefore be stated as the rotation rate must be small enough to satisfy dynamical and collision similarity and large enough to avoid large flocs settling down on the bottom. Eventually, we chose rotation periods of 30 s and 25 s for the big disc and for the medium and small discs respectively.

Scale Effects
The third question is answered by doing experiments using the three discs with different sizes. Fig.4.2-6 shows data for the time variation of the floc median diameter at concentrations of 5, 10, and 100 *mg/l* using these three disc flocculators. We can see from this figure that, for these conditions, the scale of the discs has no effect on flocculation. However, when the concentration

was as low as 1 or 2 *mg/l*, we found that there were differences in results between the big and medium or small discs. For the medium or small discs, only a few flocs were formed during the flocculation process and these flocs seemed to be smaller than those in the big disc. With only a few flocs, it was difficult to measure the median size or size distribution so as to obtain statistically meaningful data. Therefore, most of the tests were conducted using the small disc for solid concentrations greater than 5 *mg/l* , and the big disc was mainly used for concentrations of 1 and 2 *mg/l*.

Fig.4.2-6 Examination of the disc scale effect on flocculation, using: o — big disc, △ — small disc, and + — medium disc

Procedure

The experimental procedures for the disc flocculator tests were essentially similar to those for the Couette flocculator tests. In doing the experiments, the sediment samples were mixed with filtered sea water (which was from the Santa Barbara Channel with a salinity of 33.4) or tap water at a known concentration. The sediments were first disaggregated in a blender, and were then put into a disc flocculator. The disc was run at a constant rotation rate. At certain time intervals (such as 10 or 20 minutes, or several hours, depending on the solid concentration), the disc was stopped and samples were withdrawn from the disc for particle size measurements using a Malvern Particle Sizer 3600E. Then the disc was filled and run again. This procedure

was continued until the floc median diameter reached about 100 µ*m*, beyond which the Malvern could not be used to measure floc sizes. The reasons for this are that, first, when the flocs were big, the floc breakage became severe both during sampling with a pipette due to fluid shear and during the measurement in the cell of the Malvern due to stirring; second, when we stopped the disc to sample, big flocs settled down too fast to catch them; third, the size range that the Malvern can measure is 1 to 500 µ*m*, corresponding to a maximum median diameter of about 200 µ*m*. In the disc flocculator tests, floc sizes may be as large as 1 mm in the steady state. Therefore, when floc median sizes were greater than 100 µ*m*, the disc was kept running without sampling until the steady state was reached. During the steady state, pictures were taken using a microscope with either a 6.66- or a 4.6-fold magnification lenses. The floc median diameters at the steady state were then estimated by measuring floc sizes from the pictures, calculating the volumes of flocs, and performing a frequency analysis.

In the disc flocculator tests, the applied fluid shear is not a parameter, and the only flocculation parameter is solid concentration. In order to examine the effects of solid concentration on flocculation, we did tests at solids concentrations of 1, 2, 5, 10, 25, 50, 100, and 200 *mg/l*. Both the drilling mud and Detroit River sediment were used in the tests. Seawater was used in the drilling mud tests, while both seawater and fresh water were used in the Detroit River sediment tests.

Results and Discussion

Median Diameters

Figs.4.2-7 to 4.2-9 show the time variation of floc median diameter for the drilling mud in seawater, and for the Detroit River sediment in seawater and in fresh water respectively. Due to the three reasons mentioned above, these time variation curves are limited to floc median diameters less than 100 µ*m*.
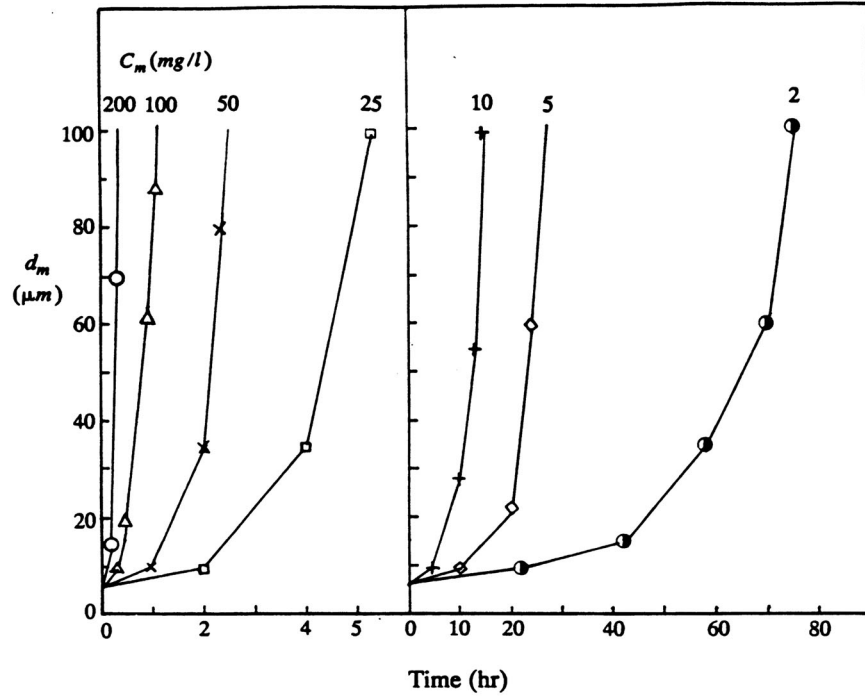
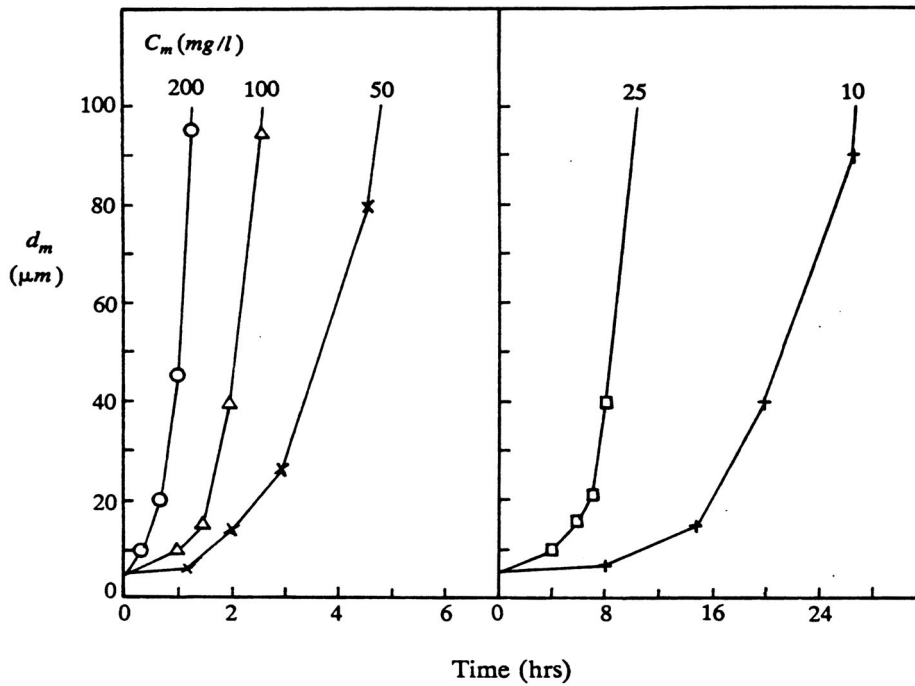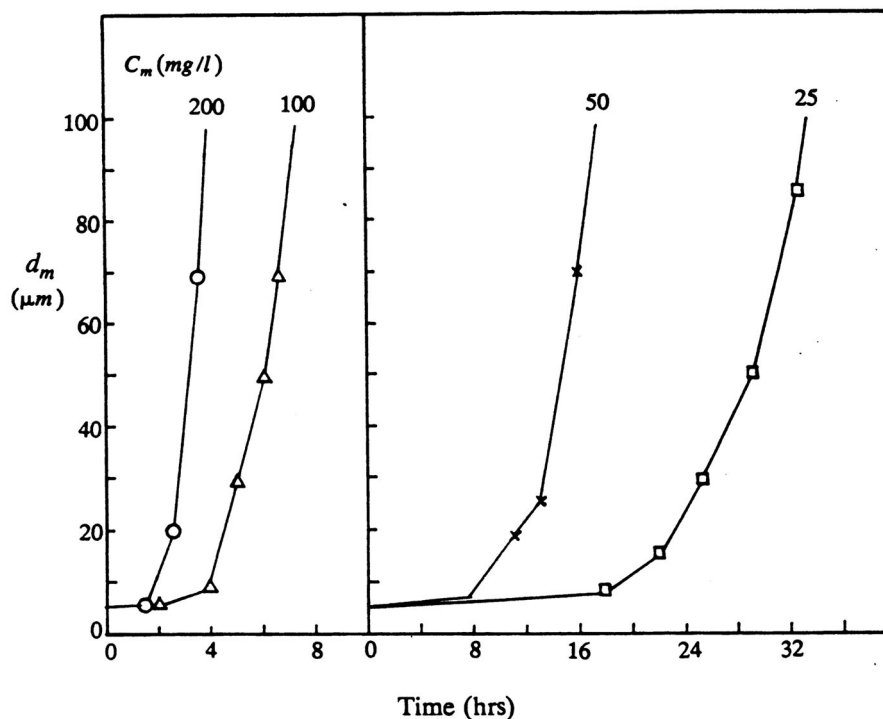**Fig.4.2-7 Time variation of the floc median diameter for the drilling mud in the disc flocculator tests**

Fig.4.2-8 Time variation of the floc median diameter for the Detroit River sediment in the disc flocculator tests (untreated samples in seawater)

**Fig.4.2-9 Time variation of the floc median diameter for the
Detroit River sediment in the disc flocculator tests
(untreated samples in fresh water)**

For the Detroit River sediment, we have noticed from Figs.4.2-8 and 4.2-9 that flocculation takes place much faster in seawater than in fresh water. This is because the electric double layer of charges, which contributes to the repulsive forces between particles, becomes much thinner in seawater than in fresh water, and consequently, the positive potential energy is much reduced. Therefore, the probability of cohesion of colliding particles is greater in seawater than that in fresh water.

Although the applied fluid shear (which is one of the main factors contributing to floc breakage in the Couette flocculator tests) is not present in a disc flocculator test, floc breakage could occur due to collisions between particles and due to fluid shear induced by the settling of flocs. Therefore, similar to the flocculation in a Couette flocculator, the flocculation in a disc flocculator is also a dynamic process in which floc growth and breakage continuously take place, and a dynamic equilibrium (i.e. steady state) will be eventually established. This is true particularly for tests at high solid concentrations such as 50, 100, and 200 *mg/l.* At very low concentrations such as 1, 2, or 5 *mg/l,* a quasi-steady state flocculation may exist. The data for the steady state floc median diameters were obtained and are shown in Table 4.2-1.

68

**Table 4.2-1 Steady state diameters (*mm*) of flocs from
the disc flocculator tests (untreated samples)**

Sediment	Solid concentration (*mg/l*)							
	1	2	5	10	25	50	100	200
DM-S	5.56*	4.48*	1.34	1.26	1.20	1.09	1.02	0.90
DR-S	7.60*	5.33*	4.50*	1.50	1.00	0.70	0.37	0.29
DR-F	–	–	5.97*	3.00*	0.42	0.41	0.39	0.36

Note: * --these data are only approximations due to a few flocs at low concentrations.
　　　DM-S --drilling mud in seawater.
　　　DR-S --Detroit River sediment in seawater.
　　　DR-F --Detroit River sediment in fresh water.

Time Scales

The time to reach the steady state is a very useful time scale to characterize the flocculation process. In the Couette flocculation tests, the time to reach the steady state is determined from the time variation curves of floc median diameter. In the disc flocculator tests, because we could not use the Malvern to measure the floc sizes during the whole flocculation process, we only obtain the time variation curves for the median diameters less than 100 μm. Consequently, the data for the time to reach the steady state can not be obtained from these limited time variation curves but were estimated roughly by observations (Table 4.2-2).

**Table 4.2-2 Time (*hrs*) to reach the steady state of flocculation
in the disc flocculator tests (untreated samples)**

Sediment	Solid concentration (*mg/l*)							
	1	2	5	10	25	50	100	200
DM-S	240	140	50	24	9	4.4	1.8	0.7
DR-S	220	165	110	48	14	7.2	4.4	2.5
DR-F	–	–	600	150	58	29.2	12.0	6.2

Note: DM-S --drilling mud in seawater.
　　　DR-S --Detroit River sediment in seawater.
　　　DR-F --Detroit River sediment in fresh water.

On the other hand, data for two other flocculation time scales T_{10} and $T_{1/10}$ can be obtained from the time variation curves of floc median diameter for the purpose of characterizing the flocculation process. T_{10} is defined as the time at which the floc median diameter becomes 10 times that of the primary solid median diameter (d_{m0}), that is:

$$d_m(T_{10}) = 10d_{m0} \tag{4.2-22}$$

$T_{1/10}$ is defined as the time at which the floc median diameter becomes one tenth of the floc median diameter at the steady state, that is:

$$d_m(T_{1/10}) = 0.1d_{ms} \tag{4.2-23}$$

where d_{ms} is a floc median diameter at the steady state and is a function of the solid concentration C_m. Therefore, both $T_{1/10}$ and $d_m(T_{1/10})$ vary with solid concentration.

The data for T_{10} are shown in Table 4.2-3 and in Figs.4.2-10 to 4.2-12 and can be fitted by a power law as follows:

$$T_{10} = 166.68\, C_m^{-1.145} \qquad \text{for } \textit{drilling mud in seawater} \tag{4.2-24}$$

$$T_{10} = 145.54 C_m^{-0.914} \qquad \text{for } \textit{Detroit River sediment in seawater} \tag{4.2-25}$$

$$T_{10} = 1002.6 C_m^{-1.096} \qquad \text{for } \textit{Detroit River sediment in fresh water} \tag{4.2-26}$$

where T_{10} is in *hrs* and C_m is in *mg/l*. The correlation coefficients are 0.9981, 0.9950 and 0.9984 respectively.

Table 4.2-3 T_{10} (*hrs*) **for the disc flocculator**
tests (untreated samples)

| Sediment	Solid concentration (*mg/l*)							
	1	2	5	10	25	50	100	200
DM-S	144*	70	24	13.5	4.4	2.2	0.9	0.33
DR-S	–	96*	60*	20.0	7.0	3.6	2.2	1.25
DR-F	–	–	288*	72*	29.0	14.6	6.0	3.10

Note: * --these data are T_2 (see Table 4.2-5) and are listed here for comparison.
  DM-S --drilling mud in seawater.
  DR-S --Detroit River sediment in seawater.
  DR-F --Detroit River sediment in fresh water.
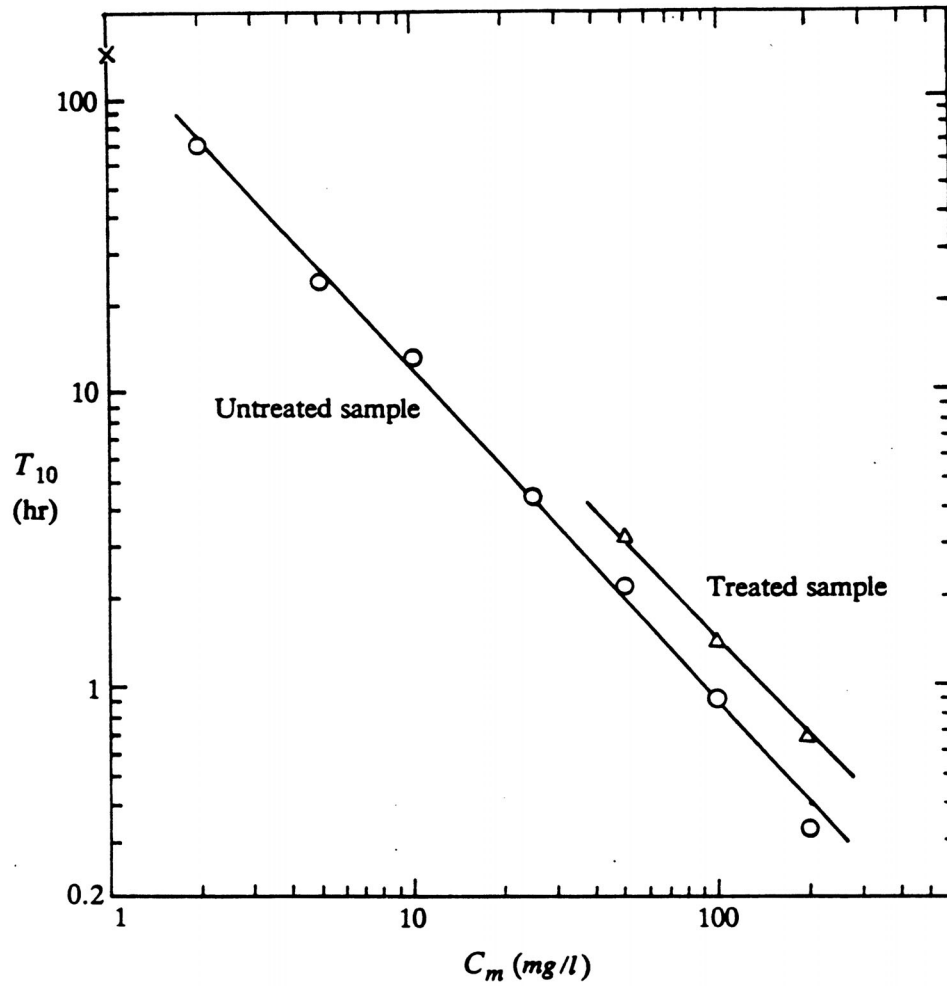
Fig.4.2-10 $T_{10} \sim C_m$ **relationship for the untreated and treated drilling mud in seawater in the disc flocculator tests. For comparison, the data for T_2 of untreated samples are also shown in this figure as $\times$.**
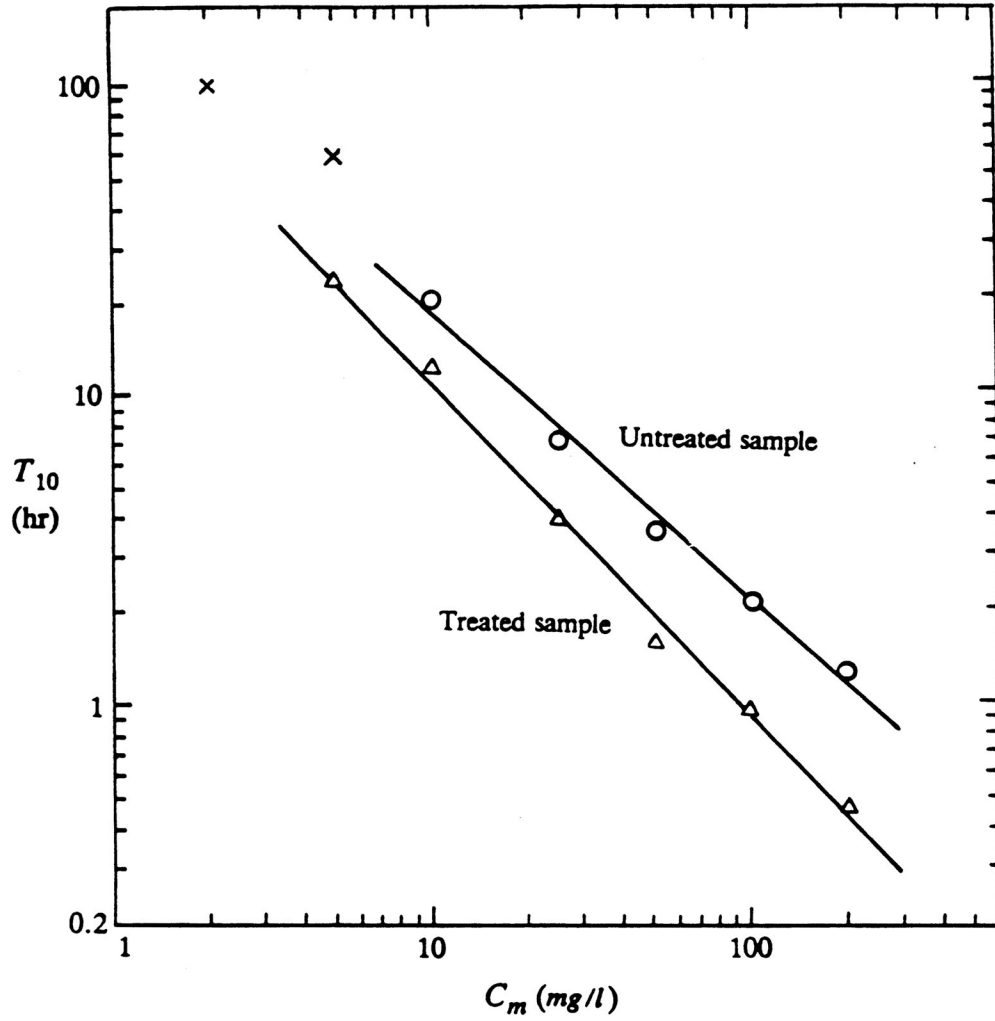
Fig.4.2-11 $T_{10} \sim C_m$ **relationship for the untreated and treated Detroit River sediment in seawater in the disc flocculator tests. For comparison, the data for T_2 of untreated samples are also shown in this figure as ×.**
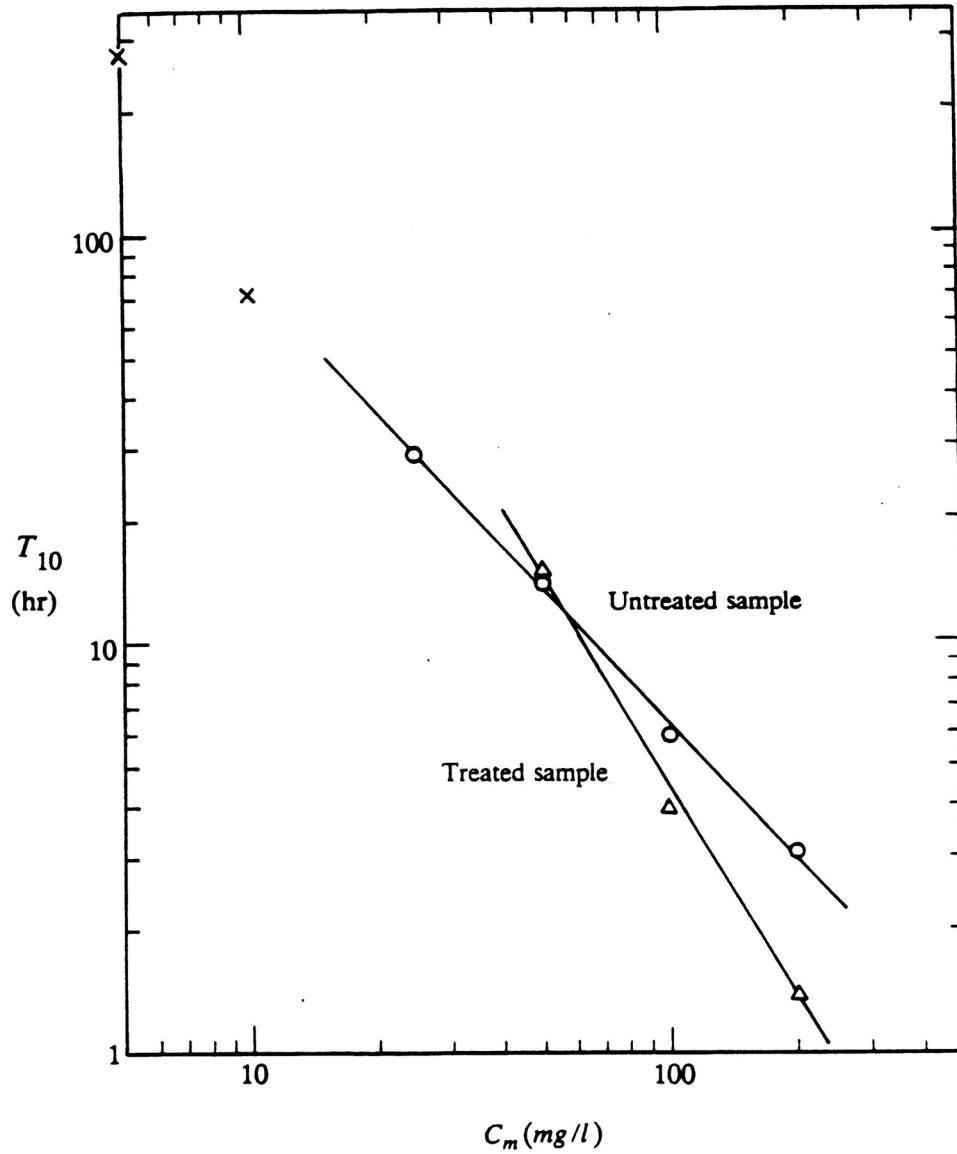
Fig.4.2-12 $T_{10} \sim C_m$ **relationship for the untreated and treated Detroit River sediment in fresh water in the disc flocculator tests. For comparison, the data for T_2 of untreated samples are also shown in this figure as ×.**

The data for $T_{1/10}$ are shown in Table 4.2-4 and in Figs.4.2-13 to 4.2-15 and can also be fitted by a power law as follows:

$$T_{1/10} = 221.78\, C_m^{-1.174} \qquad \text{for } drilling \ mud \ in \ seawater \qquad (4.2\text{-}27)$$

$$T_{1/10} = 452.64 C_m^{-1.169} \qquad \text{for } Detroit \ River \ sediment \ in \ seawater \qquad (4.2\text{-}28)$$

$$T_{1/10} = 1031.3 C_m^{-1.116} \qquad \text{for } Detroit \ River \ sediment \ in \ fresh \ water \ (4.2\text{-}29)$$

where $T_{1/10}$ is in *hrs* and C_m is in *mg/l*. The correlation coefficients are 0.9962, 0.9972 and 0.9975 respectively.

**Table 4.2-4 $T_{1/10}$ (*hrs*) for the disc flocculator
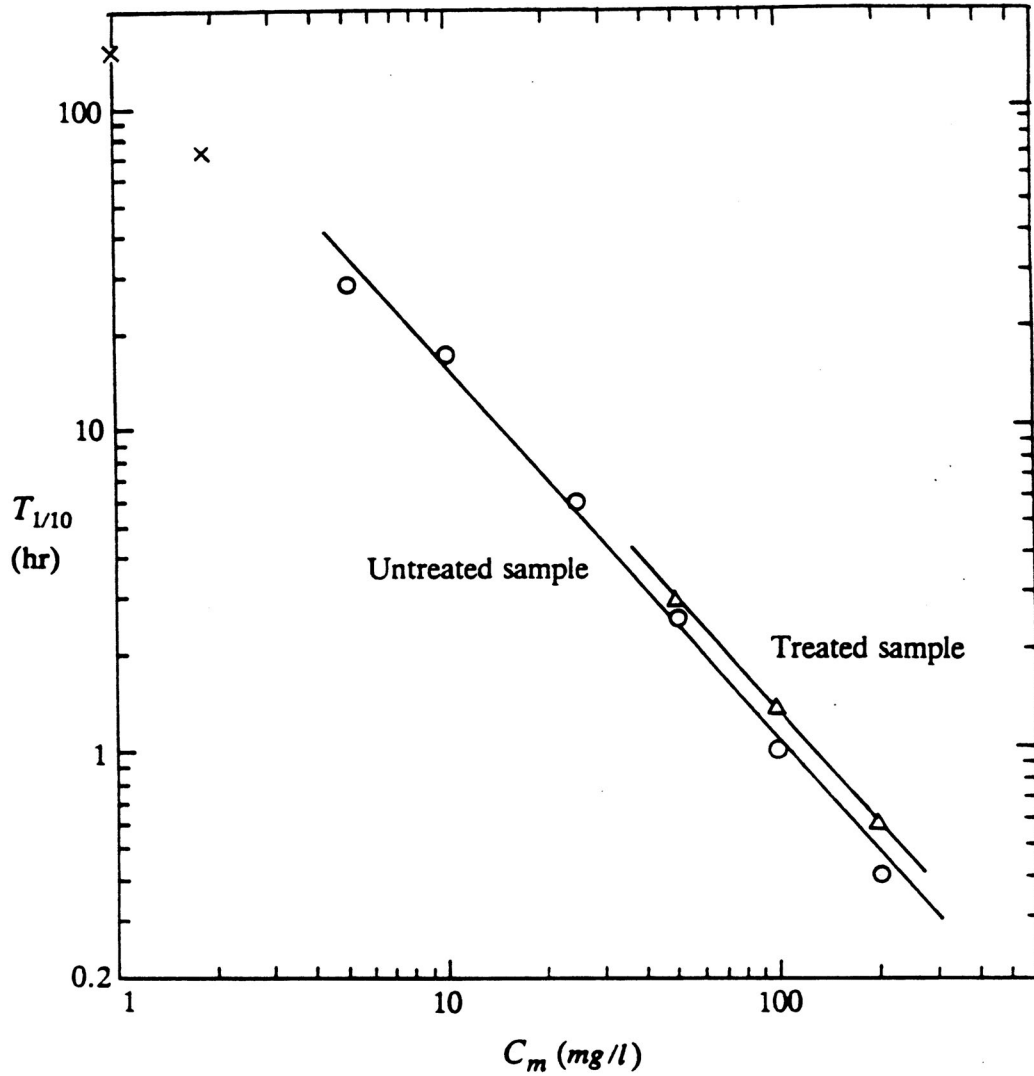tests (untreated samples)**

Sediment	Solid concentration (*mg/l*)							
	1	2	5	10	25	50	100	200
DM-S	144*	72*	27.5	16.4	5.8	2.5	1.0	0.38
DR-S	–	96*	60*	28.5	10.8	5.5	1.9	0.90
DR-F	–	–	288*	72*	28.0	14.0	5.5	2.9

Note: * --these data are T_2 (see Table 4.2-5) and are listed here for comparison.
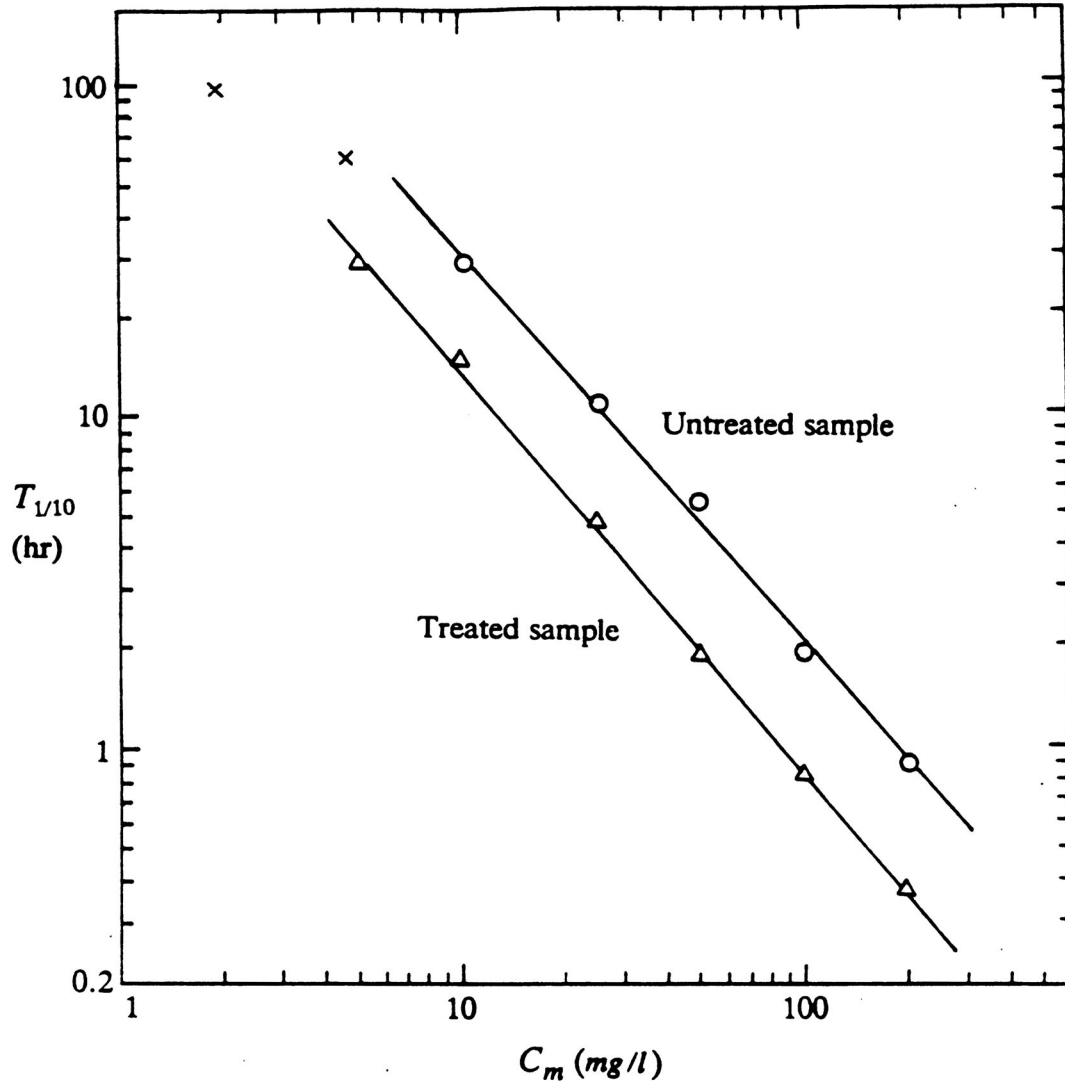   DM-S --drilling mud in seawater.
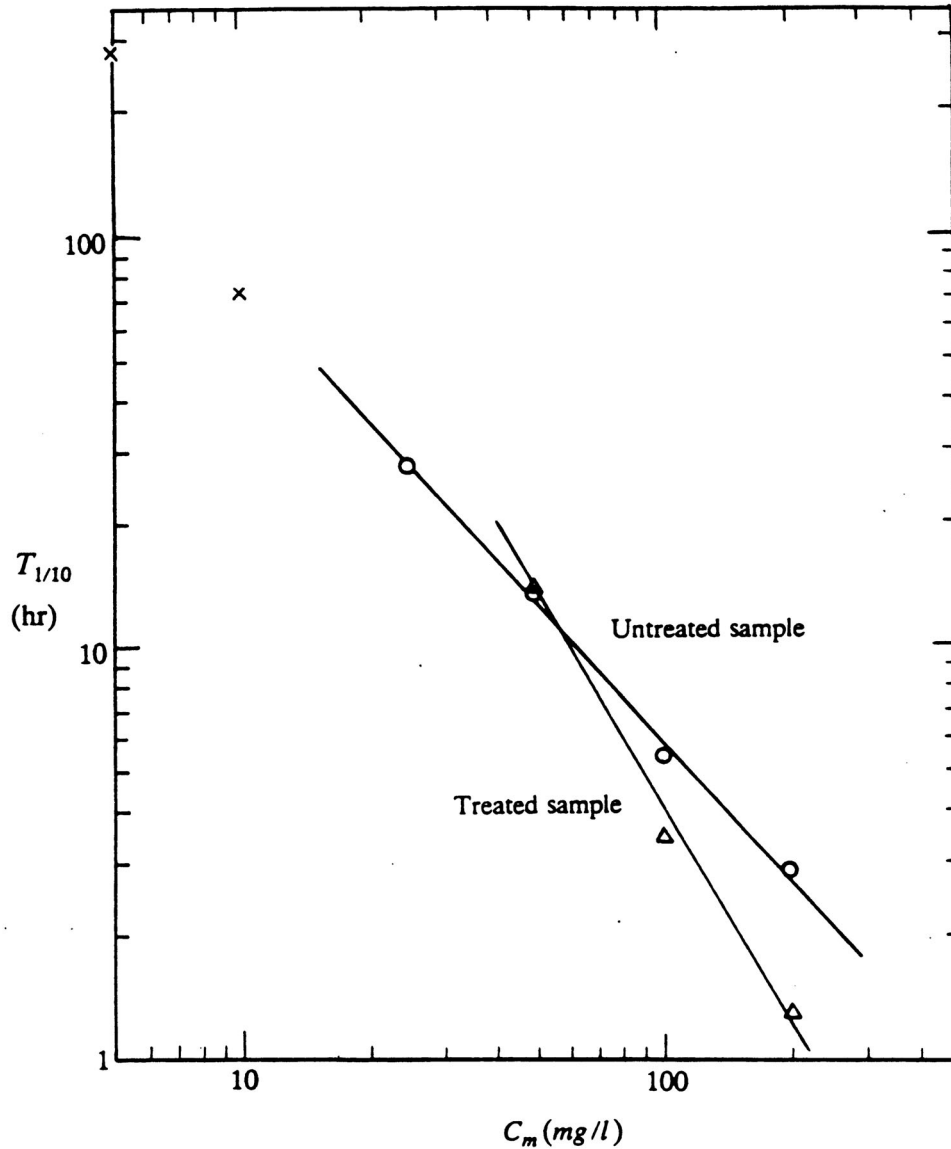   DR-S --Detroit River sediment in seawater.
    DR-F --Detroit River sediment in fresh water.

Fig.4.2-13 $T_{1/10} \sim C_m$ **relationship for the untreated and treated drilling mud in seawater in the disc flocculator tests. For comparison, the data for T_2 of untreated samples are also shown in this figure as $\times$.**

Fig.4.2-14 $T_{1/10} \sim C_m$ **relationship for the untreated and treated Detroit River sediment in seawater in the disc flocculator tests. For comparison, the data for T_2 of untreated samples are also shown in this figure as** ×.

Fig.4.2-15 $T_{1/10} \sim C_m$ **relationship for the untreated and treated Detroit River sediment in fresh water in the disc flocculator tests. For comparison, the data for T_2 of untreated samples are also shown in this figure as ×.**

We have noticed that in the Couette flocculator tests, the time to reach the steady state is about twice T_{10}. This is also a good approximation for the disc flocculator tests at high solid concentrations such as 50, 100, 200 *mg/l*. We have also noticed that $T_{1/10}$ is not much different from T_{10} for the disc flocculator tests, and within the experimental error, the time to reach the steady state is also about twice $T_{1/10}$.

In addition, in a test at a low solid concentration such as 1, 2, or 5 *mg/l*, only a few flocs were formed and the floc median diameters measured from the Malvern remained less than 10 μ*m*

even though the test had been run for more than 10 days. In this case, neither the data for T_{10} nor for $T_{1/10}$ were obtained. Instead, we determined another time scale T_2 (see Table 4.2-5) by observations. T_2 is defined as the time at which a floc with a diameter of 2 mm was observed. For comparison with T_{10} and $T_{1/10}$, the data for T_2 are also shown in Tables 4.2-3 and 4.2-4, and in Figs.4.2-10 to 4.2-15. It is interesting to note from Figs.4.2-10 to 4.2-15 that, T_2 is very close to the extrapolation lines of T_{10} or $T_{1/10}$. This may suggest that T_2 is somewhat equivalent to T_{10} or $T_{1/10}$.

Table 4.2-5 Some characteristics of flocculation in disc flocculator tests at low solid concentrations

	C_m (mg/l)	Floc No.	Floc size (mm)	R_m (% Wt)	R_v (%)	T_2 (day)	T_T (day)	w_{sm} (cm/s)
DM-S	1"	10	2.0-7.0	4.2	96.6	6	13	1.45
	2'	2	4.5,0.8	17.4	98.9	3	9	1.26
DR-S	1"	2	7.0,8.0	3.7	97.5	–	11	1.18
	2"	20	1.0-7.0	3.0	93.6	4	12	1.02
	5'	1	4.5	5.5	96.8	2.5	11	1.10
DR-F	5"	50	2.0-8.5	3.9	90.4	12	28	2.88
	10'	1	3.0	3.8	81.8	3	14	2.21

Note: DM-S --drilling mud in seawater.
   DR-S --Detroit River sediment in seawater.
   DR-F --Detroit River sediment in fresh water.
   " --the test in the big disc flocculator.
   ' --the test in the small disc flocculator.
   Floc No. --the number of flocs observed in a disc.
   R_m --the ratio of the solid mass in the flocs to the total solid mass in a disc.
   R_v --the ratio of the volume of the flocs to the volume of all particles in a disc.
   T_2 --the time at which a floc with a diameter of 2 mm was observed.
 T_T --the period of running a test.
 w_{sm} --the settling speed of a maximum floc in a disc.

Discussion

The results from the disc flocculator tests have shown that the floc median diameter is a function of solid concentration as well as time. For each test, it can be seen that the median diameter of flocs increases relatively slowly for a period of time and then very rapidly. Compared with tests in the Couette flocculator where fluid shear is dominant, particles flocculate much slower in the disc flocculators, much longer times are needed to reach the steady state, and the floc sizes at the steady state are much larger. This is because the frequency of collisions between particles is much reduced when an applied fluid shear is not present. Moreover, the breakage of flocs in a disc is mainly due to collisions between flocs and the surface erosion of small particles (flocs) by the shear stress induced by the settling of the flocs. Collision effects on the breakage will become small as the solid concentration gets low. In this situation, floc sizes in the steady state may be dominated by surface erosion.

For comparison, Fig.4.2-16 shows the steady state median diameters of the drilling mud flocs from both disc and Couette flocculator tests as a function of fluid shear with solid concentration as a parameter. Similar to Fig.4.2-16, Fig.4.2-17 shows a comparison of steady state median diameters of the Detroit River sediment flocs from both disc and Couette flocculator tests. We can see from these figures that fluid shear has a significant effect on floc size. As the applied fluid shear approaches zero (i.e., in the disc flocculator tests), floc size increases dramatically.
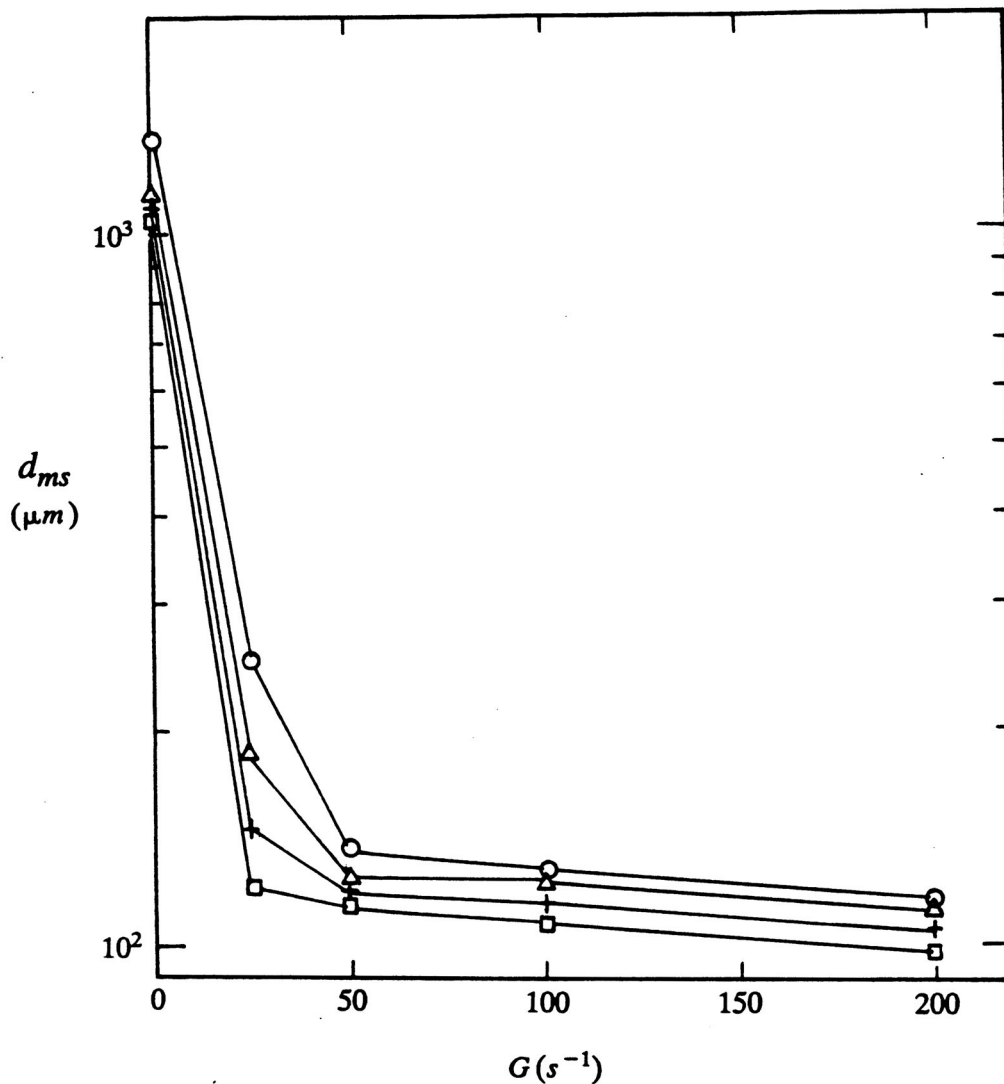
Fig.4.2-16 **Comparison of steady state median diameter of drilling mud flocs from disc and Couette flocculator tests. Solid concentration: o --5, △ --10, + --25, □ --50** *mg /l*
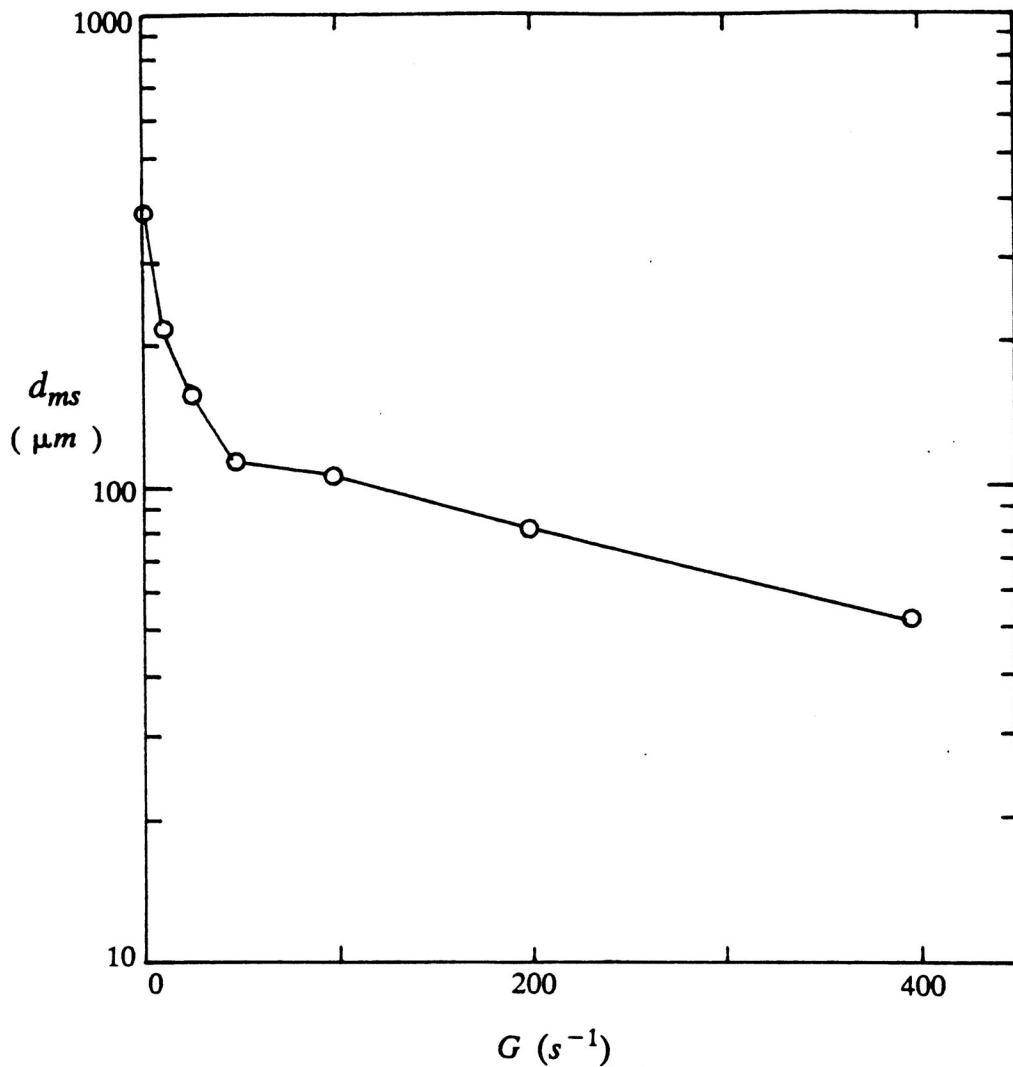
Fig.4.2-17 Comparison of steady state median diameter of Detroit River sediment flocs from disc and Couette flocculator tests in fresh water at solid concentration of 100 *mg/l* . Data at *G* = 100, 200, and 400 *s*⁻¹ are from Burban et al. (1989)

It should be noted that at very low concentrations such as 1, 2, or 5 *mg/l*, flocculation took place very slowly, very few flocs were formed in suspension, and large amounts of solid particles remained unflocculated even after they had been suspended in a disc for more than 10 days. This was determined both from direct observations and from measurements of the size distribution using the Malvern. These measurements showed that the median diameters of most suspended particles remained below 10 μ*m* even for a running period of more than 10 days. On the other hand, a few very porous flocs were usually formed at these low concentrations. The sizes and densities of these flocs probably increased slowly by sweeping small particles as they were settling. After about 10 days of running an experiment, these flocs were as large as 5 to 8 mm

and still had a loose structure. The solid mass contained in these flocs was only a small portion of the total solid mass in the disc. The solid mass of a floc was determined by measuring the orbit of the floc in the disc and estimating the settling speed of the floc from $w_s = \omega r_o$ (where ω is the rotation rate of the disc, r_o is the distance from the orbit center to the axis of the disc); then the density of the floc was calculated by the method described in Section 6 using this settling speed. Table 4.2-5 shows some characteristics of flocculation in the disc flocculator tests at low solid concentrations. It is interesting to note from this table that, for all tests except the test for the drilling mud at a concentration of 2 *mg/l,* the solid mass in flocs was only 3.0 to 5.5% of the total solid mass in a disc; the volume of these flocs, however, was 81.8 to 98.9% of the total volume of all particles (flocs and solid particles) in the disc.

From the results of all tests at solid concentrations ranging from 1 to 200 *mg/*l, we note that a change in flocculation properties occurred at certain concentrations. These concentrations were 2 *mg/l* for the drilling mud, 5 *mg/l* for Detroit River sediments in seawater, and 10 *mg/l* for Detroit River sediments in fresh water. At concentrations equal to or lower than these values, large amounts of solid particles remained unflocculated even after they had been suspended in a disc for more than 10 days. On the other hand, at concentrations higher than these values, almost all solid particles could be flocculated and a steady state of flocculation could be eventually established. The former was demonstrated from size measurements using the Malvern. These measurements showed that in a test, when the floc median diameter reached about 100 µ*m,* the volume of particles less than 10 µ*m* were usually less than 3% of the total volume of particles in suspension. As time went on, these small particles would continually flocculate to form large flocs. So that, at the steady state, the volume of unflocculated solid particles might be much less than 3%.

4.3 EFFECTS OF ORGANIC COATINGS ON FLOCCULATION

The effects of organic coatings on flocculation were examined by doing experiments in disc flocculators using samples with the organic matter removed and then comparing these results with the previous tests where organic matter was naturally present. Both the drilling mud and Detroit River sediment samples were treated in this manner. The experimental procedures for the flocculation tests were the same as those described in subsection 4.2. In this subsection, we first describe the procedures for removing organic matter, then present the results from the tests using treated samples and compare them with the results from the tests using untreated samples (subsection 4.2).

Removal of Organic Matter

Organic matter removal was accomplished by treating samples with a sodium hypochlorite (NaOCl) solution. This method was proposed by Anderson (1963). He has demonstrated that this method is both efficient and rapid for the destruction of organic matter in samples, and accomplishes this without destruction of carbonates or removal of sesquioxide or silica coatings. Moreover, quantities of organic matter left in samples by this method are commonly less than remain after hydrogen peroxide (H_2O_2) treatment of samples (Anderson, 1963; Lavkulich and Wiens, 1970).

The sodium hypochlorite solution used in the treatment was obtained from the Fisher Scientific Company and contained 4 to 6% available chlorite. The treatment includes two steps as described in the following:

Step 1, oxidation of organic matter: A 20 ml sodium hypochlorite solution was added to an 8 g sediment sample in a 50 ml centrifuge tube. The pH of the solution was adjusted to 9.5 using hydrochloric acid. The tube was placed in a boiling water bath for 15 min, then centrifuged for 8 min at 800 rpm. The solution was decanted, and the treatment was repeated at least three times.

Step 2, washing and dispersing: A 40 ml 2 percent sodium carbonate-sodium bicarbonate solution with a pH of 9.5 was added to the sample in the centrifuge tube. The solution was stirred and heated in a boiling water bath for 10 min to promote flocculation. Then the tube was centrifuged for 10 min at 800 rpm. The solution was decanted, and the treatment was repeated for a total of three treatments. After the final decantation, the sample was shaken for 12 hr with distilled water. Finally, the samples were washed using filtered water (the same water as that used for flocculation tests) with the same procedures as above for the sodium carbon-sodium bicarbonate solution.

To examine the effectiveness of the NaOCl treatment on the removal of organic matter, samples were treated consecutively up to 6 times. At the end of each treatment, a small amount of the sediment was withdrawn from the centrifuge tube and later used for a CHN (C--carbon, H--hydrogen, N--nitrogen) analysis. The CHN analysis was performed by the Marine Science Institute (at UCSB) Analytical Lab using a Control Equipment Corporation Model 240XA.

Tables 4.3-1 and 4.3-2, and Figs.4.3-1 to 4.3-3 show the total CHN (including organic and inorganic CHN) contents of the drilling mud and Detroit River sediment after the consecutive NaOCl treatments. From these data, we can see that the CHN contents are significantly reduced at the end of the first treatment; as the treatment time increases, the CHN values approach constant values, which are considered to be the inorganic CHN contents in the sediments.

Table 4.3-1 Total carbon, hydrogen, and nitrogen contents (% *Wt*) of the drilling mud after consecutive NaOCl treatments

Component	Treatment (times)						
	0	1	2	3	4	5	6
Carbon	1.89	1.10	0.72	0.64	0.61	0.60	0.58
Hydrogen	0.60	0.40	0.38	0.38	0.37	0.36	0.34
Nitrogen	0.120	0.053	0.045	0.042	0.042	0.037	0.036

Table 4.3-2 Total carbon, hydrogen, and nitrogen contents (% *Wt*) of Detroit River sediment after consecutive NaOCl treatments
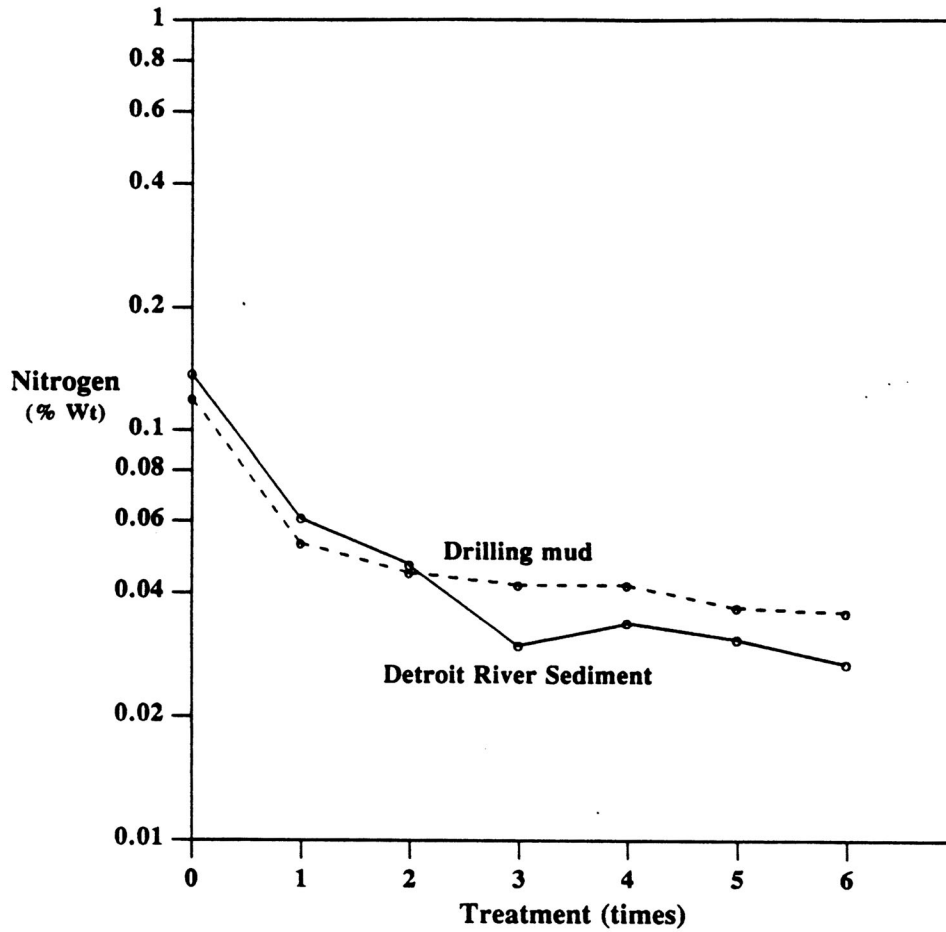
Component	Treatment (times)						
	0	1	2	3	4	5	6
Carbon	4.06	3.24	2.54	2.67	2.38	2.43	2.56
Hydrogen	0.56	0.40	0.39	0.34	0.31	0.29	0.27
Nitrogen	0.138	0.061	0.047	0.030	0.034	0.031	0.027
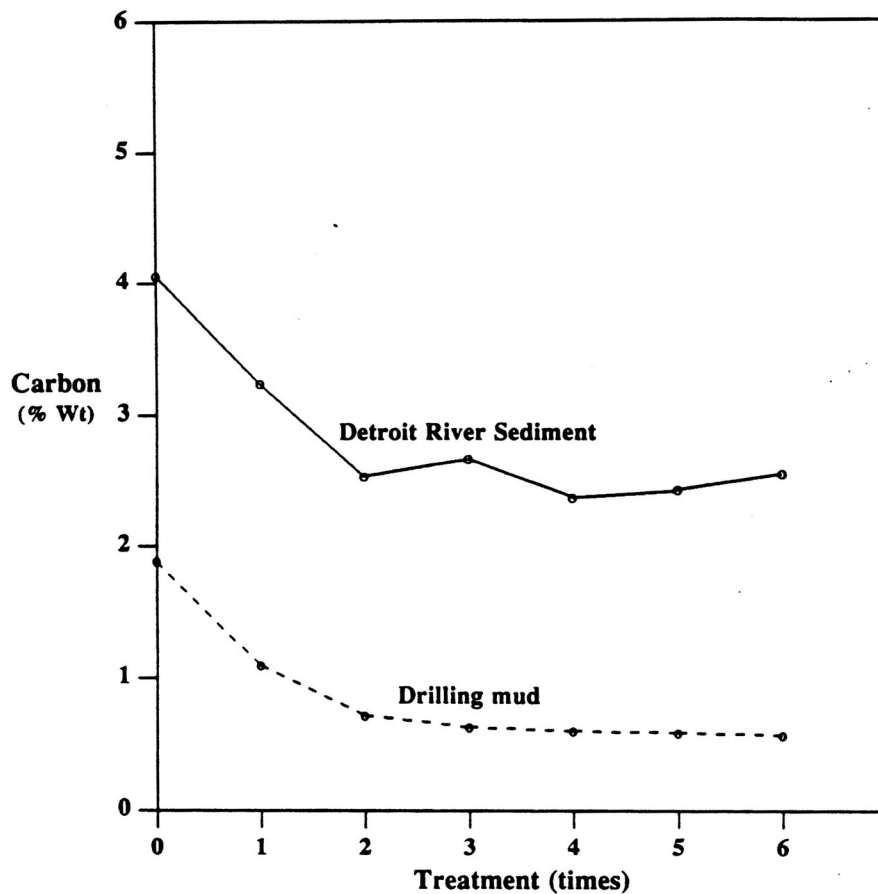
Fig.4.3-1 Total carbon contents of the sediments after consecutive NaOCl treatments
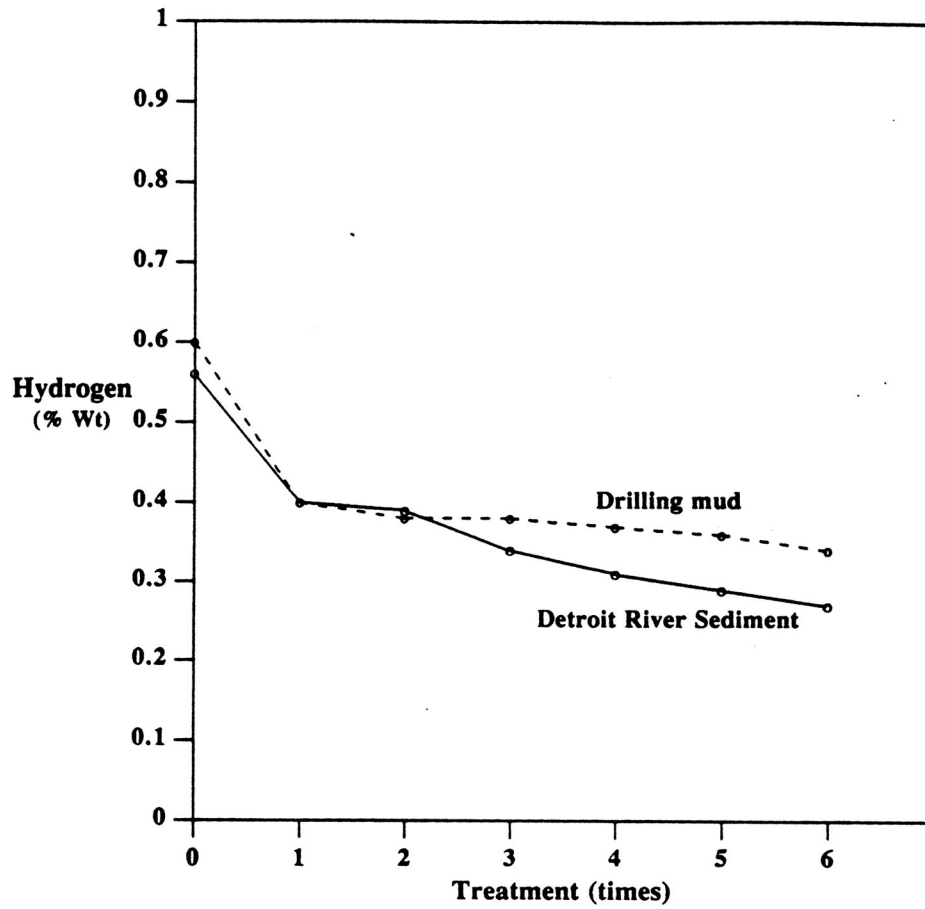
Fig.4.3-2 Total hydrogen contents of the sediments after consecutive NaOCl treatments

**Fig.4.3-3 Total nitrogen contents of the sediments
after consecutive NaOCl treatments**

Table 4.3-3 shows the organic CHN contents of the drilling mud and Detroit River sediment. From this table we can see that the Detroit River sediment contains 1.99 percent (by weight) organic matter (the sum of the organic carbon, hydrogen, and nitrogen); this is believed to be natural organic matter such as humic substances. The drilling mud contains 1.77 percent organic matter which are probably due to added polymers and organic matter from drilling cuttings.

Table 4.3-3 Organic matter contents (% *Wt*) of the sediments

| Sediment	Carbon	Hydrogen	Nitrogen
Drilling mud	1.29	0.24	0.24
Detroit River sediment	1.60	0.28	0.11

Results and Discussion

Drilling Mud

Fig.4.3-4 shows the time variation of the floc median diameter for the treated drilling mud in the disc flocculator tests. Fig.4.3-5 shows the comparison of the time variation of the floc median diameter for the treated and untreated samples. The data for the floc median diameters less than 100 μm were from the Malvern Particle Sizer measurements and are very accurate. The curves shown in Fig.4.3-5 are approximate and are determined by fitting the data for floc median diameters less than 100 μm and the data for floc median diameters in the steady states. The floc median diameters at the steady states are determined from the photographs as described in subsection 4.2 and shown in Table 4.3-4. The time to reach the steady state were estimated by observations and are shown in Table 4.3-5. The data for T_{10} are shown in Table 4.3-6 and can be fitted by a power law as follows:

$$T_{10} = 189.89 \, C_m^{-1.057} \qquad \textit{treated drilling mud in seawater} \qquad (4.3\text{-}1)$$

where T_{10} is in *hrs* and C_m is in *mg/l*. The correlation coefficient is 0.99997.
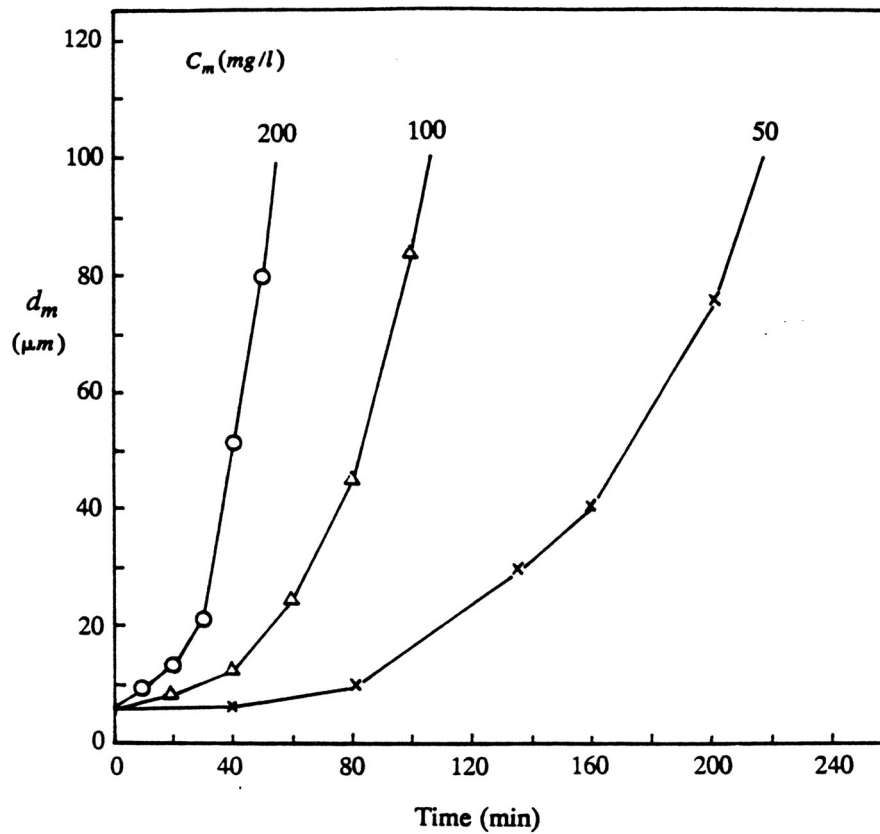
Fig.4.3-4 Time variation of the floc median diameter for the treated drilling mud in the disc flocculator tests
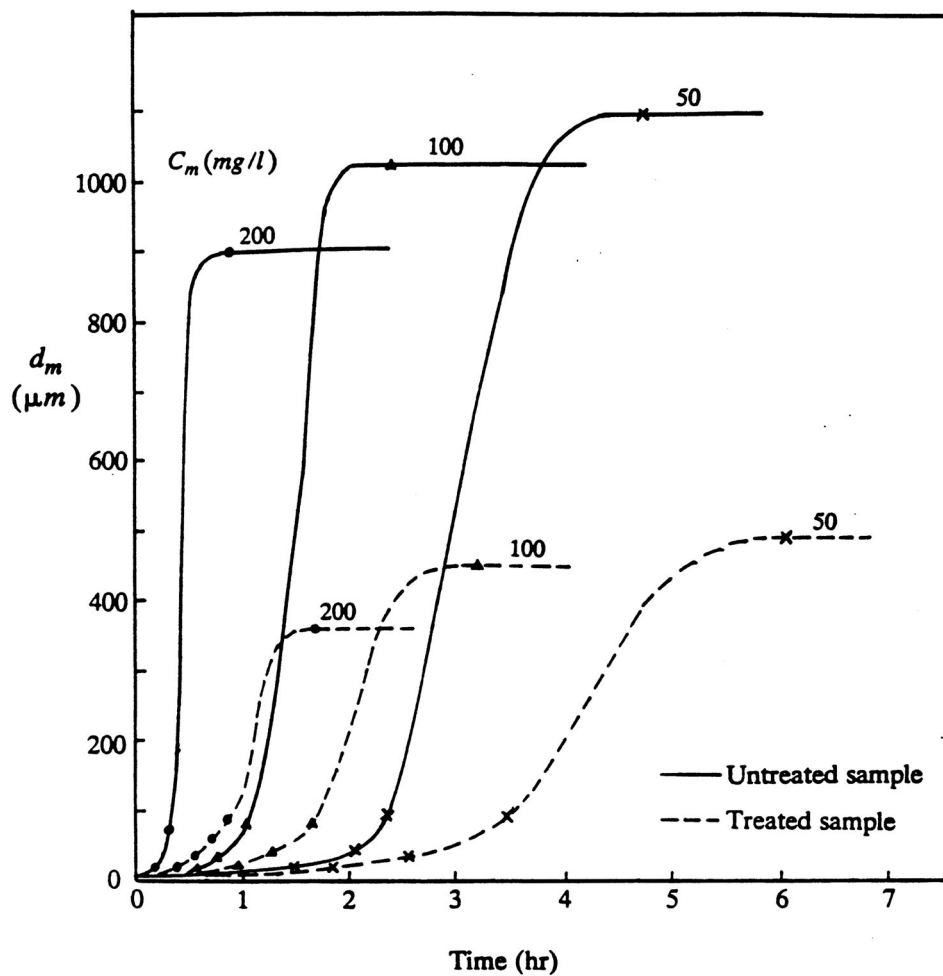
87

Fig.4.3-5 Comparison of the time variation of the floc median diameter for the treated and untreated drilling mud in the disc flocculator tests

Table 4.3-4 Steady state diameters (μm) of flocs from the disc flocculator tests (treated samples)

Sediment	Solid concentration (mg/l)					
	5	10	25	50	100	200
DM-S-T	–	–	–	490	450	360
DR-S-T	940	880	810	670	320	240
DR-F-T	–	–	–	450	350	300

Note: DM-S-T --treated drilling mud in seawater.
DR-S-T --treated Detroit River sediment in seawater.
DR-F-T --treated Detroit River sediment in fresh water.

Table 4.3-5 Time (hrs) to reach the steady state of flocculation in the disc flocculator tests (treated samples)

Sediment	Solid concentration (mg/l)					
	5	10	25	50	100	200
DM-S-T	–	–	–	6.0	3.0	1.4
DR-S-T	48	25	8	3.2	2.0	1.0
DR-F-T	–	–	–	30.0	8.0	2.8

Note: DM-S-T --treated drilling mud in seawater.
DR-S-T --treated Detroit River sediment in seawater.
DR-F-T --treated Detroit River sediment in fresh water.

Table 4.3-6 T_{10} (*hrs*) **for the disc flocculator tests (treated samples)**

Sediment	Solid concentration (*mg/l*)					
	5	10	25	50	100	200
DM-S-T	–	–	–	3.03	1.47	0.70
DR-S-T	23.7	12.5	3.95	1.58	0.97	0.47
DR-F-T	–	–	–	15.0	4.0	1.4

Note: DM-S-T --treated drilling mud in seawater.
      DR-S-T --treated Detroit River sediment in seawater.
      DR-F-T --treated Detroit River sediment in fresh water.

The data for $T_{1/10}$ are shown in Table 4.3-7 and can also be fitted by a power law as follows:

$$T_{1/10}=251.01\ C_m^{-1.143} \qquad \textit{treated drilling mud in seawater} \qquad (4.3\text{-}2)$$

where $T_{1/10}$ is in *hrs* and C_m is in *mg/l*. The correlation coefficient is 0.9996.

Table 4.3-7 $T_{1/10}$ (*hrs*) **for the disc flocculator tests (treated samples)**

Sediment	Solid concentration (*mg/l*)					
	5	10	25	50	100	200
DM-S-T	–	–	–	2.83	1.33	0.58
DR-S-T	28.0	14.6	4.78	1.83	0.83	0.37
DR-F-T	–	–	–	15.4	3.5	1.3

Note: DM-S-T --treated drilling mud in seawater.
      DR-S-T --treated Detroit River sediment in seawater.
      DR-F-T --treated Detroit River sediment in fresh water.

The comparisons of T_{10} and $T_{1/10}$ for treated and untreated samples are shown in Figs.4.2-10 and 4.2-13 respectively.

We can see from Figs.4.3-4 and 4.3-5 that, for the drilling mud, the treated samples flocculated slower than did the untreated samples, and the floc sizes at the steady state of the treated samples were much smaller than those of the untreated samples. This is probably due to small amounts of polymers such as drispac (a polyanionic cellulose polymer) contained in the drilling mud. Polymers at a very low concentration have the function of enhancing flocculation of mineral particles by a bridging mechanism (e.g., Gregory, 1989). After treatment by sodium hypochlorite, these polymers were removed.

Detroit River Sediment

Figs.4.3-6 and 4.3-7 show the time variation of the floc median diameter for the treated Detroit River sediment in the disc flocculator tests in seawater and in fresh water. Figs.4.3-8 and 4.3-9 show the comparison of the time variation of the floc median diameter for the treated and untreated samples. The curves in Figs.4.3-8 and 4.3-9 are obtained in the same way as that for the curves in Fig.4.3-5. The data for the steady state median diameters are shown in Table 4.3-4. The estimated time to reach the steady state are shown in Table 4.3-5. The data for T_{10} are shown in Table 4.3-6, and for $T_{1/10}$ in Table 4.3-7. The empirical expressions for T_{10} and $T_{1/10}$ are as follows:
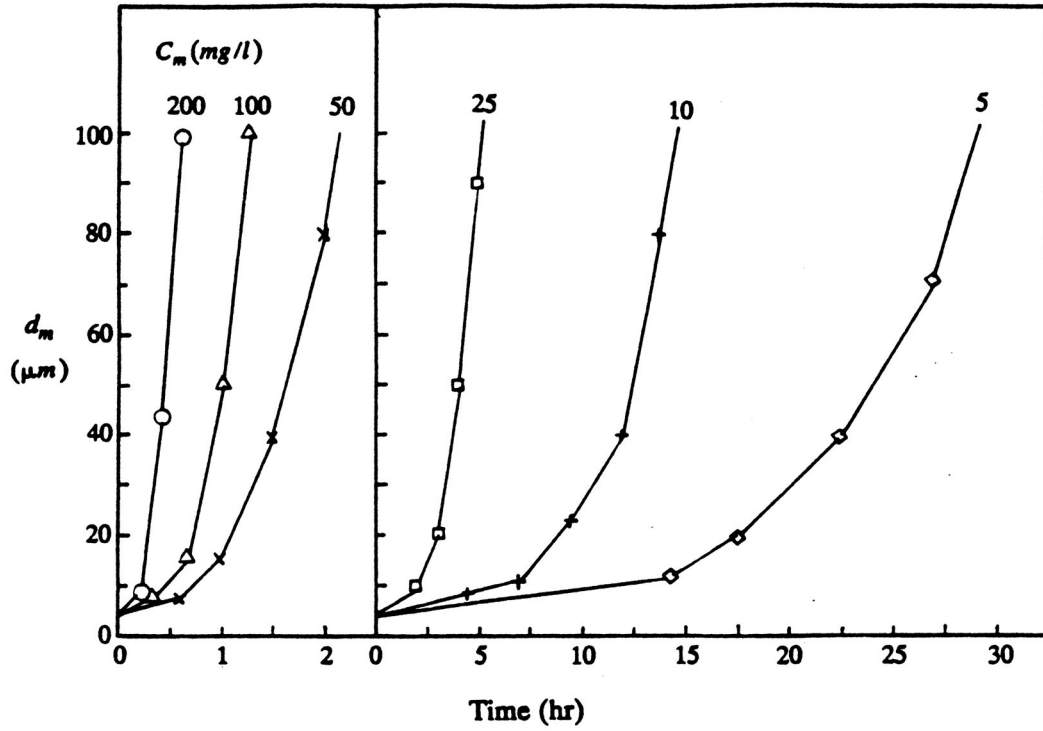
$$T_{10} = 135.76 C_m^{-1.085} \quad \textit{treated Detroit River sediment in seawater} \quad \text{(4.3-3)}$$

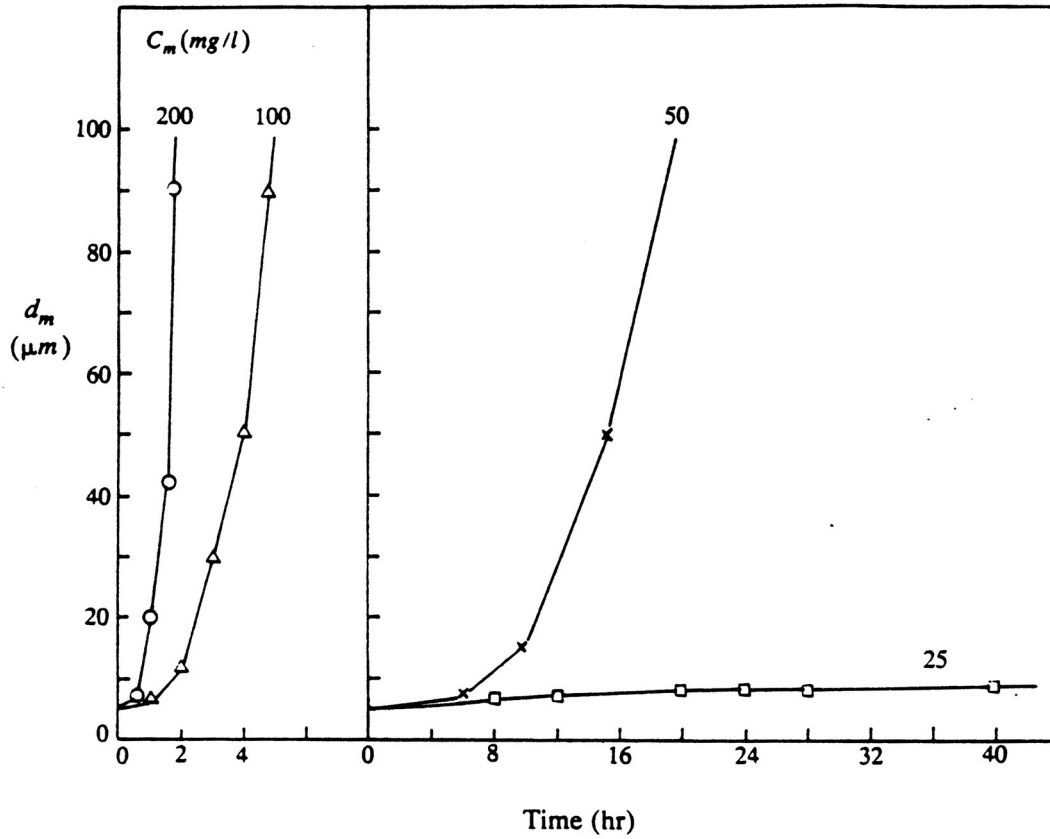$$T_{10} = 11558.2 C_m^{-1.711} \quad \textit{treated Detroit River sediment in fresh water} \quad \text{(4.3-4)}$$

$$T_{1/10} = 210.26 C_m^{-1.198} \quad \textit{treated Detroit River sediment in seawater} \quad \text{(4.3-5)}$$

$$T_{1/10} = 15188.8 C_m^{-1.783} \quad \textit{treated Detroit River sediment in fresh water} \quad \text{(4.3-6)}$$

with correlation coefficients 0.9970, 0.9978, 0.9991, and 0.9935 respectively. T_{10} and $T_{1/10}$ are in *hrs* and C_m is in *mg/l*. Additionally, the comparison of T_{10} and $T_{1/10}$ for both treated and untreated samples are shown in Figs.4.2-11, 4.2-12, 4.2-14, and 4.2-15.
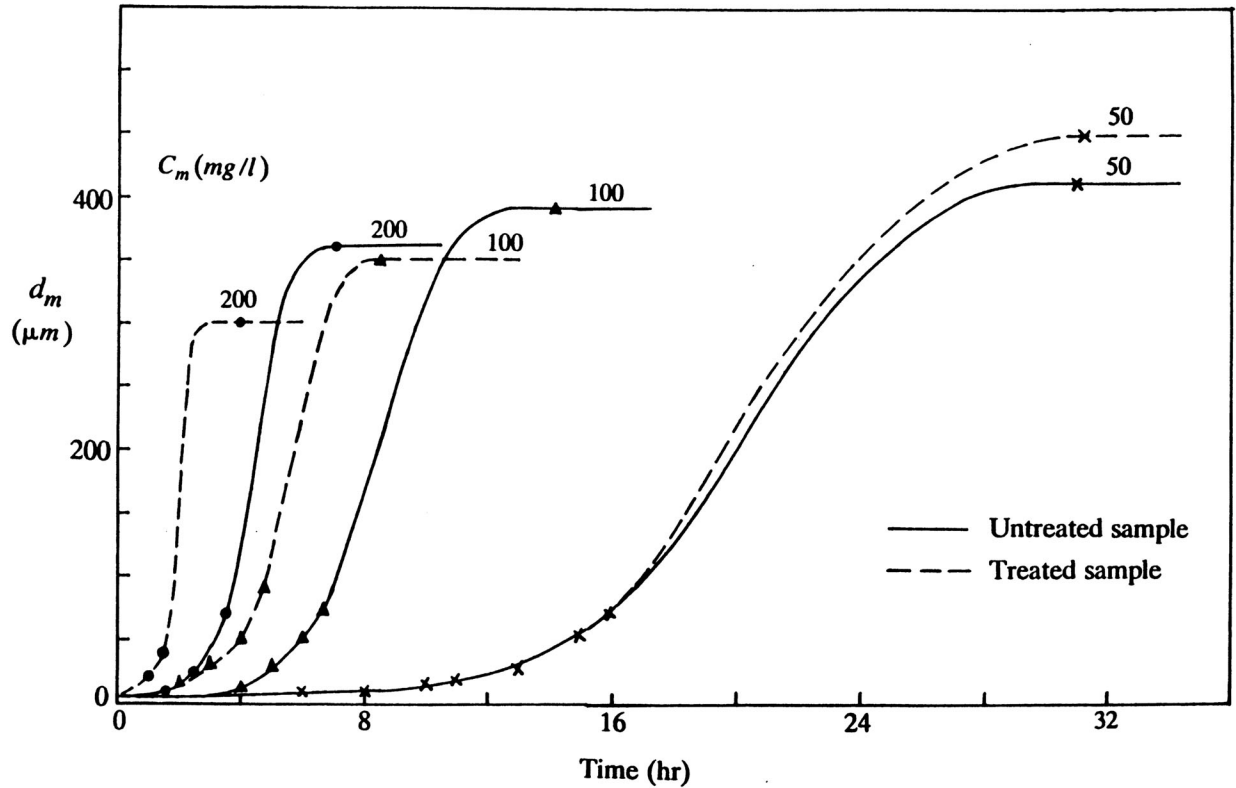
**Fig.4.3-6 Time variation of the floc median diameter for the
Detroit River sediment in the disc flocculator tests
(treated sample in seawater)**

Fig.4.3-7 Time variation of the floc median diameter for the Detroit River sediment in the disc flocculator tests (treated sample in fresh water)
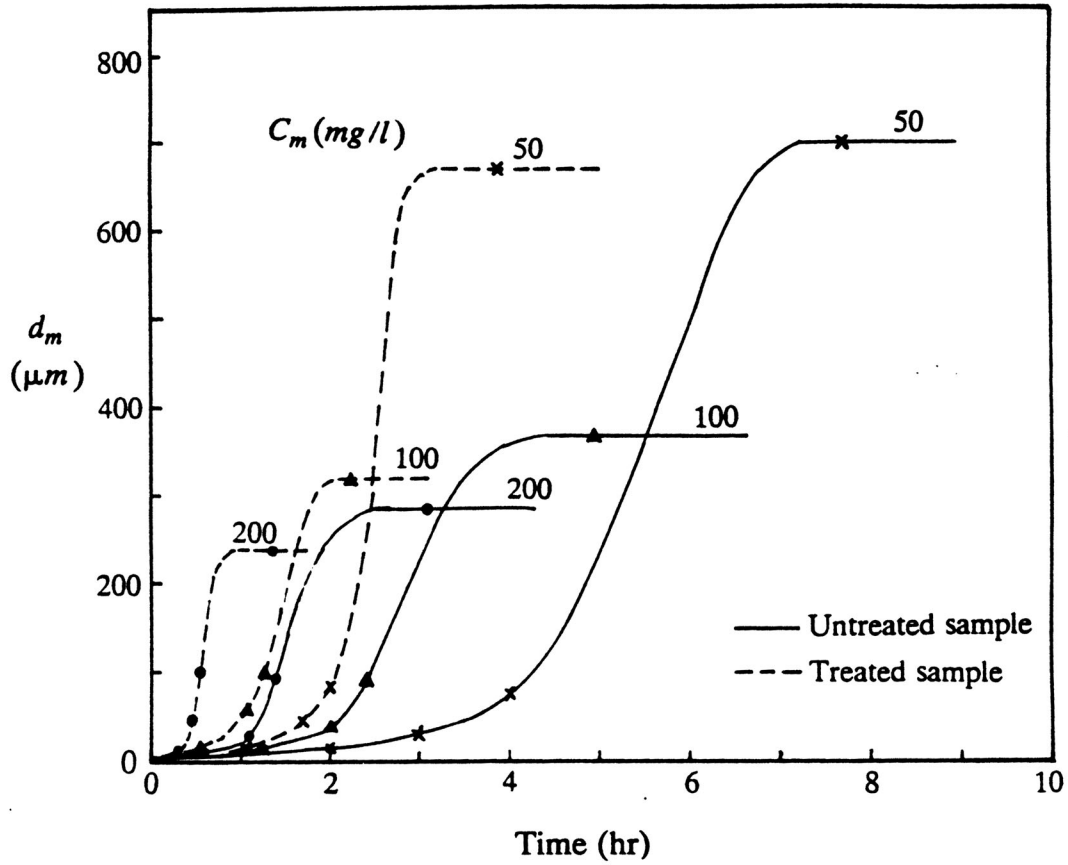
Fig.4.3-8 Comparison of the time variation of the floc median diameter for the treated and untreated Detroit River sediment in seawater in the disc flocculator tests

**Fig.4.3-9 Comparison of the time variation of the floc median
diameter for the treated and untreated Detroit River
sediment in fresh water in the disc flocculator tests**

We can see from Figs.4.3-6 and 4.3-8 that, for the Detroit River sediment in seawater, the treated samples flocculated faster than did the untreated samples at all solid concentrations tested. In fresh water (see Figs.4.3-7 and 4.3-9), however, the treated sediment flocculated faster at high concentrations (100 and 200 *mg/l*), and slower at low concentrations (e.g., 25 *mg/l*).
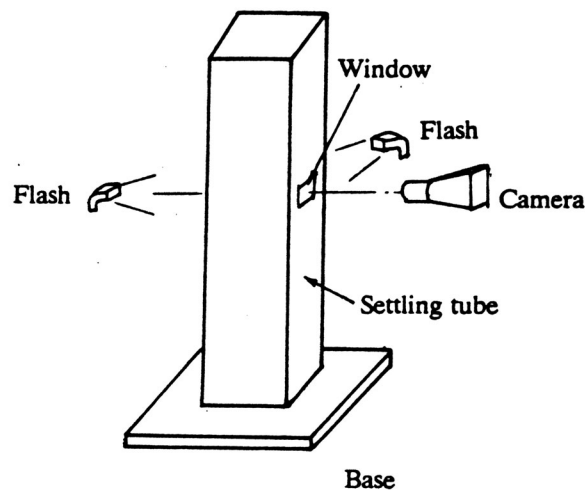
5. SETTLING SPEEDS OF FLOCS

The settling speeds of the drilling mud flocs and Detroit River sediment flocs produced from the flocculation tests in the Couette and disc flocculators were measured in a settling tube by a double-exposure photographic method. The effects of floc formation conditions (mainly fluid shear and solid concentration) on the settling speeds of flocs were examined.

In this section, we first describe the experimental methods, including the experimental apparatus and procedures. Results and a discussion of the results are then presented.

Experimental Methods

Experimental Apparatus

Fig.5-1 shows the apparatus used in the floc settling speed measurements. The settling tube made from plexiglass is 1 m high and l0xl0 cm wide in cross-section. The outer surfaces of this tube are covered by a layer of 0.5 cm styrofoam board to reduce heat transfer between the air in the room and the water in the tube. Such heat transfer may produce convection currents in the settling tube and affect the settling of flocs. Three windows (one for photography, the other two for flashing) are located at a distance of 35 cm below the water surface in the tube; at this distance, flocs will have reached their terminal settling speeds. A horizontal-axis Nikon SMZ-2T microscope-camera system is mounted against the photography window. The magnifications of this microscope-camera system can be 4.6-, 6.7-, 16-, or 20-fold. A flash for exposing films is placed either on the opposite side of the tube from the camera (in the case that flocs were small and the 16- or 20-fold magnification lens was used) or beside the camera (in the case that flocs were large and the 4.6- or 6.7-fold magnification lens was used). A lantern always accompanies the flash, lighting up the flocs in the tube for observation and focusing from the microscope. Polaroid 667 Coaterless black-and-white, professional instant pack films were used for photography.

**Fig.5-1 Experimental apparatus for the floc
settling speed measurement**

Procedure

The flocs used in the settling speed measurements were produced in the Couette and disc flocculator tests. When the steady state of flocculation in a test had been reached, a small amount (1 to 3 ml) of suspension containing flocs was taken using a pipette from the flocculator and immediately introduced into the settling tube for the settling speed measurement. It should be noted that, at high concentrations such as 100 and 200 *mg/l*, the suspension may contain too many flocs. In this case, the suspension must be diluted prior to being introduced into the settling tube to minimize the effects of the interactions between flocs during their settling on the settling speeds of these flocs.

In performing measurements, the suspension containing flocs was poured gently into the water surface in the settling tube. Then the flocs began to settle down. As one (usually more than one) floc arrived in the scope of the camera, two flashes were consecutively lighted with a time between the flashes varying from 1 to 5 seconds, depending on the settling speed of the floc. This resulted in two positions of a floc shown on one photograph. This is called a double-exposure photographic method. For each test, eight to fourteen such double-flash, single-frame photographs were taken, and about 10 to 20 flocs were shown on these photographs.

The settling speed of a floc was determined by the distance between two successive positions of the floc on the photograph and the time interval between the two flashes. The size of a floc was measured by averaging its long and short axis from the photograph.

Results and Discussion

Drilling Mud Flocs from Couette Flocculator Tests

The settling speeds and sizes of a total of 216 drilling mud flocs from the Couette flocculator tests were measured. These flocs were in the size range from 30 to 300 µ*m*. Flocs larger than 300 µ*m* were difficult to catch due to their fast settling speeds and the high magnification (20-fold) of the lens used. On the other hand, the sizes of flocs less than 30 µ*m* could not be determined accurately from the photographs.

Figs.5-2a through 5-2e show the floc settling speeds as a function of floc size with fluid shear as a parameter for the solid concentrations of 10, 50, 100, 200, and 400 mg/l respectively. From these figures we can see that the fluid shear at which the flocs are formed has a significant effect on the floc settling speeds. Although some scattering exists, the overall tendency of the data suggests that for the same size, the flocs formed at higher shears have higher settling speeds than do the flocs formed at lower shears. The main reason for this is that the flocs formed at higher fluid shears are more compact and more dense than those formed at lower fluid shears.
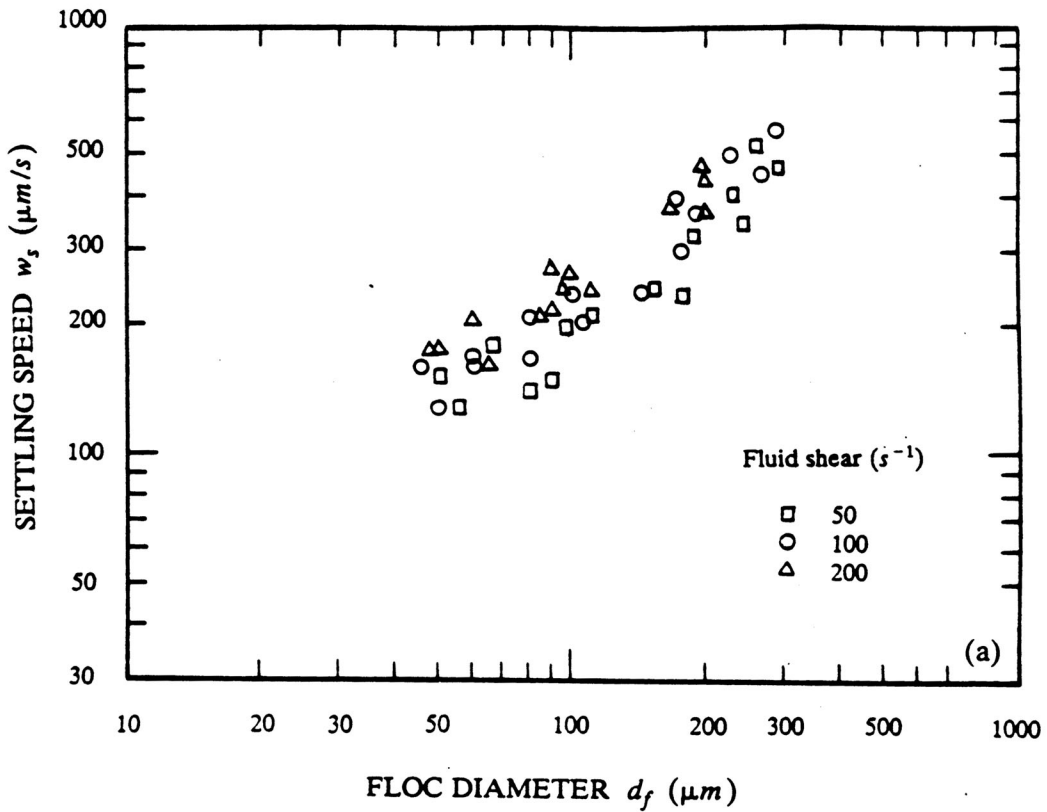
Fig.5-2 Relationship between settling speed and size for drilling mud flocs from the Couette flocculator tests with fluid shear as a parameter, at solid concentrations: (a) 10 mg/l, (b) 50 mg/l,(c) 100 mg/l, (d) 200 mg/l, (e) 400 mg/l, respectively.
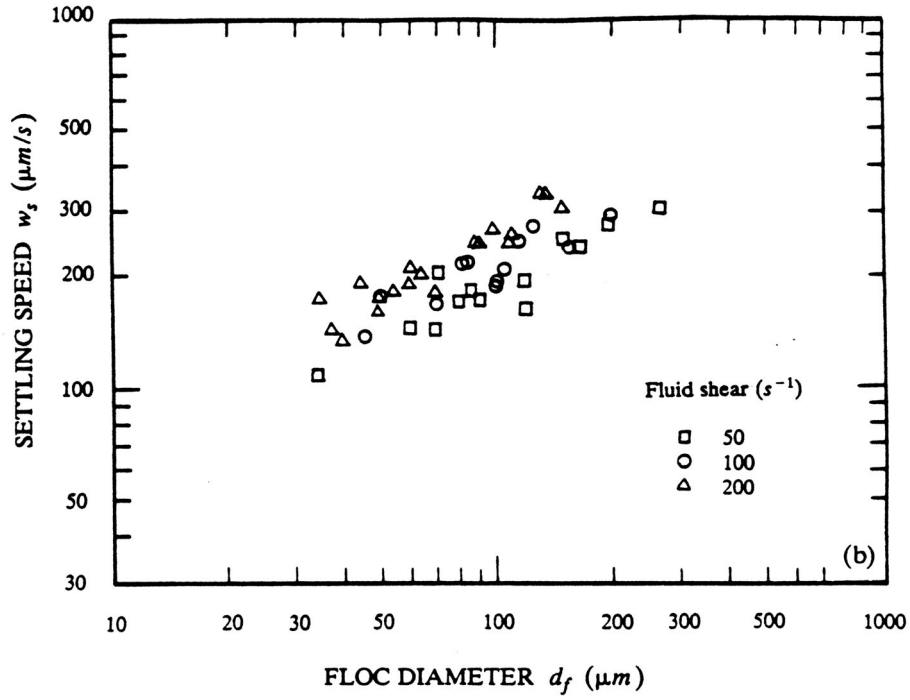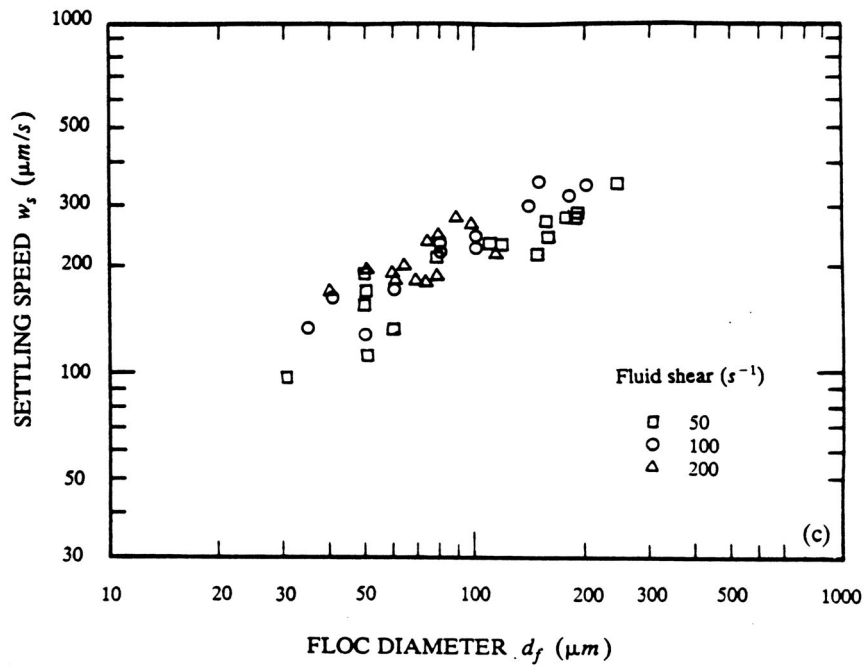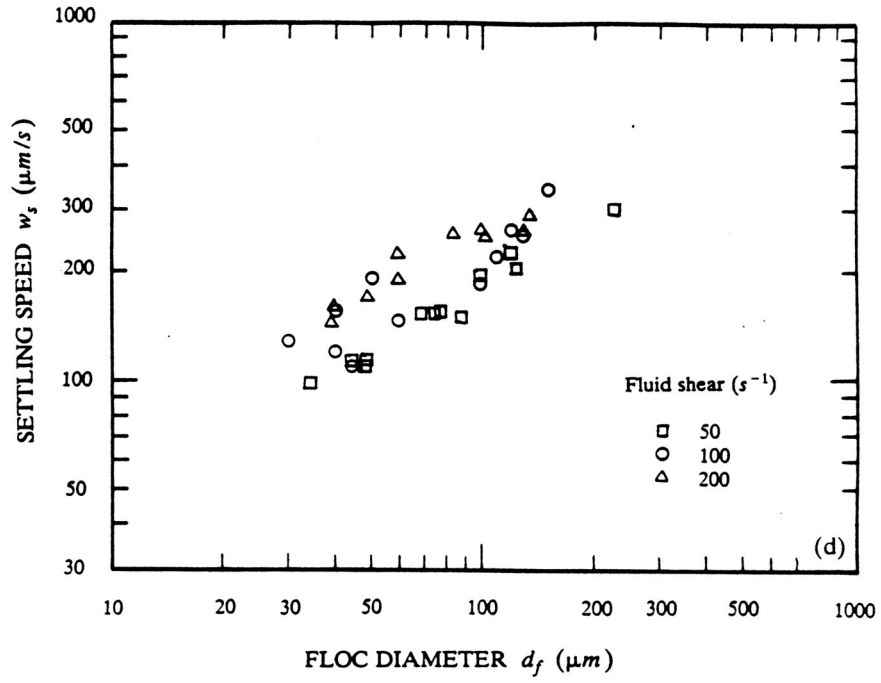
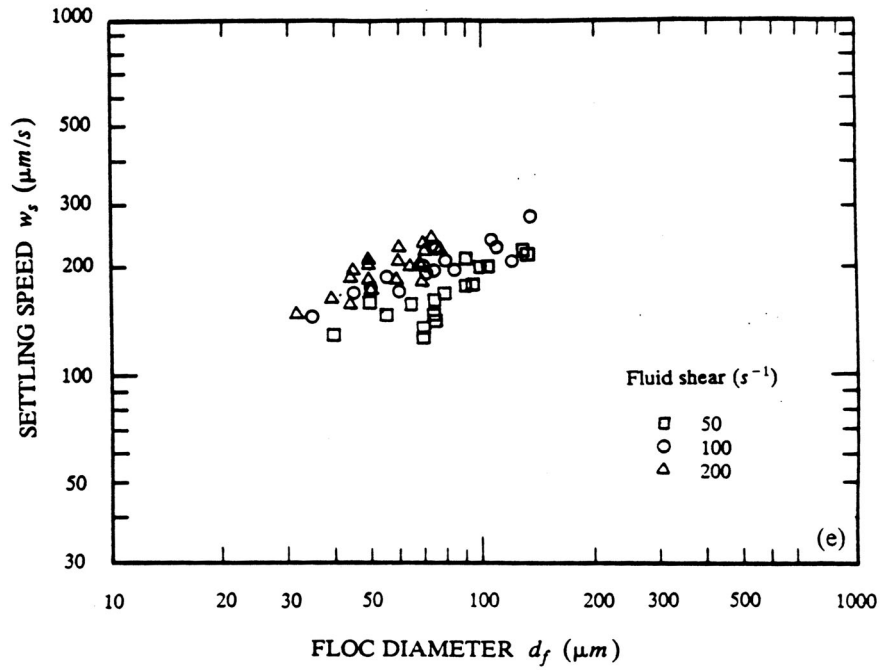**Fig.5-2a**

Fig.5-2b

Fig.5-2c

Fig.5-2d

Fig.5-2e

In order to examine the influence of solid concentration, the other main parameter of floc formation, on the settling speeds of flocs, we plot the settling speeds as a function of floc size with solid concentration as a parameter for the fluid shears of 50, 100, and 200 s^{-1} respectively (Figs.5-3a, b, c). We can see from Figs.5-3a, b, and c that the concentration at which the flocs are formed has no distinguishable effects on the floc settling speeds. This suggests that for the same size, the flocs formed at different solid concentrations but at the same fluid shear, probably have the same density.
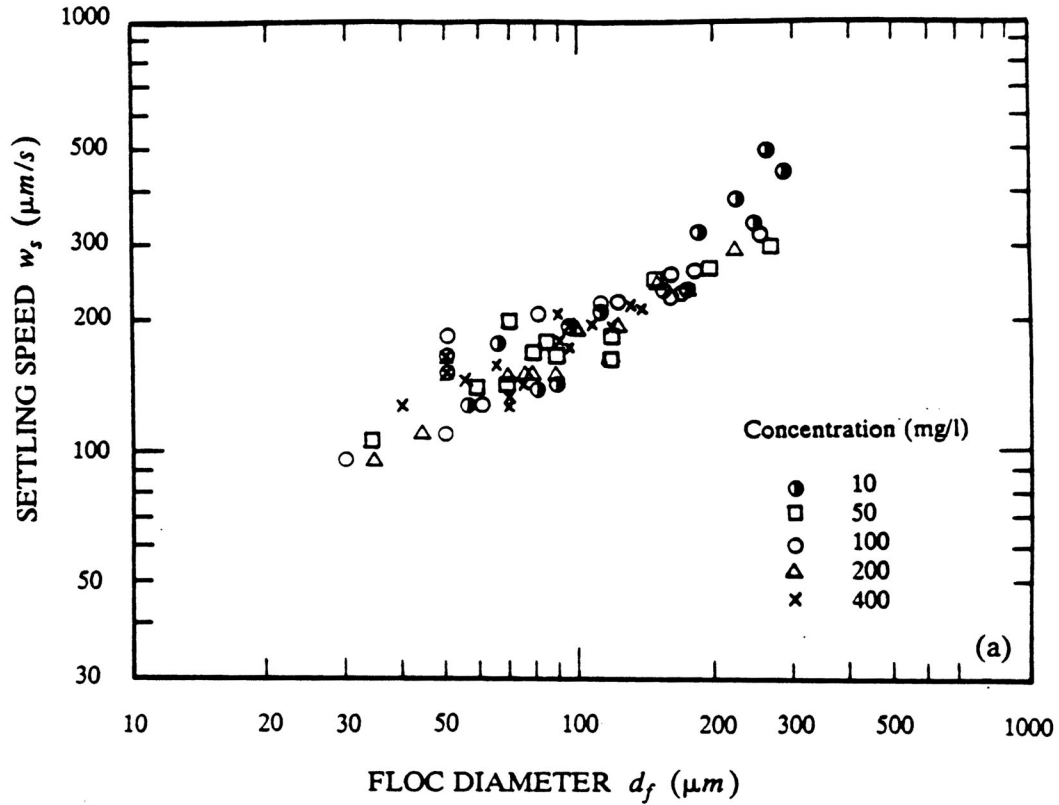
Fig.5-3 Relationship between settling speed and size for
drilling mud flocs from the Couette flocculator tests
with solid concentration as a parameter, at fluid shears:
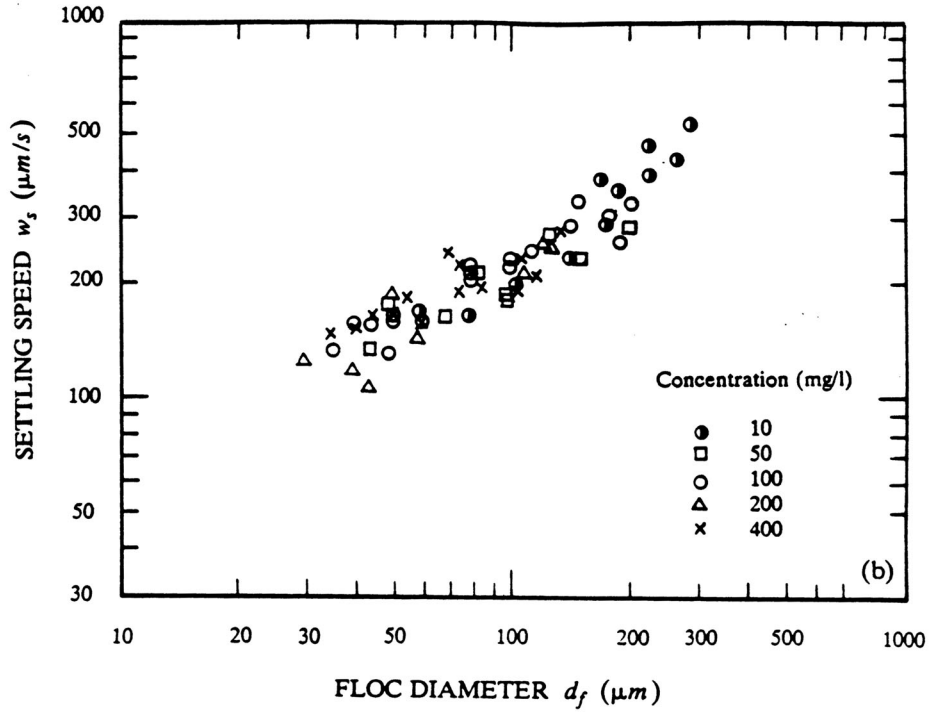(a) 50 s^{-1} ,(b) 100 s^{-1} , (c) 200 s^{-1} , respectively.
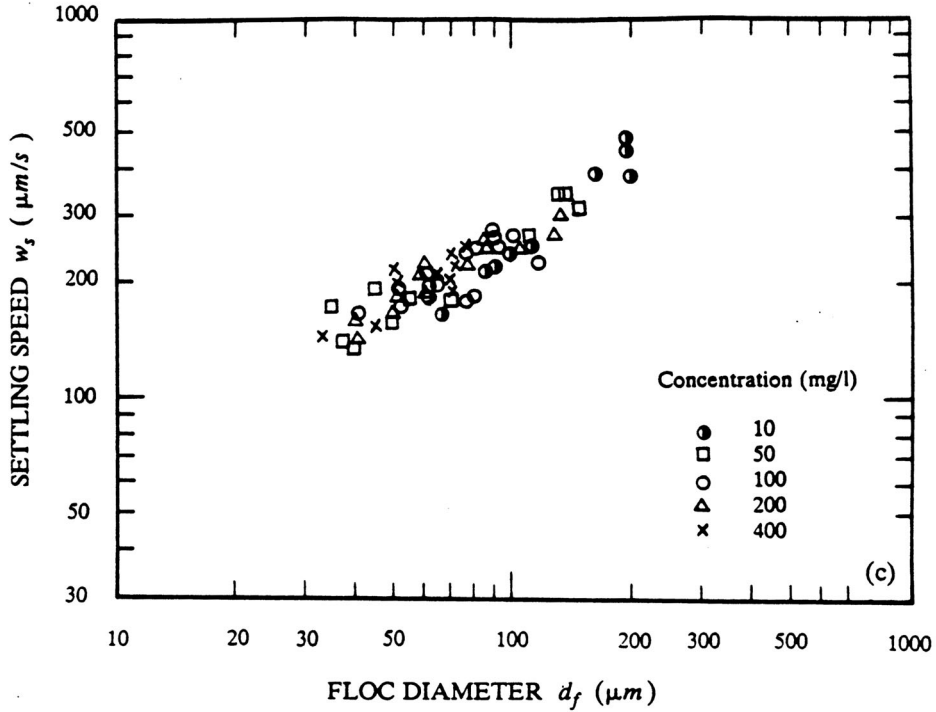
Fig.5-3a

Fig.5-3b

Fig.5-3c

We can also see from these figures that the data for any combination of fluid shear and solid concentration can be fitted by a power law:

$$w_s = A d_f^m \qquad\qquad (5\text{-}1)$$

where A and m are the constants to be determined experimentally.

Since solid concentrations have no distinguishable effects, we do the power regression for each fluid shear for all solid concentrations. Using the least-square method, we determine that $m = 0.59$, 0.58, and 0.52 for fluid shears of 50, 100, and 200 s^{-1} respectively with corresponding correlation coefficients of 0.92, 0.91, and 0.90.

Since the slopes, m, at different fluid shears are nearly the same, we set $m = 0.56$ for all the fluid shear conditions. By this slight adjustment, we find that the constants A in Eq.(5-1) are 14.61, 17.32, and 19.24 for the fluid shears of 50, 100, and 200 s^{-1} respectively. The fitted lines of the power regressions are shown in Fig.5-4.
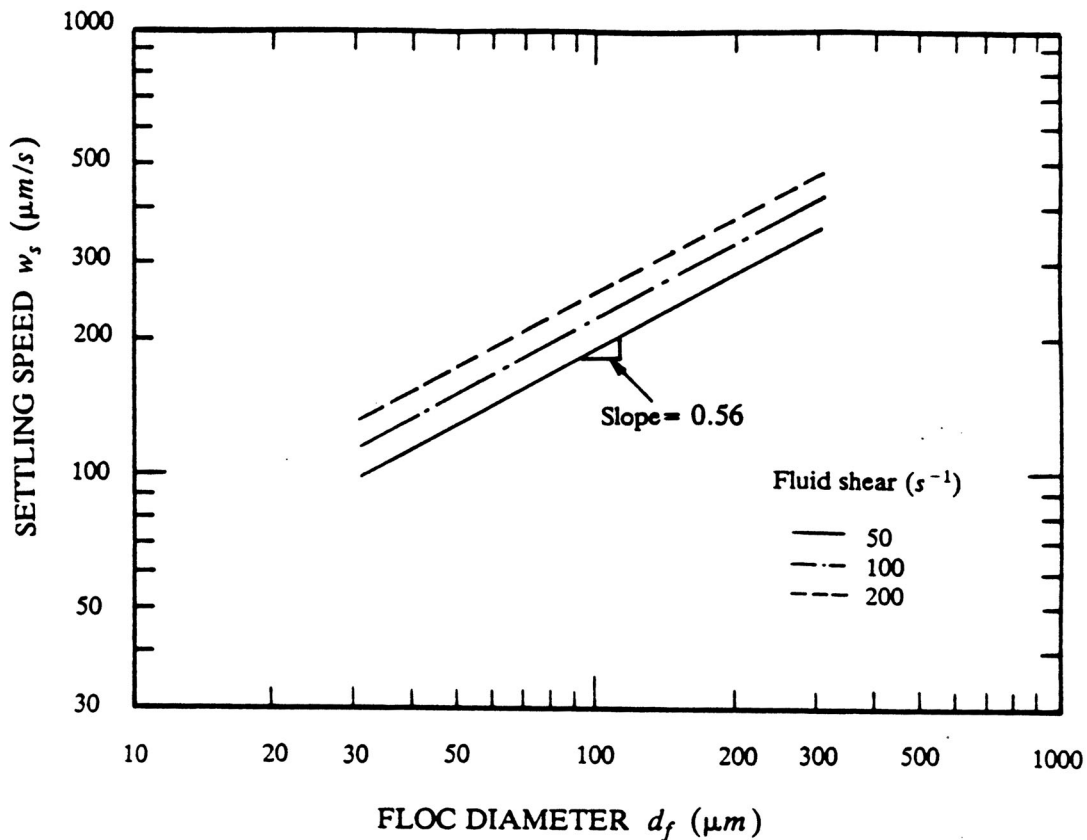

Fig.5-4 Fitted lines of the power regression for the settling speed of drilling mud flocs from the Couette flocculator tests

103

In order to obtain an empirical expression for the floc size-settling speed relationship including the effects of fluid shear, we plot A versus fluid shear G (Fig.5-5) and find that the data can also be fitted by a power expression:

$$A = 6.75G^{0.20} \qquad\qquad 50 \leq G \leq 200 \ s^{-1} \qquad\qquad (5\text{-}2)$$

where G is in s^{-1}.
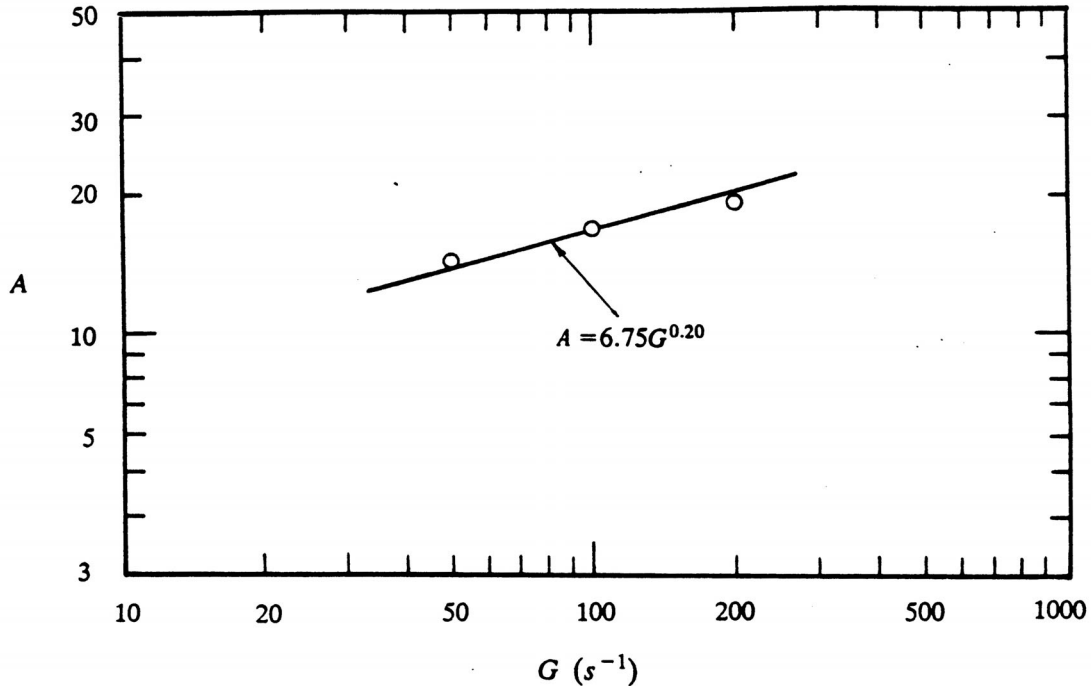
Fig.5-5 Relationship between A and G .

Then combining Eq.(5-2) with Eq.(5-1) and substituting $m = 0.56$, we obtain an empirical expression for the settling speeds of drilling mud flocs as a function of floc size and the fluid shear at which the flocs are formed:

$$w_s = 6.75G^{0.20}d_f^{0.56} \qquad\qquad (5\text{-}3)$$

where w_s is in $\mu m \ s^{-1}$ and d_f is in μm.

Drilling Mud Flocs from Disc Flocculator Tests

In the steady state, the flocs produced in the disc flocculator tests were very large, in the size range of 0.08 to 1.8 mm. Therefore, the lens with the magnification of 4.6 fold was used for

photography. A total of 129 measurements were made, including flocs made of untreated and treated samples.

It should be mentioned that because the flocs were very large and fragile, breakage of these flocs during sampling from the flocculators and introducing them into the settling tube became a critical problem. To prevent flocs from breakage, a big pipette with a tube of 4 mm in inner diameter was used. With this big pipette, we found that no significant breakage occurred when samples were withdrawn from the discs very slowly. However, no matter how careful we were, flocs broke when they were introduced into the settling tube by pushing the pipette. By trying many times, we solved this problem by simply hanging the pipette over the settling tube, with the end of the pipette just beneath the water surface. In this way, the flocs in the pipette settled out into the settling tube due to gravity, and no applied fluid shear was involved. So that, the breakage of flocs was minimized.

Figs.5-6 and 5-7 show the settling speeds of drilling mud flocs made from untreated and treated samples respectively. Some differences in settling speeds are observed from these two figures. This may reflect the effects of organic matter (1.77 % by weight in the drilling mud) on settling speeds.
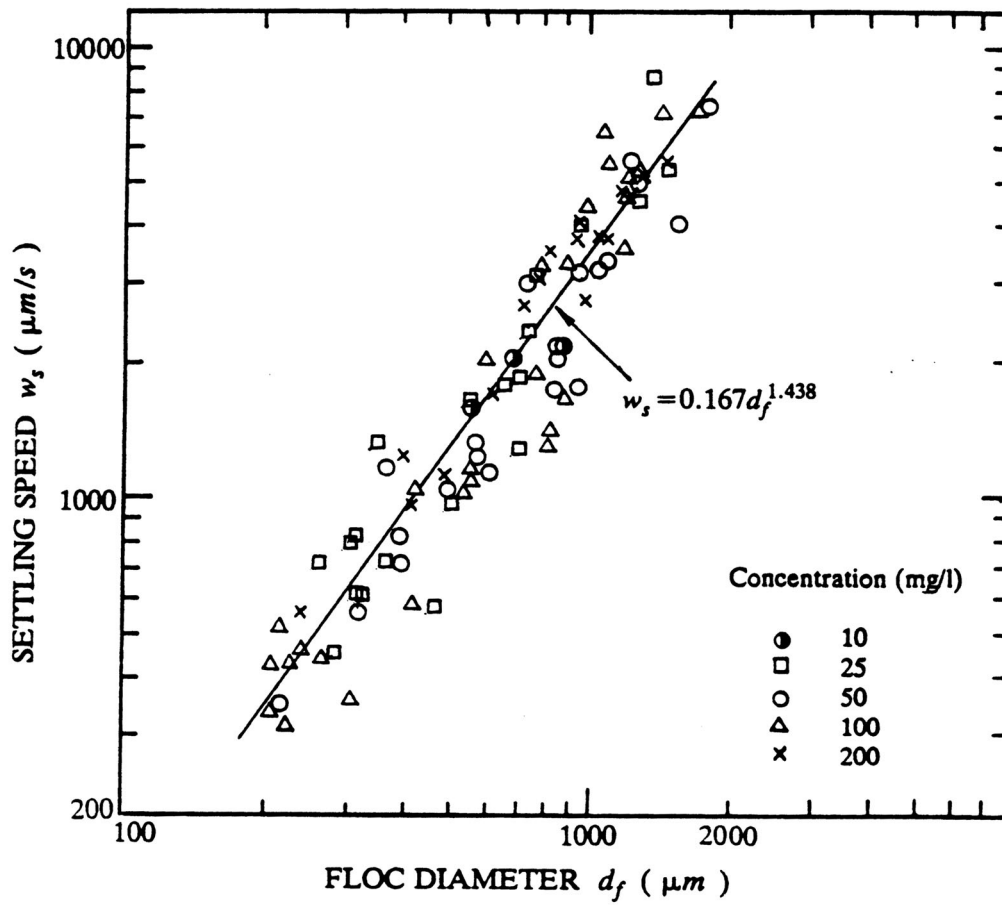
Fig.5-6 Settling speeds of drilling mud flocs from the disc flocculator tests (untreated samples)
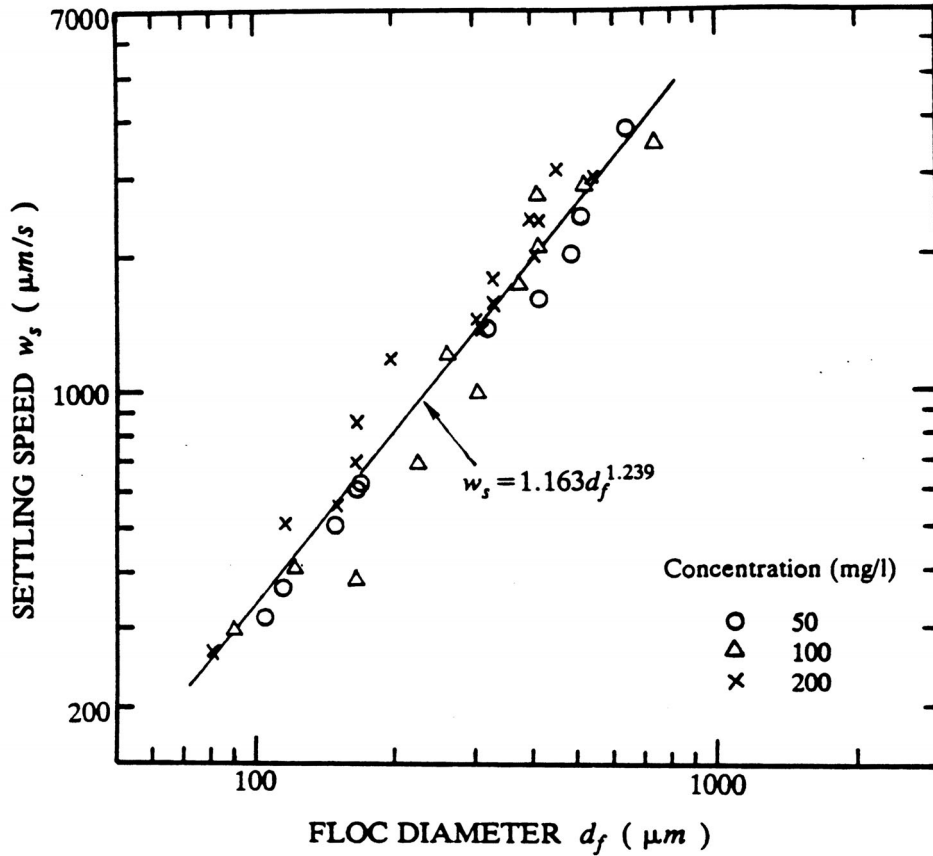
Fig.5-7 Settling speeds of drilling mud flocs from the disc flocculator tests (treated samples)

We also see from Figs.5-6 and 5-7 that the solid concentration at which flocs were formed does not have a strong effect on the settling speeds of flocs. This is consistent with the results for the flocs from the Couette flocculator tests.

Furthermore, using the least square method, empirical expressions for the settling speed-size relationship are obtained and are as follows:

$$w_s = 0.167 d_f^{1.438} \qquad \text{for } \textit{untreated samples} \qquad (5\text{-}4)$$
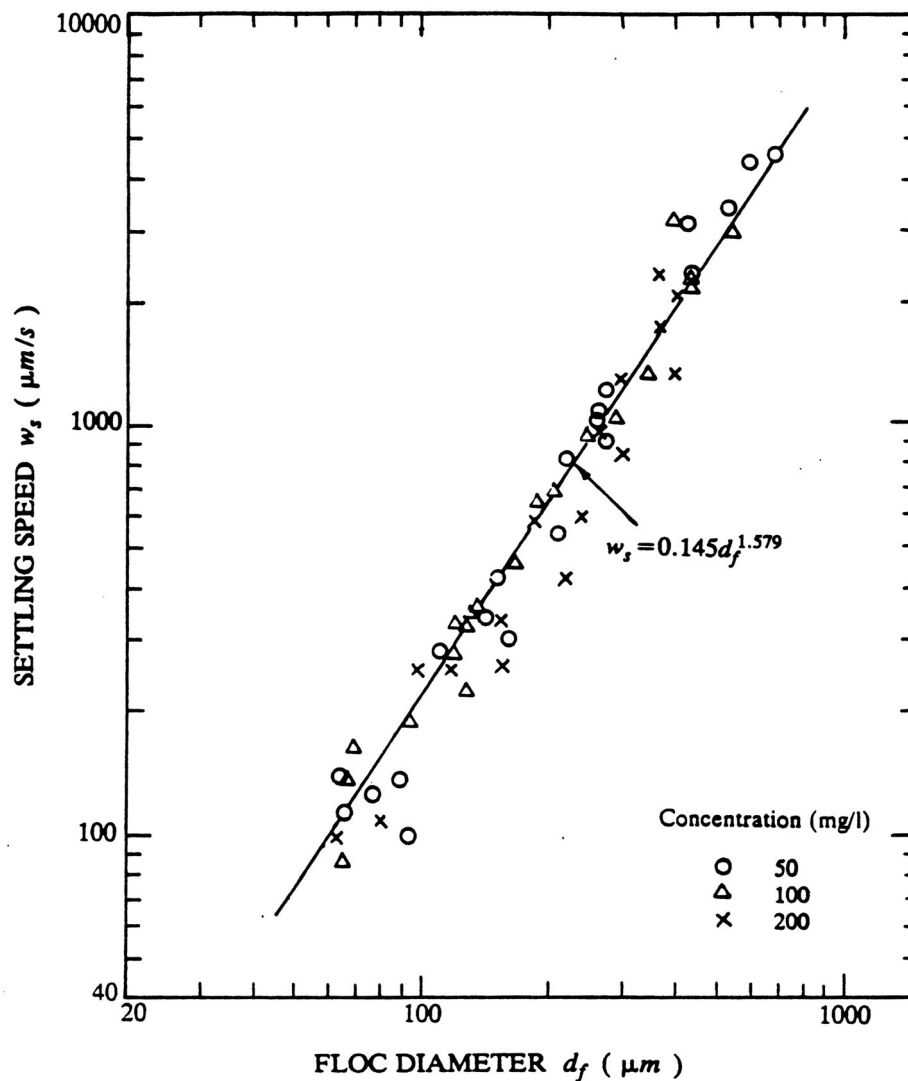
$$w_s = 1.163 d_f^{1.239} \qquad \text{for } \textit{treated samples} \qquad (5\text{-}5)$$

where w_s is in $\mu m/s$ and d_f is in μm. The correlation coefficients are 0.9362 and 0.9631 respectively.

Detroit River Sediment Flocs from Disc Flocculator Tests

A total of 202 measurements were made for the settling speeds of Detroit River sediment flocs from the disc flocculator tests. The sizes of these flocs ranged from 0.06 to 0.8 mm

Figs.5-8 and 5-9 show the settling speeds of flocs made from untreated and treated Detroit River sediment in seawater. Figs.5-10 and 5-11 show the settling speeds of flocs made from untreated and treated Detroit River sediment in fresh water. Similar to the drilling mud flocs, differences in settling speeds of flocs made from untreated and treated samples are also observed. Moreover, the settling speeds of flocs formed in fresh water are found to be larger than those of flocs formed in seawater.

The chart shows settling speed w_s ($\mu m/s$) versus floc diameter d_f (μm), with the fitted relation $w_s = 0.145 d_f^{1.579}$. The legend indicates Concentration (mg/l): ○ 50, △ 100, × 200.

Fig.5-8 Settling speeds of Detroit River sediment flocs from the disc flocculator tests (untreated samples in seawater)
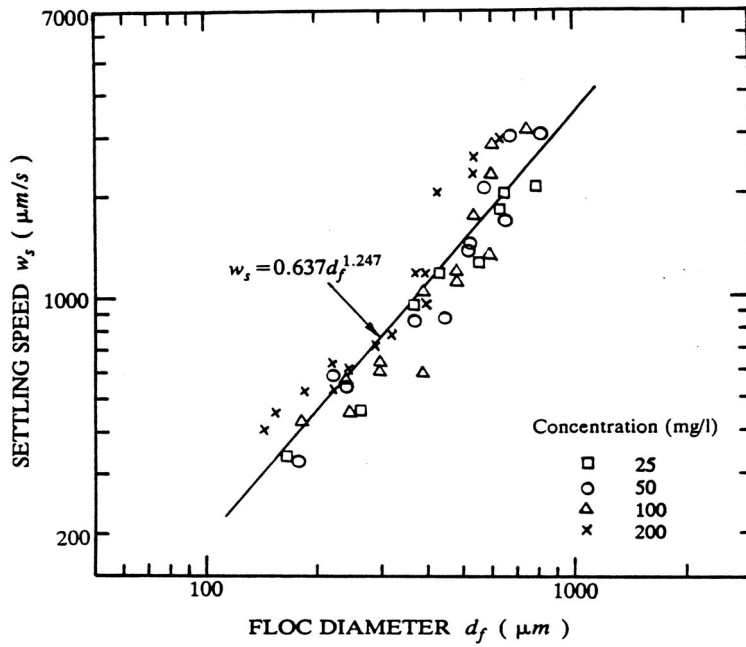
Fig.5-9 Settling speeds of Detroit River sediment flocs from the disc flocculator tests (treated samples in seawater)
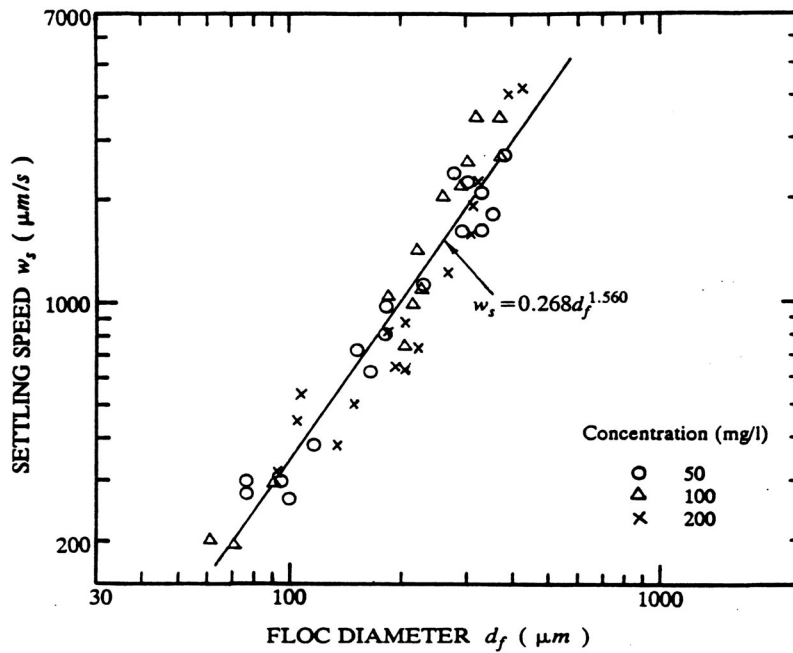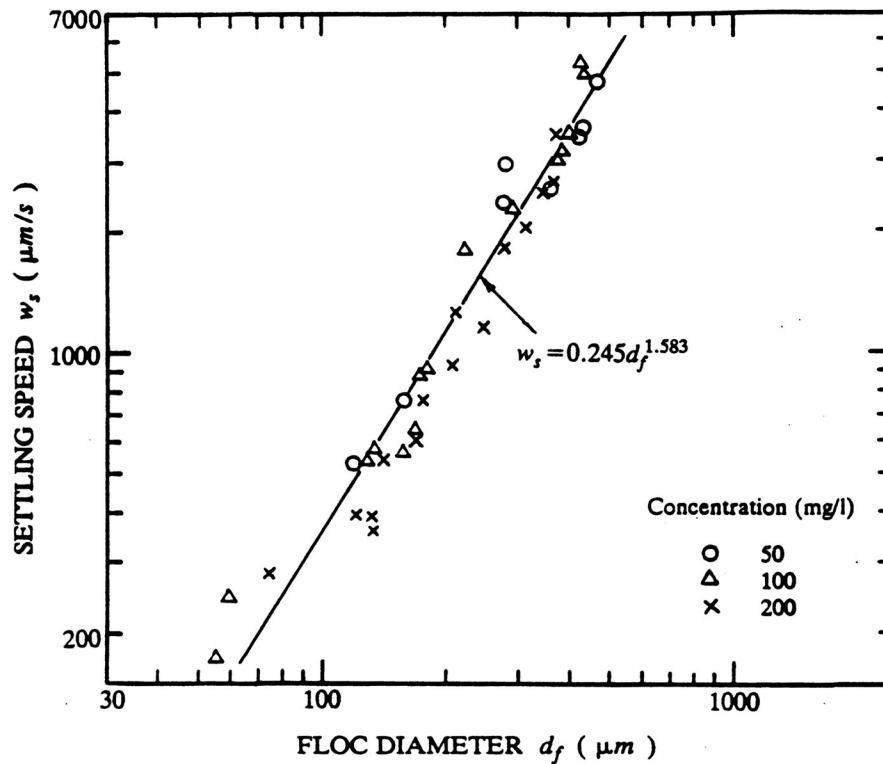

Fig.5-10 Settling speeds of Detroit River sediment flocs from the disc flocculator tests (untreated samples in fresh water)

Fig.5-11 Settling speeds of Detroit River sediment flocs from the disc flocculator tests (treated samples in fresh water)

The power regressions are also used for the data shown in Figs.5-8 to 5-11. The resulting empirical expressions are:

$$w_s = 0.145 d_f^{1.579} \qquad \text{for } \textit{untreated samples in sea water} \qquad (5\text{-}6)$$

$$w_s = 0.637 d_f^{1.247} \qquad \text{for } \textit{treated samples in sea water} \qquad (5\text{-}7)$$

$$w_s = 0.268 d_f^{1.560} \qquad \text{for } \textit{untreated samples in fresh water} \qquad (5\text{-}8)$$

$$w_s = 0.245 d_f^{1.583} \qquad \text{for } \textit{treated samples in fresh water} \qquad (5\text{-}9)$$

where w_s is in $\mu m/s$ and d_f is in μm. The correlation coefficients are 0.9765, 0.9228, 0.9505 and 0.9687 respectively.

Table 5-1 summarizes all experimental constants in the settling speed-size relationship $(w_s = A d_f^m)$ for the drilling mud and Detroit River sediment flocs from the disc flocculator tests.

110

Table 5-1 Summary of experimental constants in the settling speed-size relationship ($w_s = Ad_f^m$) for the drilling mud and Detroit River sediment flocs from the disc flocculator tests

Sediment	A	m	r	Size (μm)	R_e
DM-S	0.167	1.438	0.9362	200-1800	0.11-13.41
DM-S-T	0.245	1.583	0.9631	80-800	0.02-2.68
DR-S	0.281	1.435	0.9542	60-700	0.01-3.10
DR-S-T	0.637	1.247	0.9228	120-800	0.06-2.46
DR-F	0.268	1.560	0.9505	60-500	0.01-1.87
DR-F-T	0.245	1.583	0.9687	60-500	0.01-2.23

Note: DM-S --untreated drilling mud in seawater.
   DM-S-T --treated drilling mud in seawater.
   DR-S --untreated Detroit River sediment in seawater.
   DR-S-T --treated Detroit River sediment in seawater.
   DR-F --untreated Detroit River sediment in fresh water.
   DR-F-T --treated Detroit River sediment in fresh water.
   R_e --Reynolds number.
   r --correlation coefficient.

Discussion

From all experimental data shown above, we have noticed that the settling speeds of flocs show large deviations from Stokes' law:

$$w_s = \frac{gd_p^2}{18\mu}(\rho_p - \rho_w)$$
(5-10)

where μ is the dynamic viscosity of the water, d_p is the diameter of a solid sphere, and ρ_p and ρ_w are the density of the solid sphere and water respectively.

Although several factors, such as the relative density, permeability, roughness of surface, and shape of a floc, may affect the settling speed of the floc, the main cause of this deviation is that, the floc has a smaller average density (due to its porous structure) than that of a solid particle with the same (effective) diameter as that of the floc, and this density is not a constant but a function of the floc size. The average relative density is defined as (Tambo and Watanabe, 1979):

111

$$\Delta\rho_p = \rho_p - \rho_w \qquad \text{for } \textit{solid particles} \qquad (5\text{-}11)$$

$$\Delta\rho_f = \rho_f - \rho_w \qquad \text{for } \textit{flocs} \qquad (5\text{-}12)$$

where ρ_f is the average density of a floc and is defined by:

$$\rho_f = \frac{M_s + M_w}{V_f} \qquad (5\text{-}13)$$

where M_s and M_w are the masses of solid and water in the floc respectively, and V_f is the volume of the floc. V_f can be defined in several ways. In this study, we define V_f as:

$$V_f = \frac{\pi}{6}\left(\frac{d_{max} + d_{min}}{2}\right)^3 \qquad (5\text{-}14)$$

where d_{max} and d_{min} are the long and short axes of the floc shown in a photograph.

To obtain a better understanding of the structure of flocs, we will discuss the densities of flocs in detail in the following section.

Fig.5-12 shows a comparison of settling speeds of drilling mud flocs from both disc and Couette flocculator tests as a function of fluid shear and with solid concentration as a parameter. These settling speeds correspond to the flocs with median diameters and formed at certain conditions (i.e., fluid shear and solid concentration). In the numerical modeling of sediment transport, it is often convenient to use the settling speed corresponding to the floc with median diameter as a characteristic settling speed. From this figure, we can see that for fluid shears ranging from 25 to 200 s^{-1} and solid concentrations ranging from 25 to 50 *mg/l*, the settling speed decreases as fluid shear decreases. As the fluid shear approaches zero (i.e., in the disc flocculator tests), however, the settling speed increases dramatically. This is because, in a disc flocculator test, the steady state floc median diameter becomes as large as about 1 mm. Such a floc has a much larger settling speed than that of a floc formed in a Couette flocculator test and with a diameter about 100 µ*m*, though the latter is more dense than the former.
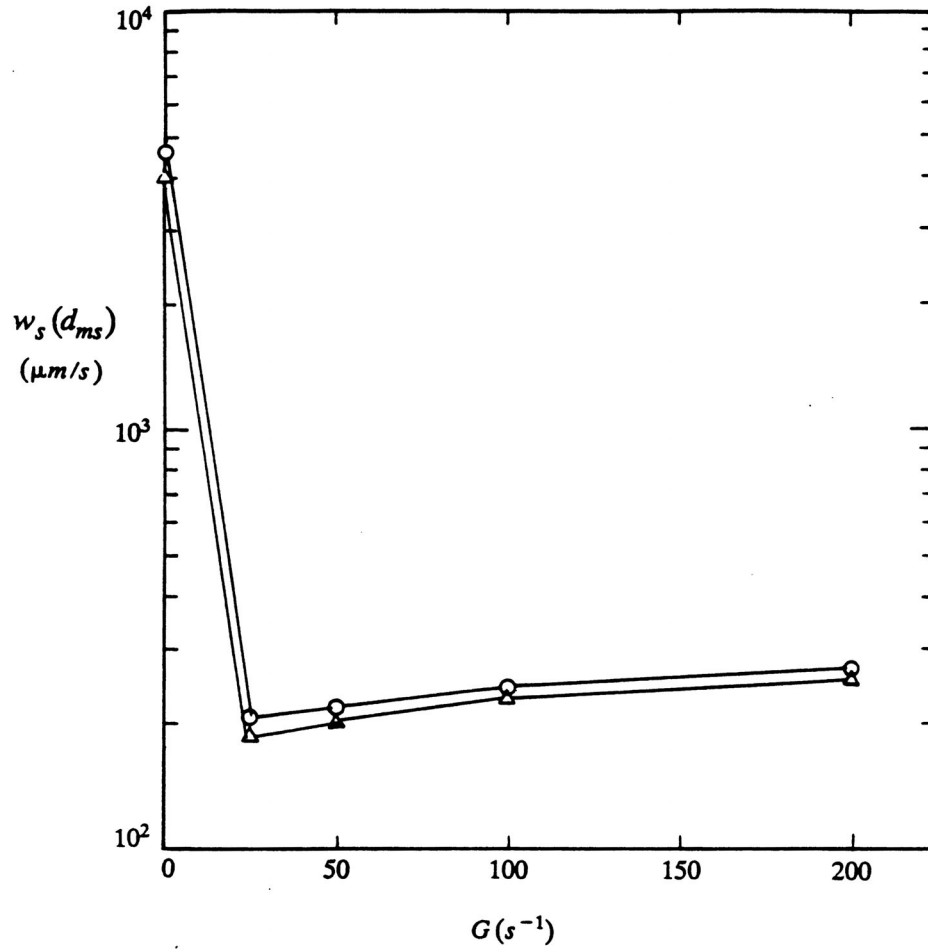
Fig.5-12 Comparison of settling speeds of drilling mud flocs from the disc and Couette flocculator tests. Solid concentration: ο -- 25, Δ -- 50 *mg/l*

Similar to Fig.5-12, Fig.5-13 shows a comparison of settling speeds of Detroit River sediment flocs from both disc and Couette flocculator tests. The same tendency as seen in Fig.5-12 is observed.
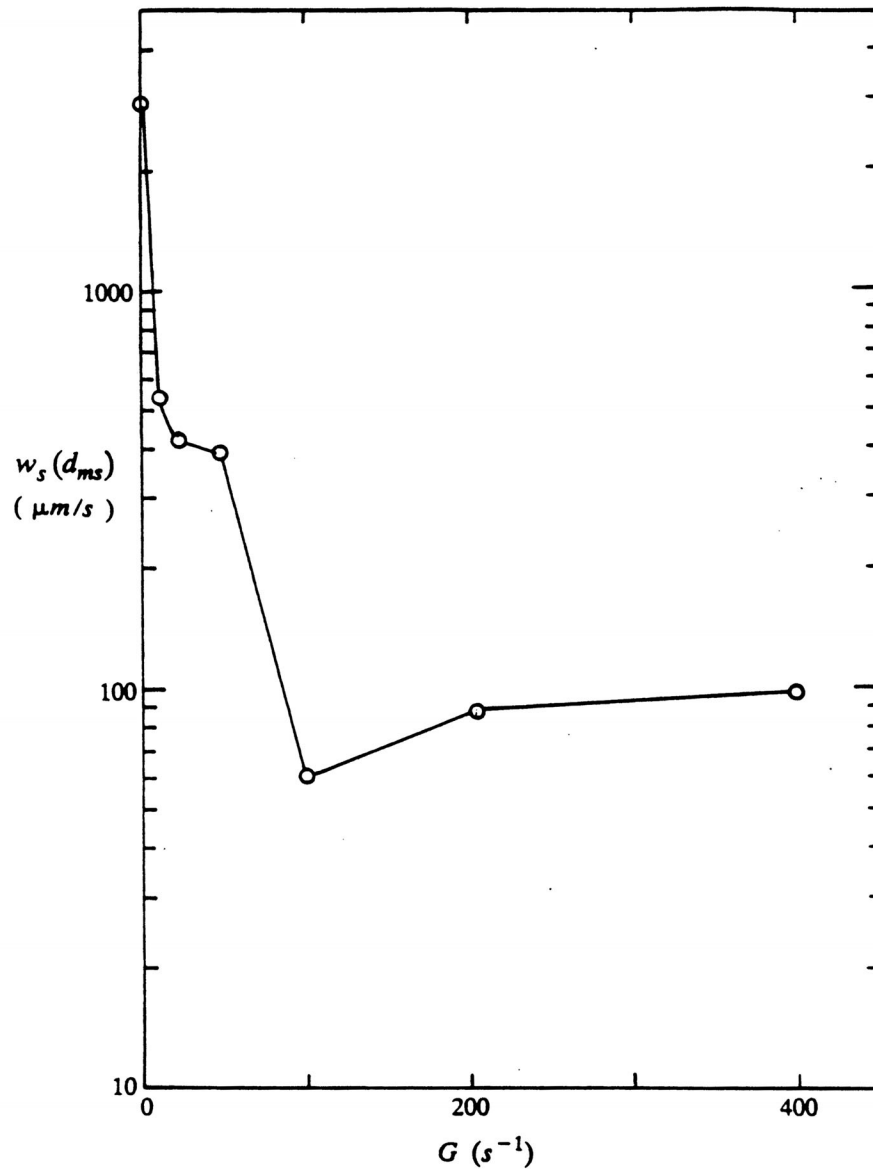
Fig.5-13 Comparison of settling speeds of Detroit River sediment flocs from disc and Couette flocculator tests in fresh water at solid concentration of 100 *mg/l* **. Data at** $G = 100, 200,$ **and** 400 s^{-1} **are from Burban et al. (1990)**

6. EFFECTIVE DENSITIES OF FLOCS

The effective densities of flocs from the Couette and disc flocculator tests were determined using settling speed data. A floc settling speed model (Brinkman, 1947a, b) as well as Stokes' law was employed in the calculation of the floc effective density. Unlike Stokes' law, the floc settling speed model applies to permeable particles, because the effect of the creeping flow through a floc on its settling speed is considered in the model.

In the following, we first describe the floc settling speed model. Then the effective densities of drilling mud and Detroit River sediment flocs are presented.

A Floc Settling Speed Model

The problem of the creeping flow relative to a floc was initially studied theoretically by Brinkman (1947a,b) and later by Sutherland and Tan (1970), Ooms *et al* (1970), Neale *et al* (1973), Epstein and Neale (1974), and Adler (1981). It should be pointed out that the term "floc" was originally used by Brinkman (1947a, b) in his analysis, and actually referred to an isotropic porous sphere.

In Brinkman's analysis, Darcy's law (which applies to a low porosity medium) was extended to describe the flow through a floc which is of high porosity. The resulting equation is:

$$\nabla p = -\frac{k}{\mu}V + \mu\Delta V \qquad (6\text{-}1)$$

where k is the permeability of the floc, μ is the dynamic viscosity of the fluid, p is the pressure, and V is the velocity of the flow.

Outside of the floc, the governing equation for the flow is:

$$\nabla p = \mu\Delta V \qquad (6\text{-}2)$$

By solving Brinkman's flow equation (Eq.(6-1)) in a floc and Stokes' flow equation (Eq.(6-2)) outside of the floc and coupling them on the floc surface, Brinkman obtained Ω, the ratio of the resistance experienced by a floc to an equivalent solid sphere which has the same diameter and the same density as those of the floc:

$$\Omega = \frac{2\beta^2[1-(\tanh\beta/\beta)]}{2\beta^2+3[1-(\tanh\beta/\beta)]} \qquad (6\text{-}3)$$

where β is the normalized floc radius given by:

$$\beta = \frac{d_f}{2\sqrt{k}}$$

(6-4)

and where k is the permeability of the floc. This permeability can be estimated by the following expression (Brinkman, 1947):

(6-7)

$$k = \frac{d_p^2}{72}(3 + \frac{4}{1-e} - 3\sqrt{\frac{8}{1-e} - 3})$$

(6-5)

where d_p is the diameter of the solid particles in the floc and e is the porosity of the floc. Assuming that a floc consists only of two parts, solid particles and water, then according to the mass balance in the floc, the floc porosity can be related to its density by the following expression:

$$1 - e = \frac{\rho_f - \rho_w}{\rho_p - \rho_w}$$

(6-6)

where ρ_p is the density of the solid particles in the floc, and ρ_f and ρ_p are the densities of the floc and water respectively.

Then the settling speed of a floc can be expressed as follows:

$$w_s = [\frac{4}{3}\frac{g}{\Omega C_D}\frac{\rho_f - \rho_w}{\rho_w}d_f]^{1/2}$$

(6-7)

where C_D is the drag coefficient for a solid sphere.

The effective density of a floc can be obtained from Eq.(6-7):

$$\Delta\rho_f = \frac{3}{4}\frac{\rho_w}{g}\frac{\Omega C_D}{d_f}w_s^2$$

(6-8)

For a Reynolds number ($R_e = w_s d/v$) less than unity, the drag coefficient is expressed as:

$$C_D = \frac{24}{R_e} \qquad\qquad R_e \leq 1$$

(6-9)

For a Reynolds number larger than unity, there are well over 30 equations in the literature relating the drag coefficient to the Reynolds number (Haider and Levenspiel, 1989). Here we adopt an expression developed by Concha and Almendra (1979):

$$C_D = 0.28(1 + \frac{9.06}{R_e^{1/2}})^2 \qquad\qquad R_e \leq 10^3 \qquad\qquad (6\text{-}10)$$

Experimental results for settling speeds of steel wool porous spheres (Reynolds number < 0.6, Matsumoto and Suganuma, 1977) and of porous spheres made from semi-rigid plastic foam slab (Reynolds number ranges from 0.2 to 120, Masliyah and Polikar, 1980) are in excellent agreement with Eq.(6-7). Therefore, Eq.(6-8) may be more reasonable than Eq.(2-6) for determining the floc effective density and is used in this study. However, it should be noted that, in Brinkman's model, an implicit assumption is that the permeability of the flocs is uniform; this is cerntainly not true for flocs in general and only an approximation for real flocs. The accuracy of this approximation can not be determined.

Since the effective density is a function of the permeability which is also a function of the floc effective density, a numerical method must be used to solve for the effective density. A computer program named PF.FOR (Appendix 2) was written to perform the calculation.

Results and Discussion

Drilling Mud Flocs from Couette Flocculator Tests

During the settling speed experiments, the settling speeds and sizes of 216 drilling mud flocs from the Couette flocculator tests were measured. The sizes of these flocs were in the range from 30 to 300 µ*m*, and the settling speeds in the range from 95 to 550 µ*m/s*, corresponding to Reynolds numbers ranging from 0.003 to 0.165.

In the calculation of the floc effective densities, we assume that $v=0.01\ cm^2/s$, $\rho_p=2.65\ g/cm^3$, and $\rho_w=1.02466\ g/cm^3$ (which corresponds to sea water from the Santa Barbara Channel at a salinity of 33.642 and a temperature of 16.0 C). d_p is assumed to be 6 µ*m*, the median size of the disaggregated drilling mud particles.

Figs.6-la to 6-le show the floc effective density-size relationships with fluid shear as a parameter for the solid concentrations of 10, 50, 100, 200, and 400 mg/l respectively. From these figures, we can see that the fluid shear at which the flocs are formed has a significant effect on the floc effective density. Although some scattering exists, the overall tendency of the data suggests that for the same size, the flocs formed at higher shears have higher effective densities than do the flocs formed at lower shears. These results are in agreement with the concept of "mechanical syneresis" introduced by Yusa (1977). In addition, the number of the large flocs decreases with the increased fluid shear, and the lower the fluid shear, the more the large flocs.
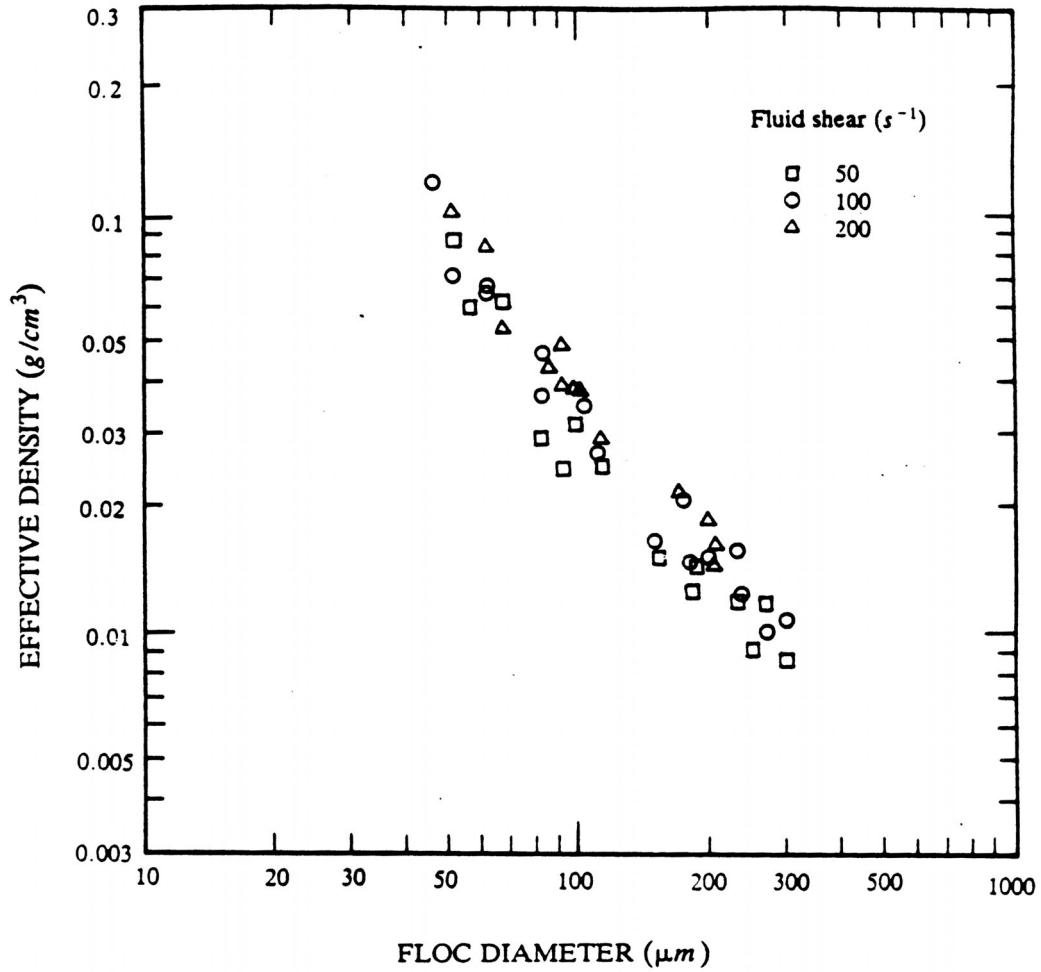
Fig.6-1 Relationship between effective density and size for drilling mud flocs from the Couette flocculator tests with fluid shear as a parameter, at solid concentrations: (a) 10 mg/l, (b) 50 mg/l,(c) 100 mg/l, (d) 200 mg/l, (e) 400 mg/l, respectively.
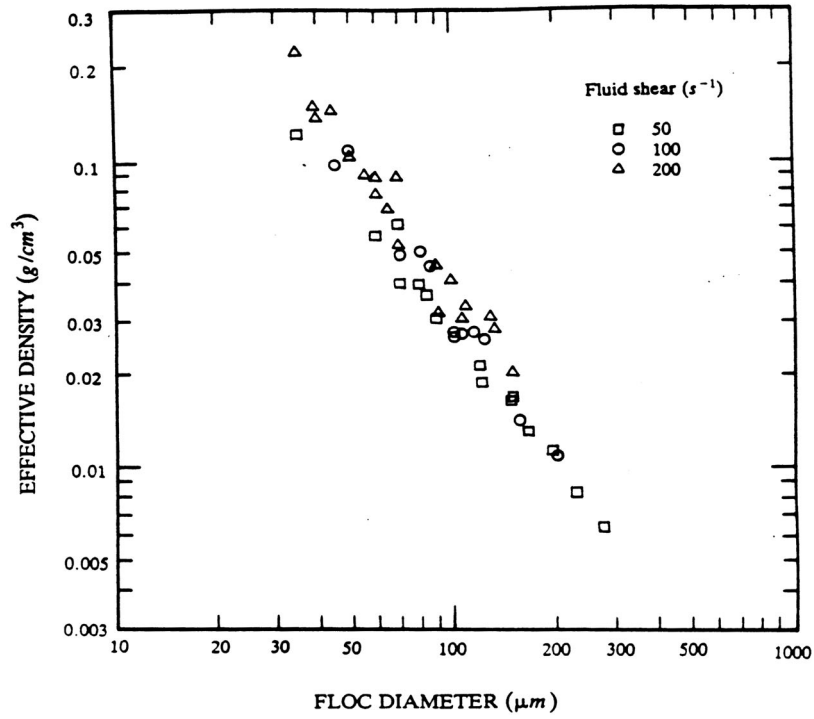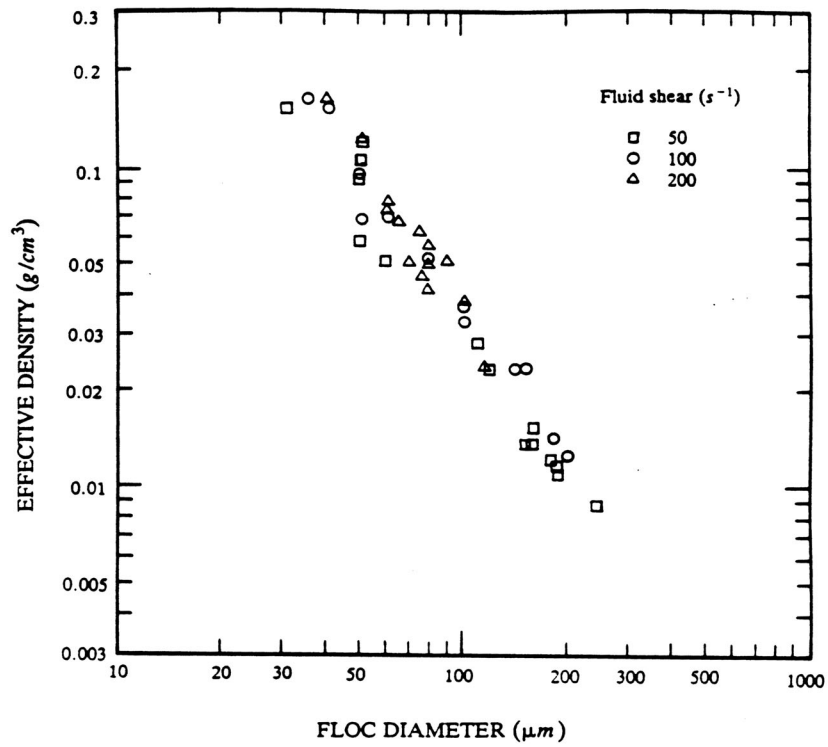
Fig.6-1a

Fig.6-1b

Fig.6-1c
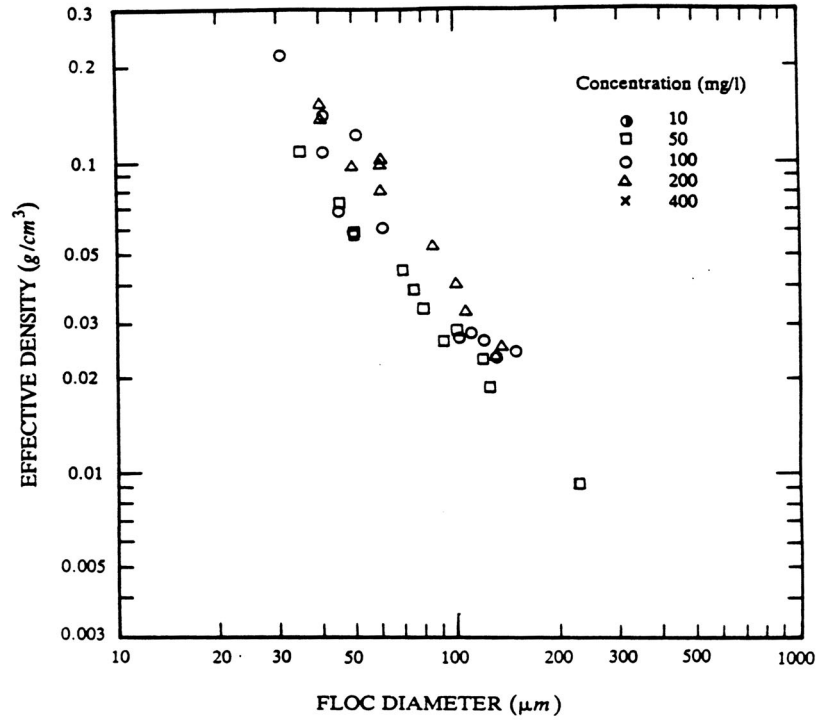
Fig.6-1d
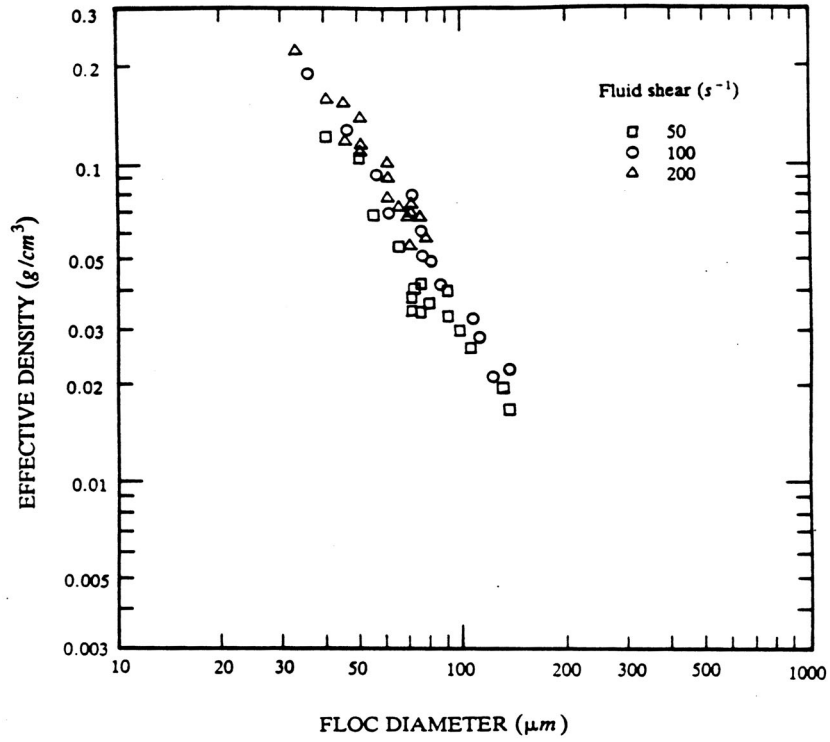
Fig.6-1e

In order to examine the influence of solid concentration, the other main parameter of floc formation, on the floc effective density-size relationship, we replot the data with the concentration as a parameter for fluid shears of 50, 100, 200 s^{-1} respectively (Figs.6-2a, 2b, and 2c). We can see from these figures that the solid concentration at which the flocs are formed has no distinguishable effects on the floc effective density. The overall tendency of the data suggests that for the same size, the flocs formed at different solid concentrations but at the same fluid shear, have the same effective density.
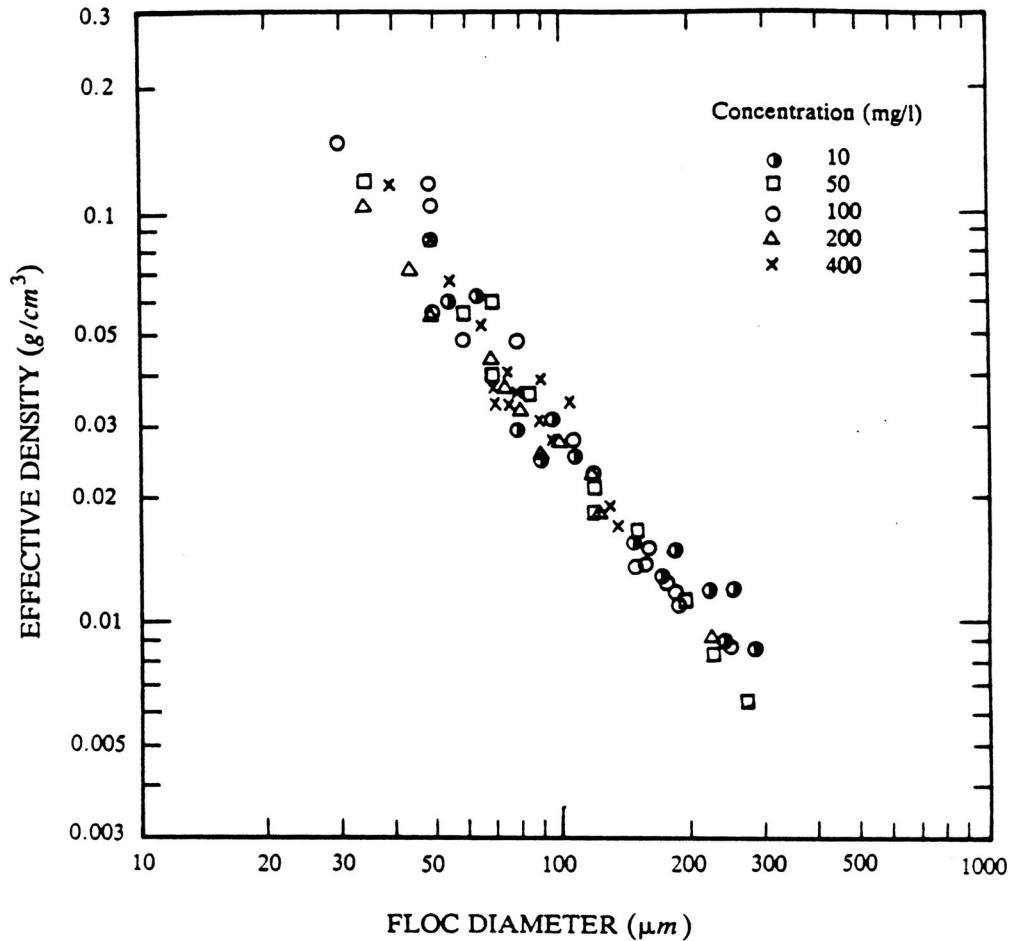
Fig.6-2 Relationship between effective density and size for drilling mud flocs from the Couette flocculator tests with solid concentration as a parameter, at fluid shears: (a) 50 s^{-1} ,(b) 100 s^{-1} , (c) 200 s^{-1} , respectively.

Fig.6-2a

121
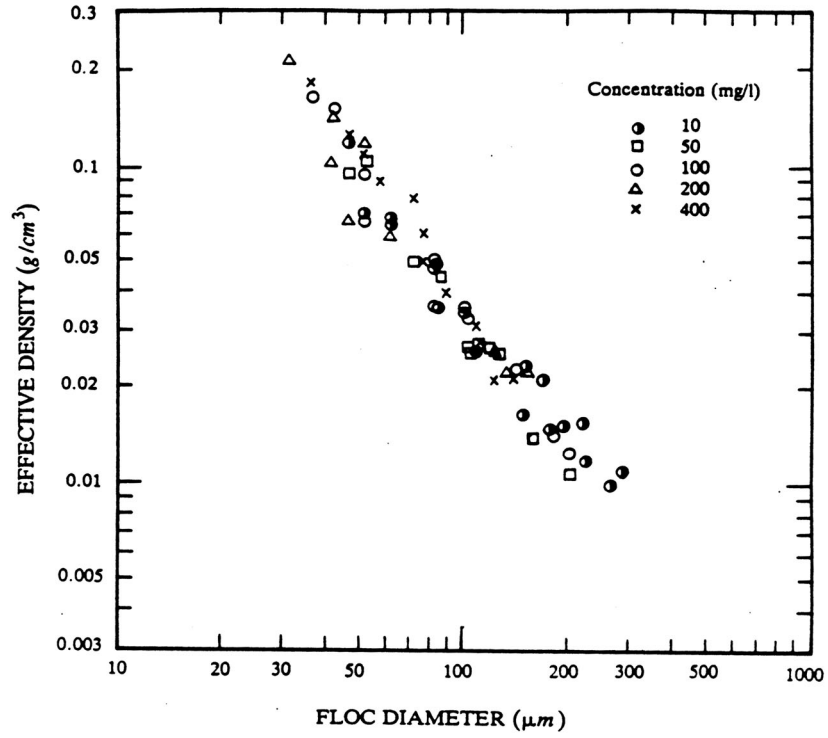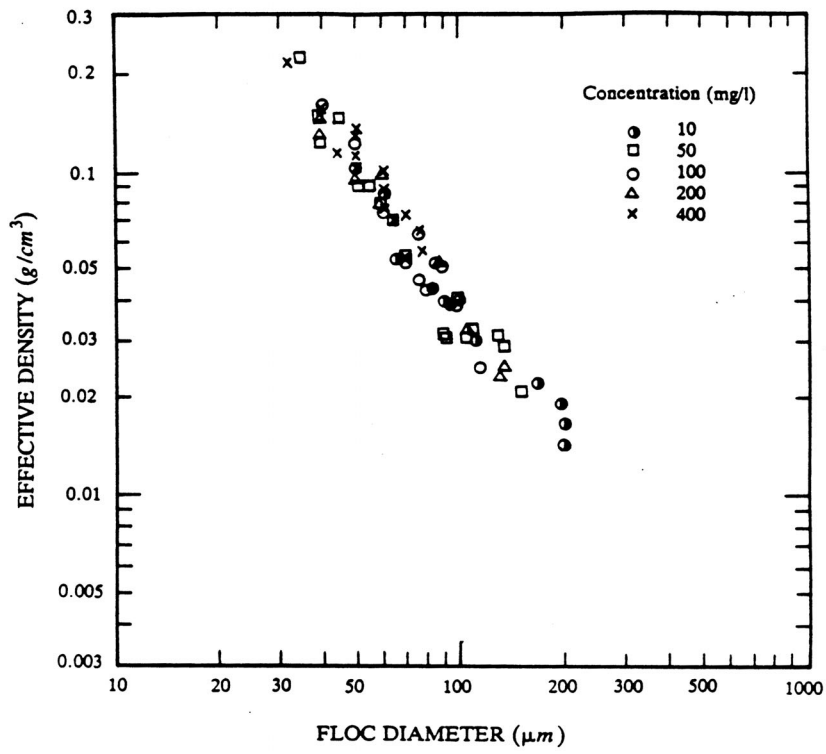
Fig.6-2b

Fig.6-2c

We can also see from these figures that for any combination of fluid shear and solid concentration, the floc effective density-size relationship over the whole size range tested can be fitted by the power expression:

$$\Delta\rho_f = A d_f^{-m} \tag{6-11}$$

where A and m are the experimentally determined constants.

Since solid concentrations have no distinguishable effects, we do the power regression for each fluid shear for all solid concentrations. Using the least-square method, we determine that $m = 1.36$, 1.39, and 1.47 for fluid shears of 50, 100, and 200 s^{-1} respectively with corresponding correlation coefficients of 0.97, 0.98, and 0.98.

Since the slopes (-m) at different fluid shears are nearly the same, we set $m = 1.4$ for all the fluid shear conditions. By this slight adjustment, we find that the constants A in Eq.(6-11) are 17.96, 22.00, and 24.86 for the fluid shears of 50, 100, and 200 s^{-1} respectively. The fitted lines of the power regressions are shown in Fig.6-3.
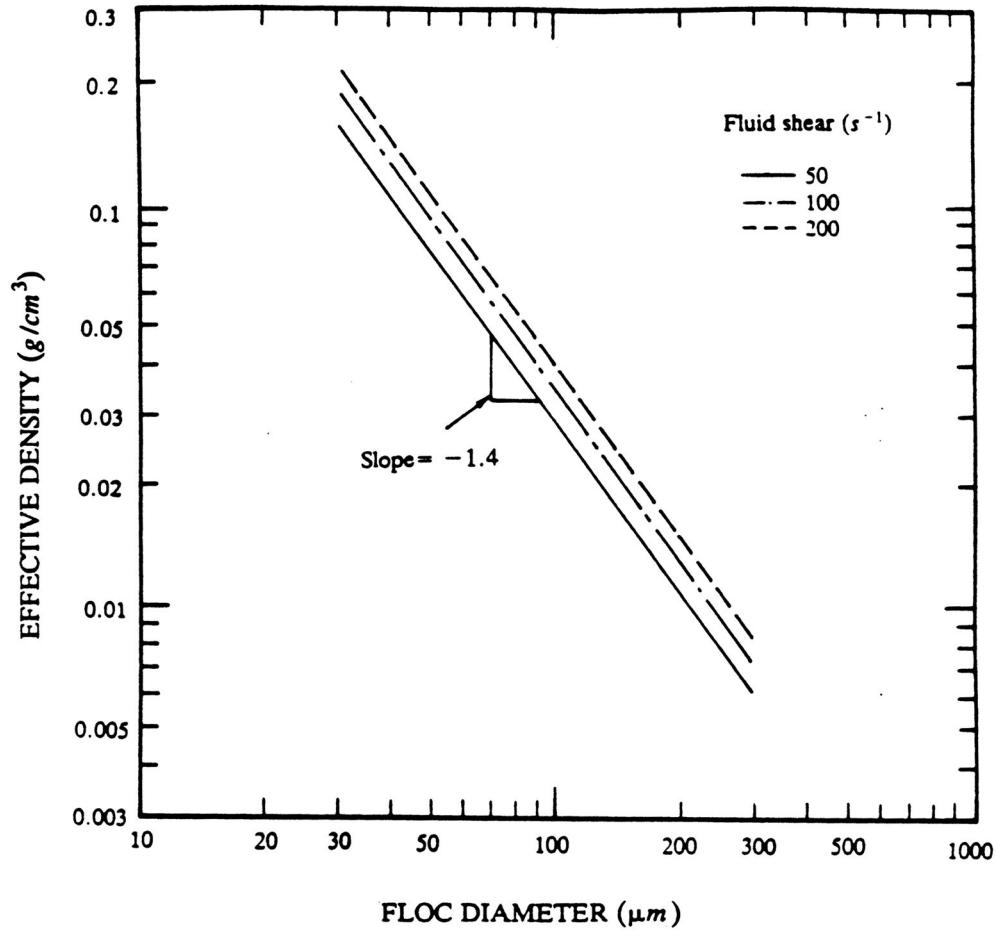
Fig.6-3 Fitted lines of the power regression for the effective density of drilling mud flocs from the Couette flocculator tests.

In order to obtain an empirical expression for the floc effective density-size relationship including the effects of fluid shear, we plot A versus fluid shear G (Fig.6-4) and find that the data can also be fitted by a power expression:

$$A = 7.43G^{0.23} \qquad\qquad 50 \leq G \leq 200 \ s^{-1} \qquad\qquad (6\text{-}12)$$

where G is in s^{-1}.
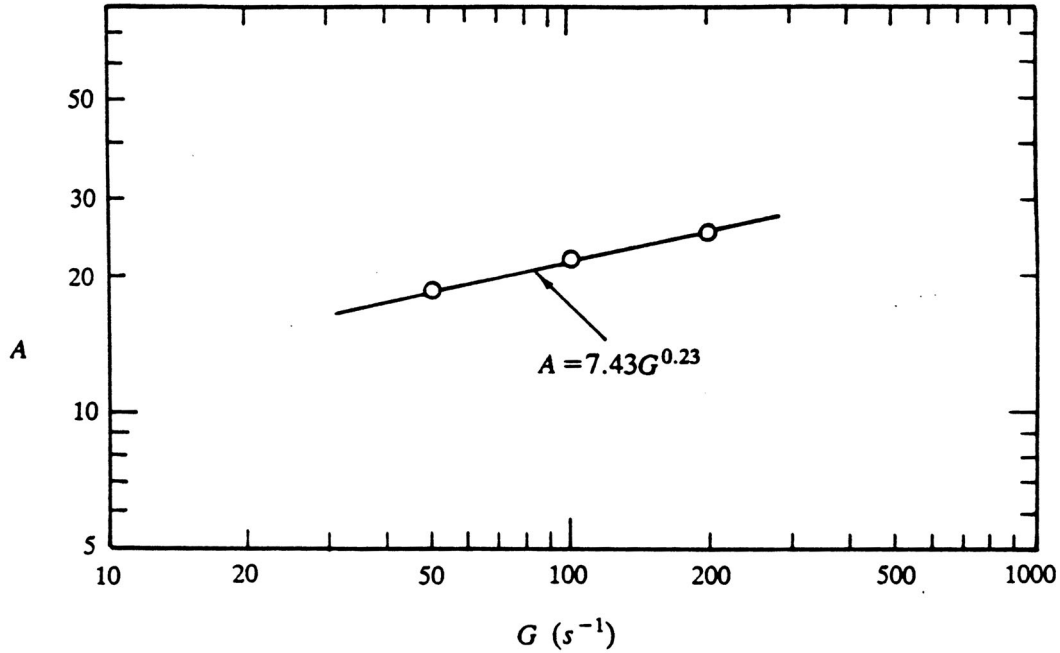
Fig.6-4 Relationship between A and G

Then combining Eq.(6-12) with Eq.(6-11), we obtain an empirical expression for the effective density-size relationship of drilling mud flocs, with fluid shear as a parameter at which the flocs would be formed:

$$\Delta\rho_f = 7.43G^{0.23}d_f^{-1.4} \qquad\qquad (6\text{-}13)$$

where d_f is in μm and $\Delta\rho_f$ is in g/cm^3.

As mentioned in Section 2, Stokes' law which applies to nonporous spheres, is used by many authors in the calculation of floc effective densities. For comparison, we also calculated effective densities using Stokes' law for the same settling speed data. The empirical expression obtained is:

$$\Delta\rho_f = 12.71G^{0.20}d_f^{-1.44} \qquad\qquad (6\text{-}14)$$

Comparing Eq.(6-14) with Eq.(6-13), 15 to 35% differences for the floc size range tested are observed between the results obtained from Stokes' law and from the floc settling speed model.

Drilling Mud Flocs from Disc Flocculator Tests

A total of 129 measurements were made of the sizes and settling speeds of the drilling mud flocs produced in the disc flocculator tests. These flocs included those made from untreated and treated samples. The sizes of these flocs ranged from 0.08 to 1.8 mm, while the settling speeds ranged from 300 to 8000 $\mu m/s$, corresponding to Reynolds numbers ranging from 0.02 to 13.4.

Figs.6-5 and 6-6 show the effective densities of drilling mud flocs made from untreated and treated samples respectively. Some differences in effective densities are observed from these two figures. This may reflect the effects of organic matter (1.77 % by weight in the drilling mud) on the densities. We also see from Figs.6-5 and 6-6 that the solid concentration at which flocs were formed does not have a distinguishable effect on the effective densities. This is consistent with the results for the flocs from the Couette flocculator tests.
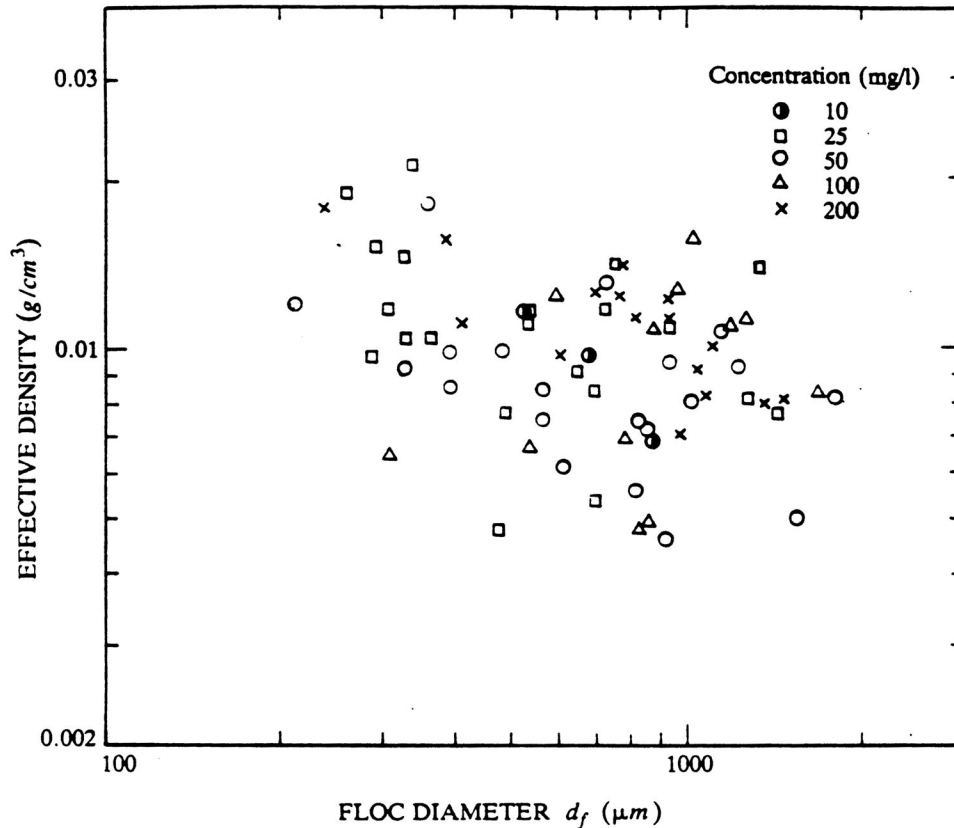
Fig.6-5 Effective densities of drilling mud flocs from the disc flocculator tests (untreated samples)
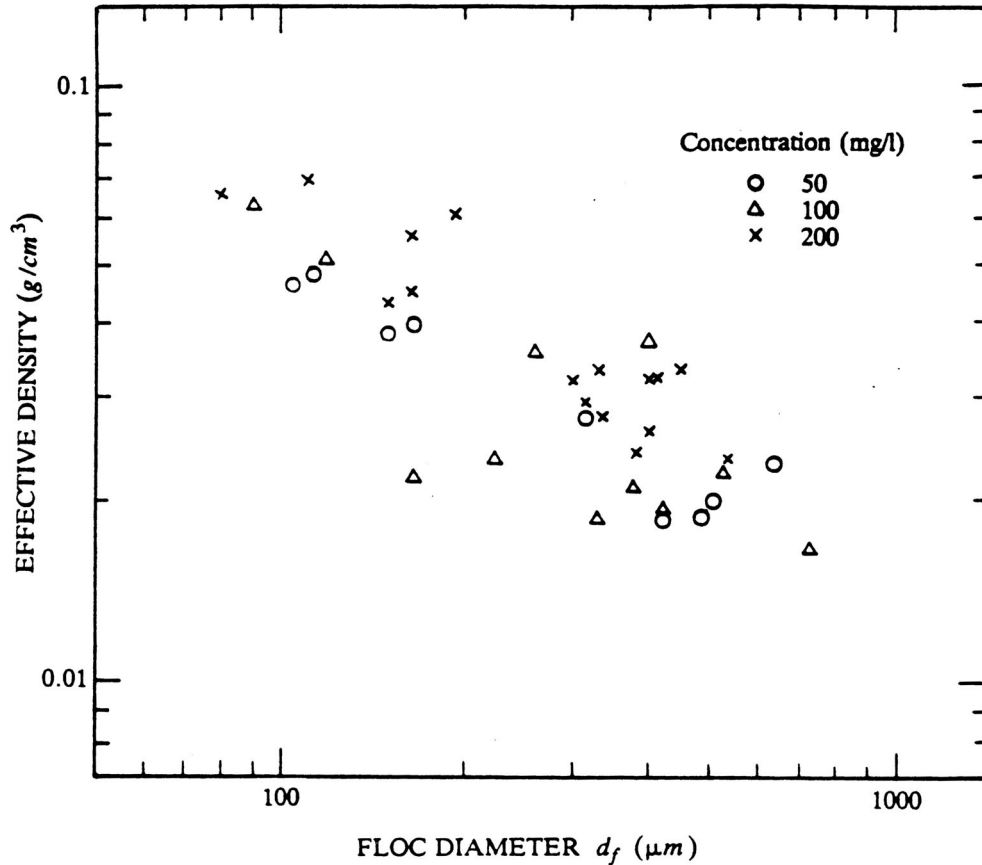
Fig.6-6 Effective densities of drilling mud flocs from the disc flocculator tests (treated samples)

We have noticed that the data shown in Figs.6-5 and 6-6 are more scattered than the data for flocs from the Couette flocculator tests (Figs.6-1 and 6-2). One possible reason for this is that in the disc flocculator tests, some flocs hit the bottom of the disc more often and became more compact than did other flocs. Nevertheless, the data suggest that the floc effective density decreases as the floc size increases.

Detroit River Sediment Flocs from Disc Flocculator Tests

A total of 202 measurements for the sizes and settling speeds of Detroit River sediment flocs from the disc flocculator tests were made. The sizes of these flocs ranged from 0.06 to 0.8 *mm*, while the settling speeds ranged from 60 to 4000 μ*m/s*, corresponding to Reynolds numbers ranging from 0.01 to 3.1.

Figs.6-7 and 6-8 show the effective densities of flocs made from untreated and treated Detroit River sediment in seawater. Figs.6-9 and 6-10 show the effective densities of flocs made from untreated and treated Detroit River sediment in fresh water. Similar to the drilling mud flocs,

differences in effective densities of flocs made from untreated and treated samples are observed. Moreover, the effective densities of flocs formed in fresh water are found to be greater than those of the flocs formed in seawater by as much as a factor of 2.
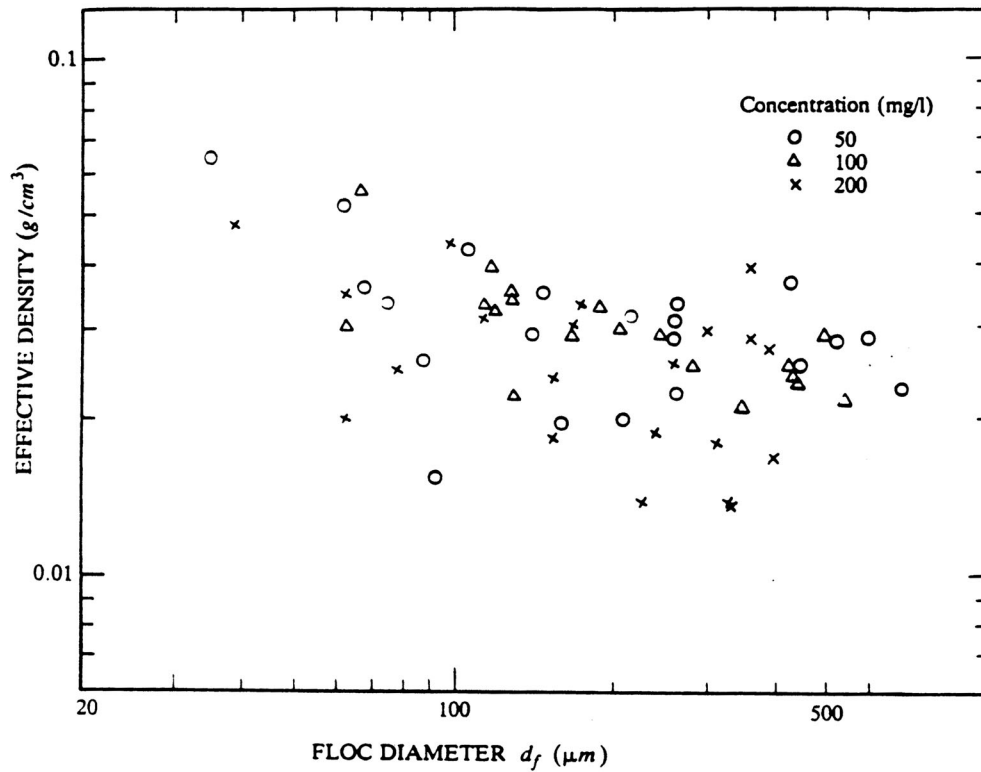
Fig.6-7 Effective densities of Detroit River sediment flocs from the disc flocculator tests (untreated samples in seawater)
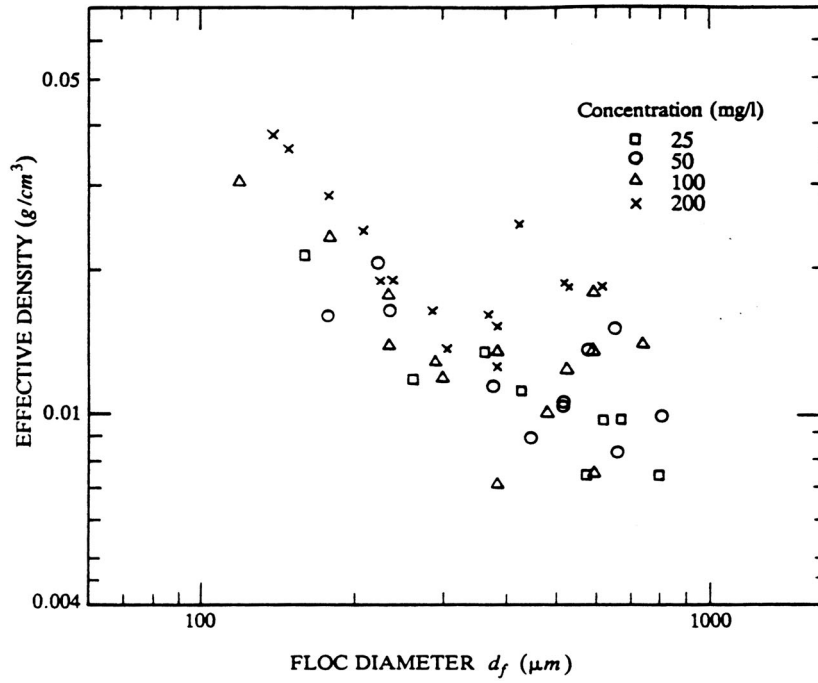
Fig.6-8 Effective densities of Detroit River sediment flocs from the disc flocculator tests (treated samples in seawater)
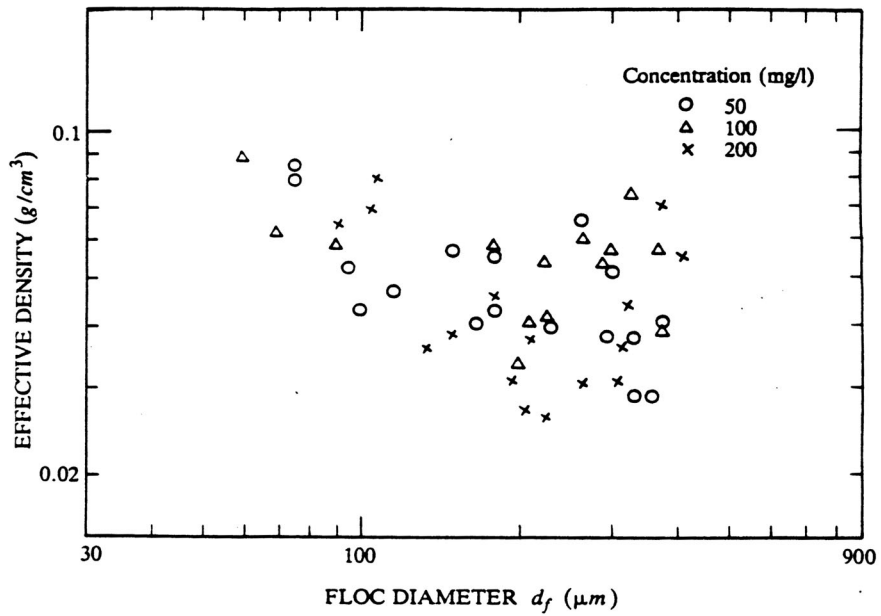
Fig.6-9 Effective densities of Detroit River sediment flocs from the disc flocculator tests (untreated samples in fresh water)
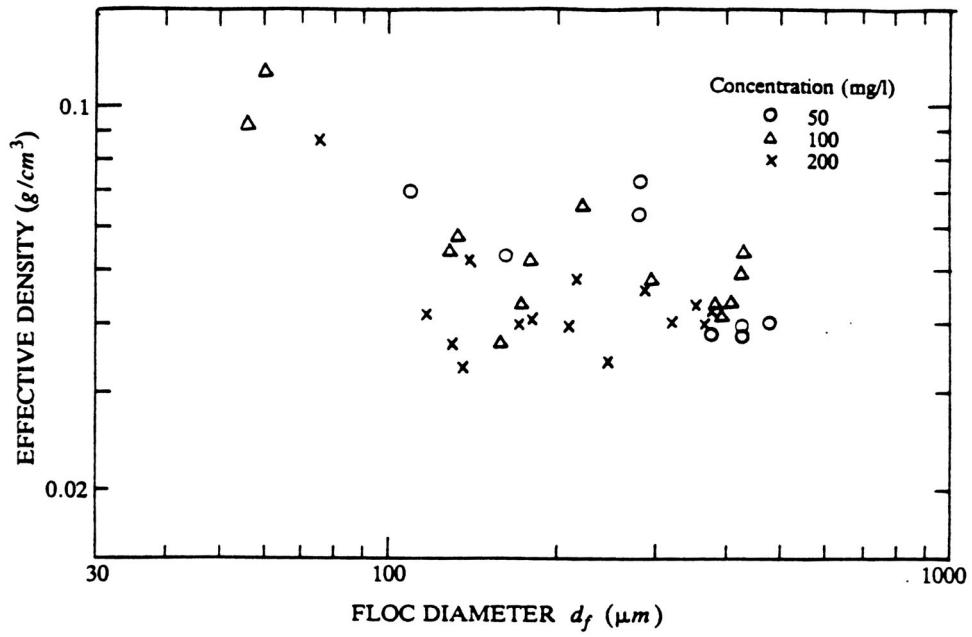
Fig.6-10 Effective densities of Detroit River sediment flocs from the disc flocculator tests (treated samples in fresh water)

7. CONCLUSIONS

In the present study, extensive experiments on the transport properties of a drilling mud and Detroit River sediments were conducted. The main findings from this study are summarized in the following:

1. From experiments in the annular flume, resuspension properties of the drilling mud were obtained as a function of fluid shear stress and bed consolidation period. Based on the experimental data, an empirical expression for ç, the amount of sediment resuspended, was obtained. Compared with bentonite, Fox River, and Green Bay sediments, ϵ for the drilling mud was less than that of bentonite by a factor of 2 to 2.5 and larger than those of Fox River and Green Bay sediments by a factor of 5 to 10. The drilling mud was therefore much easier to resuspend than the natural sediments and more difficult than bentonite. The organic matter in the sediments and the particle size and density of the sediments may be factors contributing to these differences.

2. From flocculation tests for the drilling mud in the Couette flocculator where fluid shear is present, the characteristics of flocculation (such as the median diameter, the standard deviation of the floc size distribution, and the time to reach the steady state) have been obtained as a function of fluid shear and solid concentration. Self-similar size distributions and three flocculation stages (initial stage, transition stage, and steady state) were observed. It was demonstrated by dimensional analysis for the flocculation at the steady state that the effects of fluid shear and solid concentration can be accounted for in terms of a dimensionless parameter F_l, which is defined as the flocculation number. The data on the median size at the steady state are well correlated to the flocculation number. A semi-empirical equation for this relation was obtained by power regression. The validity of the correlation was also demonstrated for other sediments.

3. Flocculation due to differential settling was studied using disc flocculators where no applied fluid shear was present. The validity of using disc flocculators to investigate flocculation due to differential settling of particles as in a settling tube or in a water body was examined. It was demonstrated both theoretically and experimentally that dynamic and collision similarity will exist and the flocculation in a disc will be independent of the rotation rate of the disc, as long as the rotation rate of the disc is low. The criteria for dynamic and collision similarity were presented. From the experiments, it was found that flocculation characteristics such as the floc median diameter are a function of solid concentration as well as time. Compared with tests in the Couette flocculator where fluid shear is dominant, particles flocculate in disc flocculators much slower, much longer times are needed to reach the steady state, and the floc sizes in the steady state are much larger.

4. Some preliminary experiments were conducted to examine the effects of organic coatings on flocculation. Sediments were treated using sodium hypochlorite to remove the organic coating, and then used in the disc flocculator tests. It was found that, for Detroit River sediments in seawater, treated samples flocculated significantly faster than did the untreated sediments at all solid concentrations tested; in fresh water, however, treated samples flocculated faster at high concentrations (100 and 200 *mg/l*), but slower at low concentrations (e.g., 25 *mg/l*). In contrast,

the treated drilling muds flocculated much slower than did the untreated mud at all concentrations tested. This was probably because the untreated drilling mud contained polymers; however, after treatment, these polymers had been removed.

5. Settling speeds of the drilling mud flocs produced from flocculation tests in the Couette and disc flocculators were measured in a settling tube by a double-exposure photographic method. The results show that the settling speed of a floc is not only a function of its size, but also of the conditions at which the floc is formed. Of the two main parameters of floc formation, fluid shear has a significant effect on the floc settling speed and must be taken into account, while solid concentration has no distinguishable effect in the present tests. Using the data for the drilling mud flocs from the Couette flocculator tests, an empirical expression for the settling speed as a function of floc size and fluid shear at which the flocs are formed is presented. Using the data for the drilling mud and Detroit River sediment flocs from the disc flocculator tests, empirical expressions for the settling speed-size relationships were obtained.

6. Effective densities of flocs were obtained using the settling speed data. A floc settling speed model was employed in the calculation of the floc effective density. For the drilling mud flocs from the Couette flocculator tests, the results show that the flocs formed at higher fluid shears are more dense than those formed at lower fluid shears, while solid concentration has much less of an effect on the floc effective density. An empirical expression for the effective density-size relationship with fluid shear as a parameter was obtained. For comparison, the effective densities of drilling mud flocs from the Couette flocculator tests were also calculated using Stokes' law. 15 to 35% differences in the results are observed between these two models. Effective densities of drilling mud and Detroit River sediment flocs from the disc flocculator tests were also obtained.

REFERENCES

Adler, P. M., Streamlines in and around porous particles, *J. Colloid and Interface Sci., 81* (2), 531-535, 1981.

Alldredge, A. L., and C. Gotschalk, In situ settling behavior of marine snow, *Limnol. Oceanogr., 33* (3), 339-351, 1988.

Amirtharajab, A., and S. L. Trusler, Destabilization of particles by turbulent rapid mixing, *J. Environ. Eng.,* ASCE, *112* (6), 1085-1109, 1986.

Anderson, J. U., An improved pretreatment for mineralogical analysis of samples containing organic matter, *Tenth National Conference on Clays Clay Minerals,* 380-388, 1961.

Argaman, Y., and Kaufman, W. J., Turbulence and flocculation, *J. Sanitary Engineering Division,* ASCE, *96,* SA2, 223-241, 1970.

Ayers, R. C., Characteristics of drilling discharges, In: *Proceedings of a Minerals Management Service Workshop entitled, An Evaluation of Effluent Dispersion and Fate Models for OCS Platforms.* Santa Barbara, California, Minerals Management Service, Los Angeles, 4-16, 1983.

Ayers, R. C., Jr., R. P. Meek, T. C. Sauer, Jr., and D. O. Stuebner, An environmental study to assess the effect of drilling fluids on water quality parameters during high-rate, high-volume discharges to the ocean, *J. Petroleum Technology, 34,* 165-173, 1982.

Beckett, R., and P. Le. Ngoc, The role of organic matter and ionic composition in determining the surface charge of suspended particles in natural waters, *Colloids and Surfaces, 44,* 35-49, 1990.

Boadway, J. D., Dynamics of growth and breakage of alum floc in presence of fluid shear, *J. Environ. Engineering Division,* ASCE, *104,* EE5, 901-915, 1978.

Brandsma, M. G., and T. C. Sauer, The OOC model: prediction of short-term fate of drilling mud in the ocean. Part 1: model description, In: *Proceedings of a Minerals Management Service Workshop entitled, An Evaluation of Effluent Dispersion and Fate Models for OCS Platforms,* Santa Barbara, California, Minerals Management Service, Los Angeles, 58-84, 1983.

Brinkman, H. C., A calculation of the viscosity and the sedimentation velocity for solutions of large chain molecules taking into account the hampered flow of the solvent through each chain molecule, *Proc. K. Ned. Akad. Wez.(A,nsterdwn), 50,* 618-625, 1947.

Brinkman, H. C., Erratum for "A calculation of the viscosity and the sedimentation velocity for solutions of large chain molecules taking into account the hampered flow of the solvent through each chain molecule", *Proc. K. Ned. Akad. Wet.(Ams:erdam), 50,* 821, 1947.

Burban, P.-Y., W. Lick, and J. Lick, The flocculation of fine-grained sediments in estuarine waters, *J. Geophys. Res., 94,* 8323-8330, 1989.

Burban, P.-Y., Y.-J. Xu, J. McNeil, and W. Lick, Settling speeds of flocs in fresh water and seawater, *J. Geophys. Res., 95,* 18213-18220, 1990.

Camp, T. R., and P. C. Stein, Velocity gradients and internal work in fluid motion, *J. Boston Society of Civil Engineers, 30,* 219-237, 1943.

Chase, R. R. P., Settling behavior of natural aquatic particulates, *Limnol. Oceanogr., 24* (3), 417-426, 1979.

Concha, F. and E. R. Almendra, Settling velocities of particulate system, 1. settling velocities of individual spherical particles, *International Journal of Mineral Processing, 5,* 349-367, 1979.

Deardorff, J. W., and S. C. Yoon, On the use of an annulus to study mixed-layer entrainment, *J. Fluid Mech., 142,* 97-120, 1984.

Deichatsios, M. A., and R. F. Probstein, Scaling laws for coagulation and sedimentation, *J. WPCF, 47* (5), 941-949, 1975.

Edzwald, J. K., J. B. Upchurch, and C. R. O'Melia, Coagulation in estuarines, *Environ. Sci. Technol., 8* (1), 58-63, 1974.

Eisma, D., Flocculation and de-flocculation of suspended matter in estuaries, *Netherlands Journal of Sea Res., 20* (2/3), 183-199, 1986.

Epstein, N., and O. Neale, On the sedimentation of a swarm of permeable spheres, *Chem. Eng. Sci., 29,* 1841-1842, 1974.

Estes, J. C., Role of water-soluble polymers in oil well drilling muds, In: Water-Soluble Polymers, Beauty with Performance, J. E. Glass (Ed.), Advances in Chemistry Series 213, American Chemical Society, Washington, D. C. 155-181, 1986.

Fair, G. M., and R. S. Gemmell, A mathematical model of coagulation, *J. Colloid Sci., 19,* 360-372, 1964.

Farley, K. J., and F. M. M. Morel, Role of coagulation in the kinetics of sedimentation, *Environ. Sci. and Technol., 20* (2), 187-195, 1986.

Findheisen, W., *Meteor. Z., 56,* 356, 1939.

Firth, B. A., and Hunter R. J., Flow properties of coagulated colloidal suspensions: I, II, and III, *J. Colloid and Interface Sci., 57,* 248-275, 1976.

Friedlander, S. K., On the particle-size spectrum of atmospheric aerosols, *J. Met. 17,* 373-374, 1960a.

Friedlander, S. K., Similarity consideration for the particle-size spectrum of a coagulating, sedimenting aerosol, *J. Met. 17,* 479-483, 1960b.

Fukuda, M. K., The entrainment of cohesive sediments in freshwater, Ph.D. dissertation, Case Western Reserve University, 1978.

Fukuda, M. K., and W. Lick, The entrainment of cohesive sediments in freshwater, *J. Geophys. Res., 85,* 2813-2824, 1980.

Gibbs, R. J., Clay mineral aggregation in the marine environment, *J. Sed. Petrol., 52,* 657-670, 1977.

Gibbs, R. J., Effect of natural organic coating on the coagulation of particles, *Environ. Sd. Technol., 17* (4), 237-240, 1983.

Gibbs, R. J., Settling velocity, diameter, and density for flocs of illite, kaolinite, and montmorillonite, *J. Sedimentary Petrology, 55* (1), 65-68, 1985a.

Gibbs, R. J., Estuarine flocs: Their size, settling velocity, and density, *J. Geophys. Res., 90,* 3249-3251, 1985b.

Gibbs, R. J., and L. Konwar, Coagulation and settling of Amazon River suspended sediment, *Continental Shelf Res., 6,* 127-149, 1986.

Gibbs, R. J., D. M. Tshudy, L. Konwar, and Jean Marie Martin, Coagulation and transport of sediments in the Gironde Estuary, *Sedimentology, 36,* 987-999, 1989.

Glasgow, L. A., and J.-P. Hsu, Floc characteristics in water and wastewater treatment, *Particulate Science and Technology, 2,* 285-303, 1984.

Goodarz-Nia, Floc density, porosity and void ratio in colloidal systems and aerosols, *J. Colloid and Interface Sci., 62* (1), 131-141, 1977.

Gregory, J., Physical properties, In *Sludge Characteristics and Behavior.* J. B. Carberry and A. J. Englande (Eds), Martinus Nijhoff Publishers, 1-27, 1983.

Gregory, J., Fundamentals of flocculation, *Critical Reviews in Environmental Control, 19* (3), 185-230, 1989.

Haider, A. and O. Levenspiel, Drag coefficient and terminal velocity of spherical and nonspherical particles, *Powder Technology, 58,* 63-70, 1989.

Harris, H. S., W. J. Kaufman, and R. B. Krone, Orthokinetic flocculation in water purification, *J. Sanitary Eng. Div.,* ASCE, *92,* SA6, 95-111, 1966.

Hawley, N., Settling velocity distribution of natural aggregates, *J. Geophys. Res., 87,* 9489-9498, 1982.

Hsu, J. -P., and L. A. Glasgow, Floc size reduction in the turbulent environment, *Parti. Sci. and Technol., 1,* 205-222, 1983.

Hunt, J. R., Prediction of oceanic particle size distributions from coagulation and sedimentation mechanisms, In: Particulates in Water: Characterization, Fate, Effects, and Removal, M. C. Kavanaugh and J. O. Leckie (Eds.), Advances in Chemistry Series 189, American Chemical Society, Washington, D. C. 243-257, 1980.

Hunt, J. R., Particle aggregate breakup by fluid shear, In: Estuarine cohesive sediment dynamics, A. J. Mehta, (Ed.), Spring, Berlin Heidelberg, New York, 85-109, 1986.

Hunt, J. R., Particle dynamics in seawater: implication for predicting the fate of discharged particles, *Environ. Sci. and Technol., 16,* 303-309, 1982.

Hunt, J R., and J. D. Pandya, Sewage sludge coagulation and settling in seawater, *Environ. Sci. and Technol., 18,* 119-121, 1984.

Hunter, R. J., and J. Frayen, Flow behavior of coagulation colloid sols, *J. Colloid and Interface Sci., 76* (1), 107-115, 1980.

Hunter, K. A., Microelectrophoretic properties of natural surface-active organic matter in coastal seawater, *Limnol. Oceanogr., 25* (5), 807-822, 1980.

Hunter, K. A., and P. S. Liss, Organic matter and the surface charge of suspended particles in estuarine waters, *Limnol. Oceanogr., 27* (2), 322-335, 1982.

Iacobellis, S., The flocculation of fine-grained lake sediments subjected to a uniform-shear stress, M.S. thesis, University of California, Santa Barbara, 1984.

Jeffrey, D. J., Aggregation and break-up of clay flocs in turbulent flow, *Advances in Colloid and Interface Science, 17,* 213-218, 1982.

Jekel, M. R., The stabilization of dispersed mineral particles by adsorption of humic substances, *Wat. Res., 20* (12), 1543-1554, 1986.

Johnson, R. J., Personal communication, 1992.

Kajihara, M., Settling velocity and porosity of large suspended particle, *J. Oceanogr. Soc. Jpn., 27,* 158-162, 1971.

Kawana, K., and T. Tanimoto, Temporal variation of suspended matter near the sea bottom in Hiro Bay, *Mer., 14.* 47-52, 1976.

Kawana, K., and T. Tanimoto, Suspended particles near the bottom in Osaka Bay, *J.Oceanogr. Soc. Jpn., 35,* 75-81, 1979.

Kawashima, Y., and C. E. Capes, An experimental study of the kinetics of spherical agglomeration in a stirred vessel, *Powder Technol., 10,* 85-92, 1974.

Klimpel, R. C., and R. Hogg, Effects of flocculation conditions on agglomerate structure, *J. Colloid and Interface Sci., 113* (1), 121-131, 1986.

Koh, P. T. L., J. R.G. Andrews, and P. H. T. Uhlherr, Floc-size distribution of scheelite treated by shear-flocculation, *Inter. J. Mineral Proce., 17,* 45-65, 1986.

Kranck, K., Sediment deposition from flocculated suspensions, *Sedimentology, 22,* 111-123, 1975.

Krone, R. B., A study of rheologic properties of estuarial sediments, *Techn Bull, 7,* Committee of Tidal Hydraulics, US Army Corps of Engr. WES, Vicksburg, 91 pp. 1963.

Krone, R. B., Aggregation of suspended particles in estuaries, In: Estuarine Transport Processes, B. Kjerfve (Ed.) Univ. S. California Press, 177-190, 1978.

Krone, R. B., The significance of aggregate properties to transport processes, In: Estuarine Cohesive Sediment Dynamics, A. J. Mehta (Ed.), Springer-Verlag, 66-84, 1986.

Krone, R. B., *Flume studies of the transport of sediment in estuarial shoaling processes,* Final Report to San Francisco District, U.S. Army Corps of Engineers, Washington, DC, 1962.

Kusuda, T., T. Umita, K. Koga, T. Futawatari, and Y. Awaya, Erosional process of cohesive sediments, *Wat. Sci. Tech., 17,* 891-901, 1984.

Lagvankar, A. L., and R. S. Gemmell, A size-density relationship for flocs, *J. AWWA, 60,* 1040-1046, 1968.

Lavkulich, L. M., and J. H. Wiens, Comparison of organic matter destruction by hydrogen peroxide and sodium hypochlorite and its effects on selected mineral constituents, *Soil Sci. Soc. Amer. Proc., 34,* 755-758, 1970.

Lee, D. Y., W. Lick, and S. W. Kang, The entrainment and deposition of fine-grained sediment in Lake Erie, *J. Great Lakes Res., 7,* 264-275, 1981.

Li, D.-H., and J. J. Ganczarczyk, Stroboscopic determination of settling velocity, size and porosity of activated sludge flocs, *Wat. Res., 21* (3), 257-262, 1987.

Lick, W., Discharge and sediment transport modeling, MMS workshop, 1989.

Lick, W., and J. Lick, Aggregation and disaggregation of fine-grained lake sediments, *J. Great L.akes Res., 14* (4), 514-523, 1988.

Lick, W., and Hening Huang, Flocculation and the physical properties of flocs, To be published, 1991.

Lick, W., and S. W. Kang, Entrainment of sediments and dredged materials in shallow lake waters, *J. Great Lakes Res., 13,* 619-627, 1987.

MacIntyre, S., W. Lick, and C. H. Tsai, Variability of entrainment of cohesive sediments in fresh water, *Biogeochemistry, 9,* 187-209, 1990.

Magara, Y., S. Nambu, and K. Utosawa, Biochemical and physical properties of an activated sludge on settling characteristics, *Wat. Res., 10,* 71-77, 1976.

Masliyah, J. H., and M. Polikar, Terminal velocity of porous spheres, *The Canadian J. Chem. Eng., 58,* 299-302, 1980.

Massion, G., The resuspension of uniform-size fine-grained sediments, M.S. thesis, University of California, Santa Barbara, 1982.

Matsumoto, K., and A. Suganuma, Settling velocity of a permeable model floc, *Chem. Eng. Sci., 32,* 445-447, 1977.

Matsumoto, K., and Y. Mori, Settling velocity of floc- new measurement method of floc density, *J. Chem. Engrs., Jpn., 8* (2), 143-147, 1975.

McCave, I. N., Vertical flux of particles in the ocean, *Deep Sea Res., 22,* 491-502, 1975.

McCave, I. N., Erosion, transport and deposition of fine-grained marine sediments, In *Fine-grained Sediments: Deep Water Process and Faces,* D. A. V. Stow, and D. J. W. Piper (Eds), Geol Soc Land, Spec Publ No 15, Blackwell, Oxford, 35-69, 1984.

Meakin, P., Effects of cluster trajectories on cluster-cluster aggregation: A comparison of linear and Brownian trajectories in two- and three-dimensional simulations, *Phys. Rev. A: Gen. Phys., 29,* 997-999, 1984.

Mehta, A. J., Depositional behavior of cohesive sediments, Ph.D. dissertation, University of Florida, 1973.

Mehta, A. J., T. M. Parchure, J. G. Dixit, and R. Ariathurai, Resuspension potential of deposited cohesive sediment beds, In *Estuarine Comparisons,* V. S. Kennedy (Ed), Academic Press, NY, 591-609, 1982.

Michaels, A. S., and Bolger, J. C., The plastic flow behaviour of flocculated kaolin suspensions, *Ind. Eng. Chem. Fund., 1,* 153-162, 1962.

Morgan, C. L., and F. T. Lovorn, Modelling the coagulation of a solid waste discharge from a manganese nodule processing plant, In: Waste in the Ocean, Vol.5, Deep-Sea Waste Disposal, D. R. Kester, W. V. Burt, J. M. Capuzzo, P. K. Park, B. H. Ketchum, and I. W. Duedall (Eds.), John Wiley & Sons, 243-258, 1986.

Mountain, R. D., G. W. Mulholland, and H. Baum, Simulation of aerosol agglomeration in the free molecular and continuum flow regimes, *J. Colloid and Interface Sci., 114,* 67-81, 1986.

Neale, G., N. Epstein, and W. Nader, Creeping flow relative to permeable spheres, *Chem. Eng. Sci., 28,* 1865-1874, 1973.

Neihof, R. A., and G. I. Loeb, The surface charge of particulate matter in seawater, *Limnol. Oceanogr., 17* (1), 7-16, 1972.

Neihof, R. A., and G. I. Loeb, Dissolved organic matter in seawater and the electric charge of immersed surfaces, *J. Mar. Res., 32,* 36-40, 1974.

Ooms, G., P. F. Mijnlieff, and H. L. Beckers, Frictional force exerted by a flowing fluid on a permeable particle, with particular reference to polymer coils, *J. Chem. Phys., 53,* 4123-4130, 1970.

Partheniades, E., Results of recent investigation on erosion and deposition of cohesive sediments, In *Sedimentation,* H. W. Shen (Ed), Fort Collins, Colorado, 20-39, 1972.

Rogak, S. N., and R. C. Flagan, Stokes drag on self-similar clusters of spheres, *J. Colloid and Interface Sci., 134* (1), 206-218, 1990.

Rotta, J. C., Turbulent stromungen, B. G. Teubner, Stuttgart, 1972.

Saffman, P. G., and J. S. Turner, On the collision of drops in turbulent clouds, *J. Fluid Mech., 1,* Part 1, 16-30, 1956.

Smoluchowski, M., Drei vortrage uber diffusion brownsche bewegung und koagulation von kolloidteilchen, *Physik Z, 17,* 557-585, 1916.

Smoluchowski, M., Versuch einer mathematischen theorie der koagulationskinetic kolloider losungen, Z. *Phys. Chem., 92,* 129, 1917.

Sricharoenchaikit, P., and R. D Letterman, Effect of AL(III) and sulefate ion on flocculation kinetics, *J. Environ. Eng.,* ASCE, *113* (5), 1120-1138, 1987.

Sutherland, D. N., A theoretical model of floc structure, *J. Colloid and Interface Sci., 25,* 373-380, 1967.

Sutherland, D. N., and C. T. Tan, Sedimentation of a porous sphere, *Chem. Eng. Sci., 25,* 1948-1950, 1970.

Swift, D. L., and S. K. Friedlander, The coagulation of hydrosols by Brownian motion and laminar shear flow, *J. Colloid Sci., 19,* 621-647, 1964.

Tambo, N., and Y. Watanabe, Physical characteristics of flocs, I, The floc density function and aluminum floc, *Wat. Res., 13,* 409-419, 1979.

Taylor, G. I., Stability of a viscous liquid contained between two rotating cylinders, *Philosophical Transactions, Royal Society, Series A, 223,* 289-345, 1923.

Taylor, G. I., Fluid friction between rotating cylinders, *Proceedings Royal Society, Series A, 157,* 546-578, 1936.

Tooby, P. F., G. L. Wick, and J. D. Isaacs, The motion of a small sphere in a rotating velocity field: a possible mechanism for suspending particles in turbulence, *J. Geophysical Research, 82* (15), 2096-2100, 1977.

Tsai, C. H., S. Iacobellis, and W. Lick, Flocculation of fine-grained sediments due to a uniform share stress, *J. Great Lakes Res., 13* (2), 135-146, 1987.

Tsai, C. H., and W. Lick, Resuspension of sediments from Long Island Sound, *Wat. Sci. Tech., 21* (6/7), 155-184, 1987.

Tsao, H.-K., and J.-P. Hsu, Simulation of floc breakage in batch-stirred tank, *J. Colloid and Interface Sci., 132* (2), 313-318, 1989.

Tsurui, M., and T. Takamori, Fundamental studies on the process of floc formation: 3. On the growing process of floc attended with its porosity change under turbulent motion, *J. Min. Metall. Inst. Jpn., 97,* 945-949(in Japanese, with English abstract), 1981.

Valioulis, I. A., Coagulation in the aquatic environment: theory and practice, *Advances in Colloid and Interface Science, 24,* 81-102, 1986.

Van Duuren, F. A., Defined velocity gradient model flocculator, *J. Sanitary Engineering Division, Proceedings of the American Society of Civil Engineers, 94* (SA4), 671-682, 1968.

Van Leussen, W., Aggregation of particles, settling velocity of mud flocs: a review, In: Physical processes in estuaries, J. Dronkers, and W. ven Leussen, (Eds.), 347-403, 1988.

Ven, T. G. van de, and Hunter, R. J., The energy dissipation in sheared coagulated sols, *Rheol Acta, 16,* 534-543, 1977.

Vold, M. J., Computer simulation of floc formation in a colloidal suspension, *J. Colloid Sci., 18,* 684-695, 1963.

Weitz, D. A., and M. Oliveria, Fractal structures formed by kinetic aggregation of aqueous gold colloids, *Physical Review Letters, 52,* 1433-1436, 1984.

Xu, Y-J, The flocculation of bentonite and barite in sea water, M.S. thesis, University of California, Santa Barbara, 1988.

Xu, Y-J., Transport properties of fine-grained sediments, Ph.D. dissertation, University of California, Santa Barbara, 1991.

Yeh, H. Y., Resuspension properties of flow deposited cohesive sediment beds, University of Florida Coastal Eng. Lab. Report, 79/018, 57-84, 1979.

Young, R. A., and J. B. Southard, Erosion of fine-grained marine sediments: Sea floor and laboratory experiments, *Bull. Geol. Soc. Am., 89,* 663-672, 1978.

Yusa, M., Mechanisms of pelleting flocculation, *Inter. J. Mineral Processing, 4,* 293-305, 1977.

ACKNOWLEDGMENTS

Appendix 1

```
C
C     SIGMA2.FOR
C
C     PROGRAM TO CALCULATE STANDARD DEVIATION OF FLOC
C     SIZE DISTRIBUTION
C
      REAL Y0(11),Y1(11)
      COMMON /AA/ Y,S
      OPEN(5,FILE='SIGMA2.I')
      OPEN(6,FILE='SIGMA2.O')
      READ(5,*)CC,SS,dm
      READ(5,*)(Y0(I),I=1,11)
      READ(5,*)(Y1(I),I=1,11)
      WRITE(0,10)CC,SS,dm
      WRITE(6,10)CC,SS,dm
10    FORMAT(///30X,'FLOC DEVIATION CALCULATION',
     1 //5X,'CONCENTRATION=',
     1F4.0,' MG/L','SHEAR STRESS=',F5.2,' DYNE/CM2',//
     14X,'dm=',F7.1,'um')
      DO 100 I=1,11
      Y0(I)=Y0(I)/100.0
100   Y1(I)=Y1(I)/100.0
      CALL SIMPSN(0.0,1.0,0.00001,2,N,Y0)
      S1=S
      CALL SIMPSN(1.0,6.0,0.00001,2,N,Y1)
      S2=S1+S
      SI=SQRT(S2)
      WRITE(0,303)dm,SI,S1,S
303   FORMAT(5X,'d50=',F6.1,8X,'Sigma=',F12.4,2F14.3)
      STOP
      END
C
C     INTERGRATING (d/d50-1)**2*d(F(x))
      SUBROUTINE SIMPSN(A,B,EPS,K,N,bb)
      REAL bb(11)
      COMMON /AA/Y,S
      N=1
      C=ABS(A)+ABS(B)
      H=0.5*(B-A)
      T1=H*(0.0000001+0.0)
1     X=A-H
      T2=0.5*T1
      DO 2 I=1,N
      X=X+2.*H
      CALL LAGR12(bb,11,A,B,1,X)
```

143

```
2      T2=T2+H*F(X)
       S=0.33333333*(4.*T2-T1)
       N=N+N
       IF(N.LE.K)GO TO 3
       IF(ABS(S-S0).LE.(1.+ABS(S))*EPS) RETURN
3      S0=S
       T1=T2
       H=0.5*H
       IF((C+H).NE.C) GO TO 1
       N=-N
       RETURN
       END
C
C      CALCULATION OF d(F(x))/dx
       SUBROUTINE LAGR12(bb,N,A,B,L,X)
       REAL bb(11)
       COMMON /AA/Y,S
       RN=FLOAT(N)
       H=(B-A)/(RN-1.0)
       I=(X-A)/H+0.5
       IF(I-1) 30,10,10
10     IF(I-(N-2)) 40,20,20
20     I=N-2
       GO TO 40
30     I=1
40     TI=FLOAT(I)
       T=(X-A)/H-TI
       IF(L.EQ.1) GO TO 50
       C0=0.5*T*(T-1.0)
       C1=1.0-T*T
       C2=0.5*T*(T+1.0)
       Y=C0*bb(I)+C1*bb(I+1)+C2*bb(I+2))
       RETURN
50     C0=0.5*(2.0*T-1.0)
       C1=-2.0*T
       C2=0.5*(2.0*T+1.0)
       Y=(C0*bb(I)+C1*bb(I+1)+C2*bb(I+2))/H
       RETURN
       END
C
C      CALCULATION OF (x-1)**2*d(F(x))/dx  x=d/d50
       FUNCTION F(X)
       COMMON /AA/Y,S
       F=(X-1.0)**2*Y
       RETURN
       END
```

Appendix 2

```
C
C     FP.FOR
C
C     PROGRAM TO CALCULATE FLOC EFFECTIVE DENSITIES USING
C     THE SETTLING SPEED DATA AND A FLOC SETTLING SPEED MODEL
C
      REAL W(114),D(114),RT(1)
      COMMON /A/ W,D,I
      OPEN(5,FILE='INP1')
      OPEN(6,FILE='OUT1')
      READ(5,*)C,S,M
      READ(5,*)W(W(I),I=1,M)
      READ(5,*)D(D(I),I=1,M)
      WRITE(0,10)C,S
10    FORMAT(///30X,'FLOC EFFECTIVE DENSITY CALCULATION',
     1 //5X,'CONCENTRATION=',
     1F4.0,' MG/L','SHEAR STRESS=',F5.2,' DYNE/CM2',//
     12X,'I   W(um/s)   d(um)   DENSITY(G/CM3)
     1      (1-e)I   (1-e)II   F      Re',/)
C
      DO 20 I=1,M
      CALL ROOT2(0.002,0.3,0.01,1,M1,1E-6,1E-6,RT)
      RE=W(I)*D(I)/1000000.0
C     X2=18.0/9.8*1.0/(2.65-1.0)*W(I)/D(I)/D(I)
      X2=18.0/9.8*1.02466/(2.65-1.02466)*W(I)/D(I)/D(I)
C     DL=(2.65-1.0)*RT(1)
      DL=(2.65-1.02466)*RT(1)
      P=6.0*6.0/72.0*(3.0+4.0/RT(1)-3.0*SQRT(8.0/RT(1)-3.0))
      B=D(I)/2.0/SQRT(P)
      Q=B/(B-TANH(B))+3.0/2.0/B/B
      WRITE(6,30)I,W(I),D(I),DL,RT(1),X2,Q,RE
20    WRITE(0,30)I,W(I),D(I),DL,RT(1),X2,Q,RE
30    FORMAT(1X,I2,F10.0,F14.5,F12.4,F11.4,F10.4,F8.2,/)
      STOP
      END
C
      SUBROUTINE ROOT2(AA,BB,H,N,M1,E1,E2,RT)
      DIMENSION RT(N)
      WT=0.0
      I=0
      X=AA
      F0=F(X)
04    X=X+H
      K=0
      F1=F(X)
      IF(ABS(F0).LE.E1) GO TO 100
```

```
        IF(ABS(F1).LE.E1) GO TO 101
        IF(F0*F1.GT.0.0) GO TO 101
        FA=F0
        FB=F1
        A=X-H
        B=X
01      C=B-(A-B)*FB/(FA=FB)
        K=K+1
        IF(WT)5,7,5
07      WT=1
        GO TO 06
05      IF(ABS(C1-C).LT.E2) GO TO 03
06      C1=C
        FC=F(C)
        IF(FC*FA.GT.0.0) GO TO 02
        FB=FC
        B=C
        GO TO 01
02      FA=FC
        A=C
        GO TO 01
100     C=X-H
03      I=I+1
        RT(I)=C
101     F0=F1
        IF(X-BB)4,8,8
08      M1=I
        RETURN
        END
C
        FUNCTION F(X)
        REAL K,W(114),D(114)
        COMMON /A/W,D,I
        K=6.0*6.0/72.0*(3.0+4.0/X-3.0*SQRT(8.0/X-3.0))
        B=D(I)/2.0/SQRT(K)
        Q=B/(B-TANH(B))+3.0/2.0/B/B)
C       A2=4.0/3.0/0.28*9.8/1000000.0*(2.65-1.0)/1.0*X*Q*D(I)**3
        A2=4.0/3.0/0.28*9.8/1000000.0*(2.65-1.02466)/1.02466*X*Q*D(I)**3
        AAA=SQRT(A2)
        RE=1.0/4.0*SQRT((9.06*9.06+4.0*AAA)-9.06)**2
        WS=1000000.0/D(I)*RE
        F=W(I)-WS
        RETURN
        END
```

146

The Department of the Interior Mission

As the Nation's principal conservation agency, the Department of the Interior has responsibility for most of our nationally owned public lands and natural resources. This includes fostering sound use of our land and water resources; protecting our fish, wildlife, and biological diversity; preserving the environmental and cultural values of our national parks and historical places; and providing for the enjoyment of life through outdoor recreation. The Department assesses our energy and mineral resources and works to ensure that their development is in the best interests of all our people by encouraging stewardship and citizen participation in their care. The Department also has a major responsibility for American Indian reservation communities and for people who live in island territories under U.S. administration.

The Minerals Management Service Mission

As a bureau of the Department of the Interior, the Minerals Management Service's (MMS) primary responsibilities are to manage the mineral resources located on the Nation's Outer Continental Shelf (OCS), collect revenue from the Federal OCS and onshore Federal and Indian lands, and distribute those revenues.

Moreover, in working to meet its responsibilities, the **Offshore Minerals Management Program** administers the OCS competitive leasing program and oversees the safe and environmentally sound exploration and production of our Nation's offshore natural gas, oil and other mineral resources. The MMS **Royalty Management Program** meets its responsibilities by ensuring the efficient, timely and accurate collection and disbursement of revenue from mineral leasing and production due to Indian tribes and allottees, States and the U.S. Treasury.

The MMS strives to fulfill its responsibilities through the general guiding principles of: (1) being responsive to the public's concerns and interests by maintaining a dialogue with all potentially affected parties and (2) carrying out its programs with an emphasis on working to enhance the quality of life for all Americans by lending MMS assistance and expertise to economic development and environmental protection.